



Chair of Process Technology and Industrial Environmental Protection

Master's Thesis



Assessment of conceivable CCU  
technologies for Austria

Alexander Paul Knaak, BSc

April 2024



**EIDESSTATTLICHE ERKLÄRUNG**

Ich erkläre an Eides statt, dass ich diese Arbeit selbstständig verfasst, andere als die angegebenen Quellen und Hilfsmittel nicht benutzt, den Einsatz von generativen Methoden und Modellen der künstlichen Intelligenz vollständig und wahrheitsgetreu ausgewiesen habe, und mich auch sonst keiner unerlaubten Hilfsmittel bedient habe.

Ich erkläre, dass ich den Satzungsteil „Gute wissenschaftliche Praxis“ der Montanuniversität Leoben gelesen, verstanden und befolgt habe.

Weiters erkläre ich, dass die elektronische und gedruckte Version der eingereichten wissenschaftlichen Abschlussarbeit formal und inhaltlich identisch sind.

Datum 23.04.2024

---

Unterschrift Verfasser/in  
Alexander Paul Knaak

## **DANKSAGUNG**

An dieser Stelle möchte ich mich bei allen bedanken, die mich bei meiner Masterarbeit unterstützt haben und auch bei all jenen, die während meines Studiums für mich da waren.

Mein größter Dank gilt meinem Betreuer DI Philipp Wolf-Zöllner, der mich mit dieser Arbeit am CaCTUS-Projekt teilhaben ließ und mir jederzeit für all meine Fragen und Anliegen mit Rat und Tat zur Seite stand. Ebenfalls bedanken möchte ich mich bei Univ.-Prof. DI Dr.-Ing. Markus Lehner, der mich mit seiner fachlichen Expertise unterstützte.

Besonderer Dank gilt meinen Eltern, Beata und Rüdiger, die mir mein Studium ermöglicht haben und deren stets positive Einstellung mich während meines gesamten Studiums dazu ermutigte, Herausforderungen lösungsorientiert gegenüberzustehen. Hier möchte ich mich auch bei Jennifer bedanken, die mich auf diesem Weg stets bestärkt und ermutigt hat.

In Leoben schließt man Freundschaften fürs Leben und ich möchte mich bei all jenen Bedanken, die mir diese unglaublich schöne Zeit im und abseits des Studiums beschert haben: Elias, Gabriel, Karin, Christoph, Iris, Lea, Cathrin, Florian, Thomas, Jonathan, Jakob, David, Richard, Patrik, Andreas, Christina und Michael.

Danke!

## **Kurzfassung**

### **Bewertung denkbarer CCU-Technologien für Österreich**

Die nachhaltige Verwertung von Kohlenstoffdioxid in Produktionsprozessen erfordert neben der Verfügbarkeit spezifischer Technologien, eine davon ausgehende, maßgebliche Reduktion von Treibhausgasemissionen im Vergleich zu konventionellen Herstellungsverfahren. Eine umfassende Literaturrecherche identifiziert zehn unterschiedliche CCU-Technologien, inklusive möglicher Umsetzungsmethoden und Betriebsbedingungen. Zur Bewertung und Gegenüberstellung derselben dienen die formulierten Klimazielkompatibilitätskriterien, welche auf den nationalen Strategien beruhen und in technologiespezifischen Emissionsfaktoren resultieren. Diese Faktoren zeigen gemeinsam mit Emissionsdaten heimischer Betriebe aus den Industrie- und Energiesektoren den Wert von CO<sub>2</sub> als alternativen Rohstoff auf und ergeben theoretische Treibhausgaseinsparungspotentiale auf Basis eines Substitutionsansatzes. Darüber hinaus behandelt diese Arbeit limitierende Aspekte, die bei der Auswahl geeigneter CCU-Routen zu beachten sind und diskutiert Hürden auf dem Weg des Kohlenstoffdioxids von seinem Ursprung bis hin zur erneuten Freisetzung am Ende eines Produktlebenszyklus.

## **Abstract**

### **Assessment of conceivable CCU technologies for Austria**

The utilization of carbon dioxide in production processes, targeted for implementation by 2030 or 2040, necessitates timely technological readiness and a substantial impact on greenhouse gas reduction compared to conventional manufacturing methods. Within this context, a comprehensive literature review has identified ten distinct CCU technologies, presenting their methodologies and possible operational conditions. Aligned with national objectives, climate target compatibility criteria are formulated for comparative analysis and to determine technology-specific emission factors. These factors, in conjunction with emissions data from domestic operators, highlight the value of CO<sub>2</sub> as an alternative raw material and potential GHG emission savings through a substitution approach. Furthermore, this thesis explores considerations and challenges involved in selecting suitable CCU pathways, tracing the journey of carbon dioxide from its origin to its re-release at the end of a product's lifecycle.

## Table of contents

	Page
<b>1 INTRODUCTION.....</b>	<b>3</b>
<b>2 DEFINITIONS AND FUNDAMENTALS.....</b>	<b>4</b>
2.1 Austria's climate targets.....	4
2.2 CO <sub>2</sub> origins and pathways .....	5
2.2.1 Utilizable CO <sub>2</sub> sources in Austria .....	7
2.3 Carbon capture .....	9
2.3.1 Chemical absorption .....	11
2.3.2 Physical adsorption.....	11
2.3.3 Membrane separation .....	12
2.3.4 Cryogenic carbon capture.....	13
2.3.5 Solid looping .....	14
2.4 CO <sub>2</sub> utilization pathways.....	15
2.4.1 Mineral carbonation .....	16
2.4.2 Chemical conversion.....	17
2.4.3 Electrochemical conversion .....	18
2.4.4 Biological conversion .....	20
2.5 Lifetime of CCU products.....	21
2.6 CCU emissions .....	21
<b>3 CLIMATE TARGET COMPATIBILITY OF CCU TECHNOLOGIES.....</b>	<b>23</b>
3.1 Harmonization of LCAs.....	23
3.1.1 Functional unit.....	23
3.1.2 System boundaries .....	23
3.1.3 Electricity mix .....	24
3.1.4 Hydrogen mix.....	24
3.1.5 Heat supply .....	25
3.1.6 CO <sub>2</sub> recovery.....	25
3.1.7 Multifunctionality .....	26
3.1.8 Storage effects.....	26
3.2 Technological Readiness Level .....	26
3.3 Compatibility limits for CCU with climate targets .....	28
<b>4 CONCEIVABLE CCU TECHNOLOGIES .....</b>	<b>29</b>
4.1 Carbonation of steel slag construction blocks .....	31

4.2	High gravity steel slag carbonation .....	33
4.3	Urea via SEWGS from BOFG .....	36
4.4	Direct hydrogenation of CO <sub>2</sub> .....	39
4.5	FT fuel from syngas via rWGS .....	41
4.6	Direct synthesis of DMM via CO <sub>2</sub> hydrogenation in methanol .....	43
4.7	Electrochemical CO <sub>2</sub> reduction to ethylene .....	44
4.8	CO <sub>2</sub> -based polyol production .....	46
4.9	CO <sub>2</sub> bio-fermentation to acetone .....	48
<b>5</b>	<b>POTENTIAL OF CCU IN AUSTRIA .....</b>	<b>52</b>
5.1	Estimating CCU potentials .....	53
5.1.1	MSWI sector .....	55
5.1.2	Methanol sector .....	57
5.2	Resulting reduction potentials for Austria's industrial sectors.....	58
<b>6</b>	<b>CONCLUSIONS.....</b>	<b>61</b>
<b>7</b>	<b>APPENDICES .....</b>	<b>63</b>
7.1	References .....	63
7.2	Nomenclature .....	74
7.3	Formulars.....	75
7.4	Tables .....	76
7.5	Figures.....	78

# 1 Introduction

The Paris Climate Agreement's commitment to limit global warming to 1.5°C has initiated a shift towards fossil-free practices across the globe. In anticipation, entities in the industry and energy sectors have devised roadmaps and strategies aimed at circumventing greenhouse gas emissions by transitioning to more sustainable production methods. Despite these efforts, certain sectors, such as cement, lime and glass industry, face inherent challenges in fully mitigating emissions due to technological and process constraints as per current advancements. In this context, carbon capture and utilization emerges as a viable solution, introducing technologies that recover CO<sub>2</sub> either from industrial processes or directly from the atmosphere to produce a variety of carbon containing products, including building materials, polymers, alternative fuels and commodity chemicals. The growing interest in these technologies has prompted the Austrian Climate Research Program to initiate the CaCTUS-Project [1], assessing their impact on Austria's journey to net-zero emissions. This thesis contributes to the CaCTUS-Project by addressing the potential of CO<sub>2</sub> as an alternative raw material through the deployment of CCU technologies.

The effectiveness of CCU technology implementation is influenced by a variety of factors, including the carbon dioxide's origin and source, the process of conversion, as well as the characteristics of the final product. Given the diversity of CCU technologies and the extensive discussion of their various methods and applications in literature, this work aims to elucidate critical considerations for CCU evaluation. Reports on current projects offer insights into their developmental status and projected availability for the target years of 2030 and 2040. Based on life cycle assessment studies, conceivable CCU technologies are evaluated for compatibility with Austrian climate objectives. By integrating emissions data from companies of the domestic industrial and energy sectors, with the identified CO<sub>2</sub> utilization opportunities, their theoretical potential for the reduction of GHG-emissions is quantitatively estimated.



## 2 Definitions and fundamentals

This chapter provides an exploration of the driving forces behind the implementation of carbon capture and utilization (CCU) in Austria, highlighting both political and industrial incentives. Furthermore, it aims to establish a foundational understanding of the various stages involved in the journey of CO<sub>2</sub>, starting from its origin, passing through capture technologies, and culminating in its transformation into valuable products.

### 2.1 Austria's climate targets

The European Climate Law [2] mandates member states to achieve a minimum 55% reduction in net greenhouse gas (GHG) emissions across the Union by 2030, relative to 1990 levels, and to reach net-zero emissions by 2050. Integral to this objective, national energy and climate plans (NECPs) for the period 2021-2030 must be developed, detailing strategies to meet these targets. In Austria, the government has placed the ambitious aim of attaining climate-neutrality by 2040 on its agenda [3], positioning itself as a pioneer in Europe's climate protection efforts. The Environment Agency Austria collaborates in a consortium of scientific institutions to calculate GHG scenarios for the monitoring tool (VO 525/2013/EG). Besides the 'With Existing Measures' (WEM) and the 'With Additional Measures' (WAM) scenarios, a 'Transition Scenario' is also modelled for the implementation of 2040 climate neutrality. This scenario demonstrates emission reductions achievable with domestically available resources and technologies, as well as taking lifestyle changes into account. [4] The latest results are detailed in the proposed NECP [5], as illustrated in Figure 1.

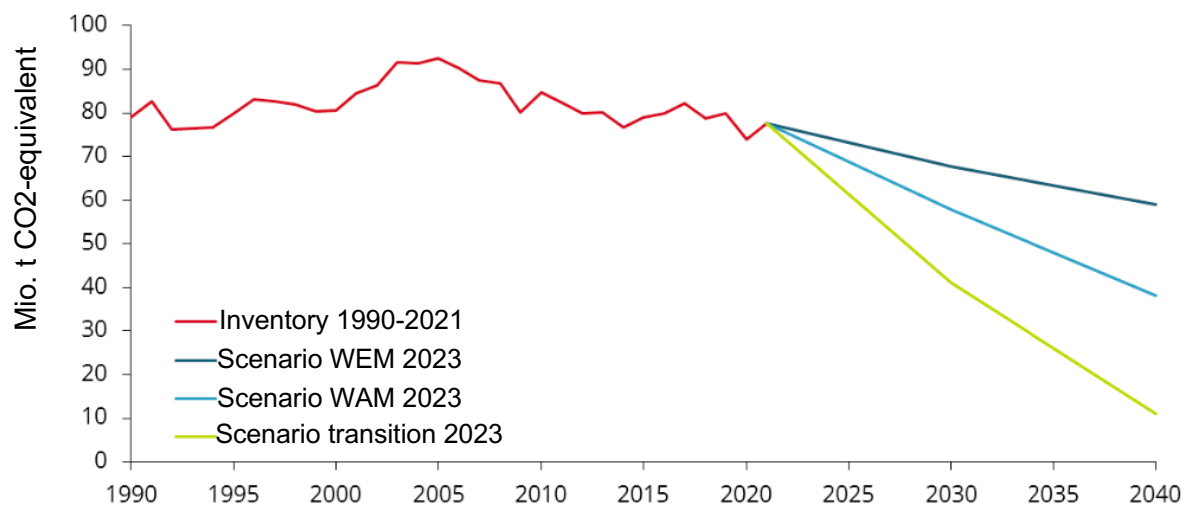


Figure 1: Development of total GHG-emissions (ETS and non-ETS) 1990-2021 and calculated GHG-scenarios [5]

Based on the 'Transition Scenario' findings, around 11 million tonnes of CO<sub>2</sub> equivalents (CO<sub>2</sub>e) are projected to persist by 2040 from hard-to-defossil sectors, such as agriculture, industry (particularly in terms of process emissions), and waste management. The journey towards national climate neutrality is marked by a distinct prioritization in terms of reducing

GHG emissions by lowering energy consumption, for instance through efficiency improvements or savings, and by transitioning to sustainable renewable energy sources. Emissions which currently seem unavoidable, especially those originating from industrial processes and partly from energy consumption, must be technologically captured and then geologically stored or utilized. [5]

The proposed NECP [5] reports key objectives, policies and measures guiding Austria towards net-zero emissions. Since this work is dedicated to CCU technologies, those objectives pertinent to evaluating their alignment with national climate targets and assessing their potential are summarized subsequent:

- Reduction of GHG emissions by 46% until 2030 compared to 2005, including ETS flexibility,
- achieving climate-neutrality by 2040,
- increasing the share of renewable energy of the domestic total energy consumption to at least 60% until 2030,
- 100% electricity from renewable sources,
- a capacity of 1 GW to produce hydrogen by electrolysis and substituting at least 80% of fossil derived hydrogen with climate neutral H<sub>2</sub> until 2030.

The connection between these targets and the analysis of chosen CCU technologies is discussed in Chapter 3.

## 2.2 CO<sub>2</sub> origins and pathways

Carbon dioxide suitable for CCU production sites can be categorized into four distinct origins. These include fossil-derived CO<sub>2</sub>, usually linked with energy-related emissions; geogenic CO<sub>2</sub>, which originates from mineral raw materials and is commonly seen in processes such as the cement industry; biogenic CO<sub>2</sub>, considered energy-related when it's a by-product of energy production and process-related in the context of biogas production; and atmospheric CO<sub>2</sub>. The categorization is crucial as not all emission sources are appropriate for carbon dioxide removal (CDR). Converting geogenic or fossil CO<sub>2</sub> into products postpones its release but ultimately results in atmospheric accumulation at the end of a products life if it's not kept in an artificial cycle. In contrast, biogenic or atmospheric CO<sub>2</sub> can be reintegrated within the existing natural carbon cycle. In this case product specific storage effects can lead to CDR. [6]

Figure 2 overviews the pathways linked to each carbon dioxide origin.

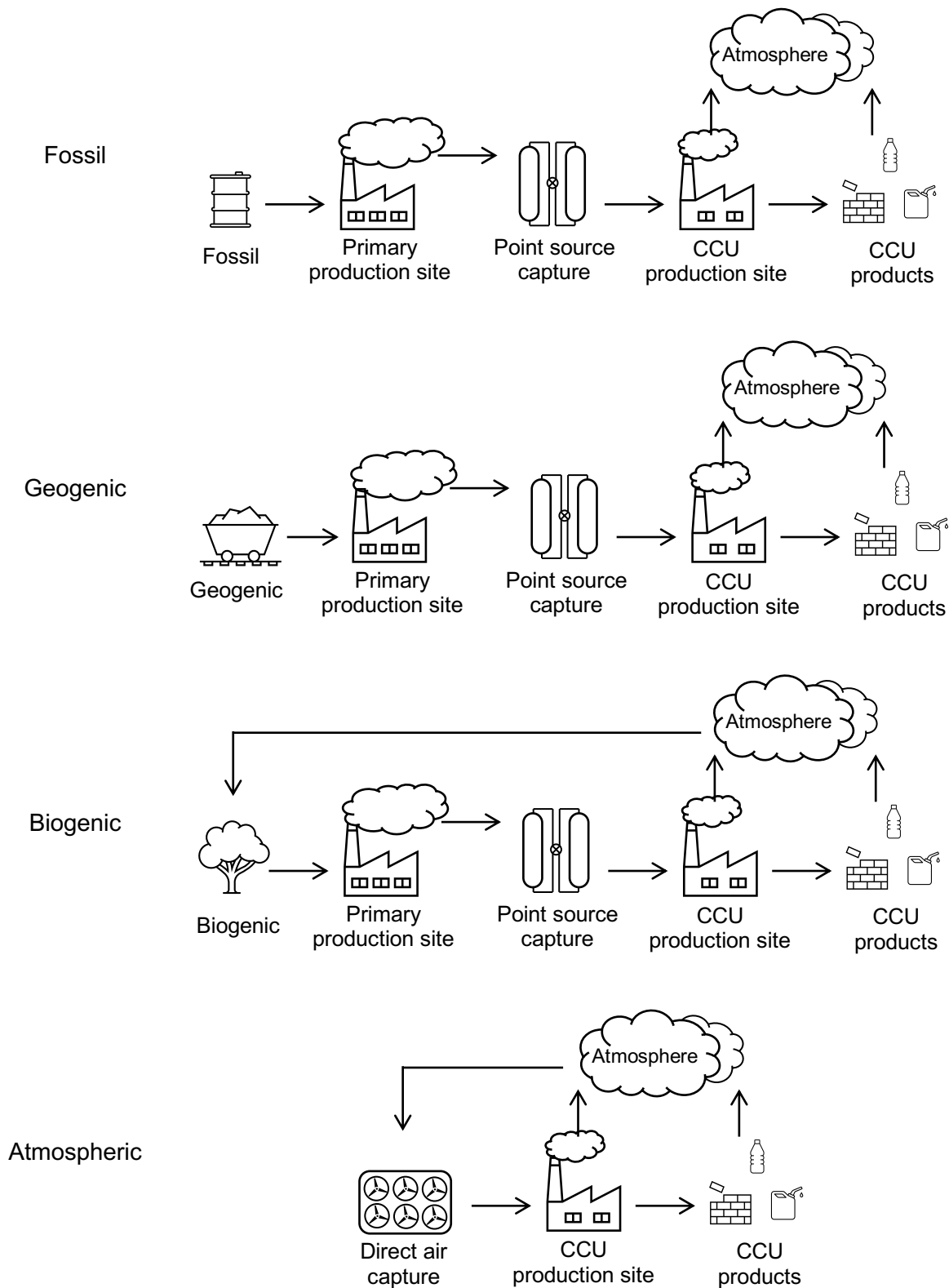


Figure 2: Overview of CO<sub>2</sub> origins and its journey on CCU pathways

Although CCU products derived from fossil or geogenic sources may not accomplish CDR, utilizing this CO<sub>2</sub> as a raw material can still result in net-emission reductions when it substitutes

a conventional product with higher GHG intensity. Under these circumstances, CCU can serve as a transitional technology, particularly in hard-to-defossil industrial processes.

### 2.2.1 Utilizable CO<sub>2</sub> sources in Austria

As a party to the United Nations Framework Convention on Climate Change (UNFCCC), Austria consistently determines and updates its national GHG inventories. The accompanying report presents the annual CO<sub>2</sub>e emissions, which are calculated using global warming potentials (GWP). In 2020, Austria's total national emissions amounted to 73.9 mio. tonnes CO<sub>2</sub>e, with the respective sectoral distribution illustrated in Figure 3. [7]

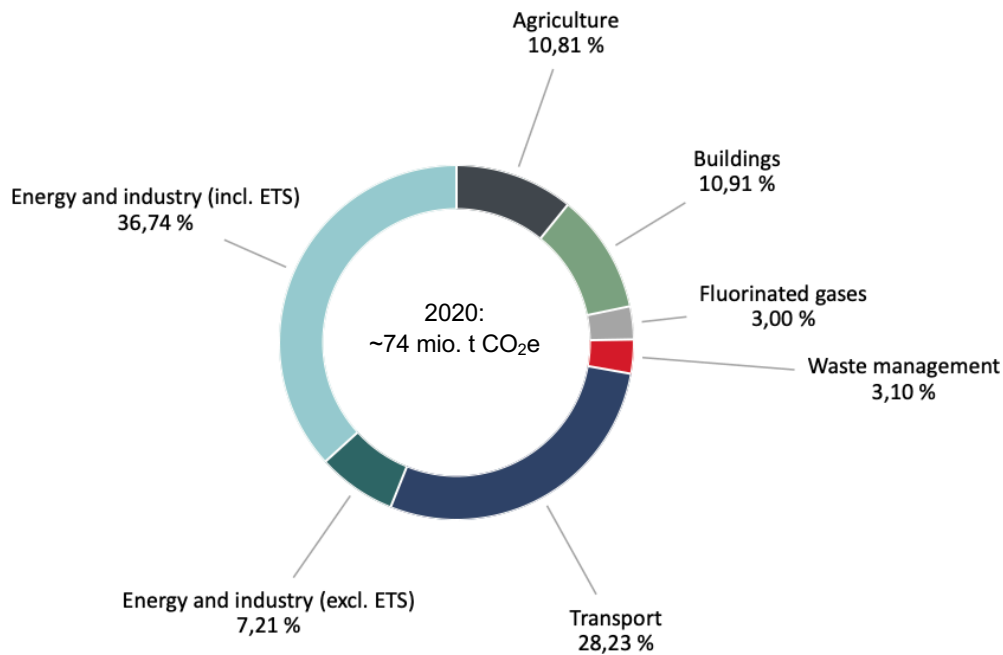


Figure 3: Share of sectors in Austria's total GHG emissions in 2020 [7]

The energy and industrial sectors currently represent the largest contributors to GHG emissions, comprising approximately 44%. These sectors host facilities emitting process exhaust gases from point sources, making them potential suppliers of CO<sub>2</sub> for CCU technologies. A data collection by Hochmeister et al. [8] on ETS registered domestic company sites and non-ETS biogenic emitters, enables a branch-specific categorization and allocation of their emissions. Furthermore, their development was projected using a progressive pathway that, similar to the transition scenario, involves ambitious measures to defossilise energy and industrial systems. Figure 4 shows emission allocations for both target years 2030 and 2040.

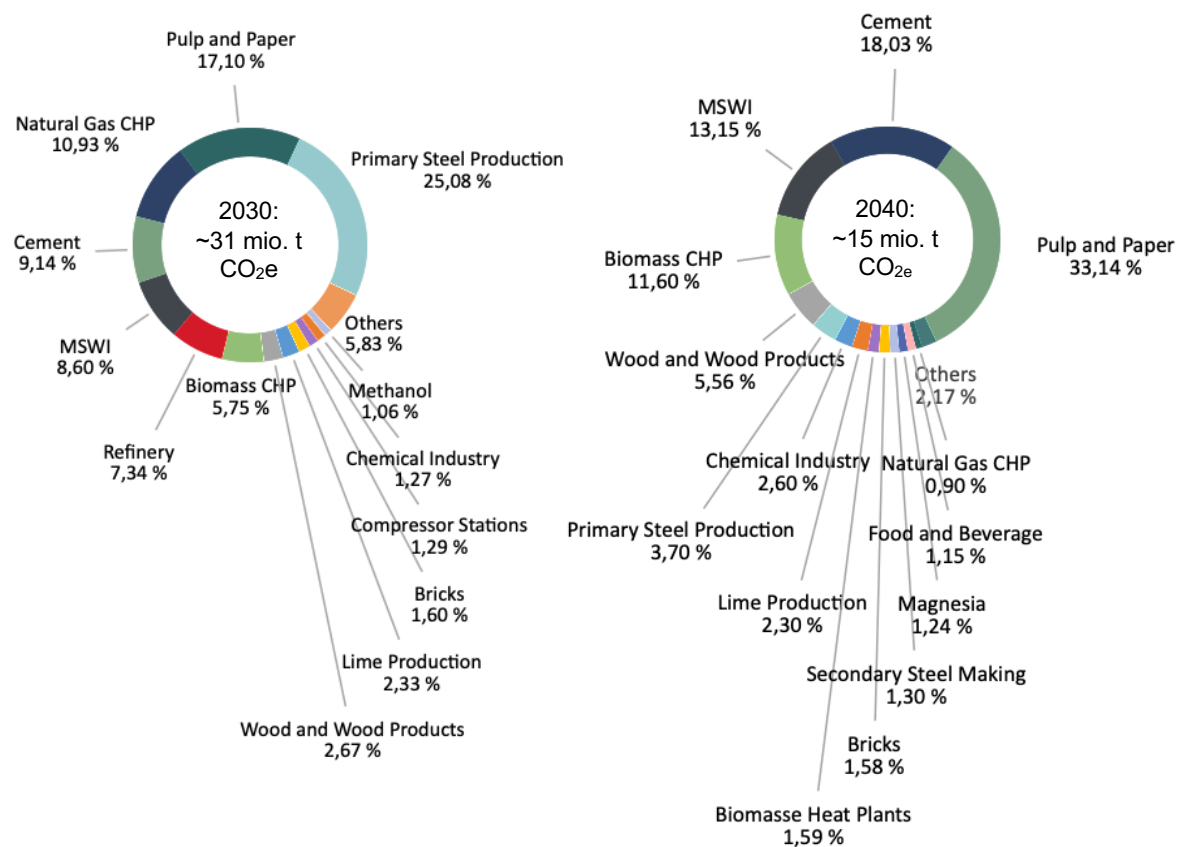


Figure 4: Branch specific allocation of GHG emissions from the energy and industry sectors for the target years 2030 and 2040 (data from Hochmeister et al. [8])

In certain sectors, emissions reduction measures are already in progress, facilitated by the adoption of available alternative technologies. For instance, Voestalpine is implementing the transition from blast furnaces to electric arc furnaces and explores hydrogen-based defossilisation of their steel production [9]. In contrast, industries like cement production continue to face challenges with hard-to-abate emissions resulting from the nature of the manufacturing process.

The emissions data collection by Hochmeister et al. [8] also provides insights into the origin of the emitted CO<sub>2</sub>. As outlined in the previous chapter, this aspect is a key criterion for evaluating whether CCU serves as a reduction measure or accomplishes carbon dioxide removal. Figure 5 illustrates the share of CO<sub>2</sub> sources according to a progressive pathway.

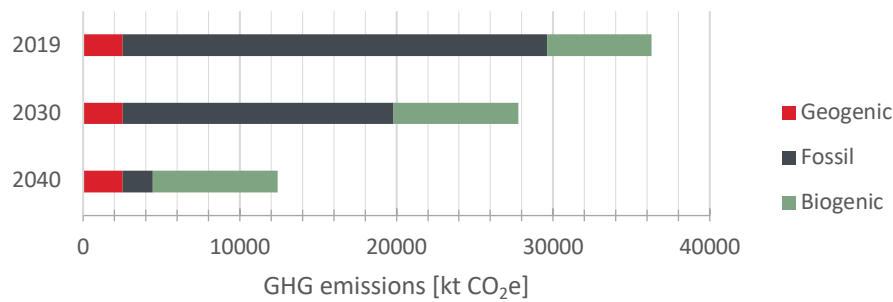


Figure 5: CO<sub>2</sub> origin distribution in 2019 and their progressive development until target years 2030 and 2040 (data from Hochmeister et al. [8])

Detailed allocation of geogenic, fossil, and biogenic CO<sub>2</sub> to their respective branches can be found in Tables 29 and 30. The classification of industrial point sources, taking into account both the origin of CO<sub>2</sub> and the type of industrial sector, significantly influences the choice for suitable CCU technologies. Later in Chapter 5, recommendations for CCU technologies are provided based on the type of point sources.

## 2.3 Carbon capture

The utilization of carbon dioxide as a raw material in CCU technologies requires its separation from the carrier gas and achieving a high purity level for most applications. Carbon capture (CC) encompasses technologies specifically engineered for extracting CO<sub>2</sub> from various gas streams. This CO<sub>2</sub> may derive from industrial emission sources or directly from the atmosphere. The process of capturing CO<sub>2</sub> directly from ambient air is known as direct air capture (DAC), whereas in industrial settings, CO<sub>2</sub> is captured at point sources [10]. Besides these technical CC approaches, natural assimilation methods are also possible, such as mineralization or biomass accumulation (photosynthesis), which actively remove CO<sub>2</sub> from the atmosphere. These natural methods include processes like reforestation, as well as technical-biological approaches, such as the cultivation of algae in bioreactors. [11] However, due to the diversity of industrial processes and the resulting variations in exhaust gas characteristics, there is no one-size-fit-all scenario for technical CO<sub>2</sub> capture. As a result, a wide range of CC systems exists to ensure compatibility with each specific emission source. [12]

Technical processes for CO<sub>2</sub> capture are categorized based on the employed chemical or physical separation methods. This categorization includes absorption, adsorption, membrane technology, cryogenic processes, and gas/solid reactions. Figure 6 provides an overview of potential CC technologies capable of achieving CO<sub>2</sub> capture efficiencies of up to 99%. [11]

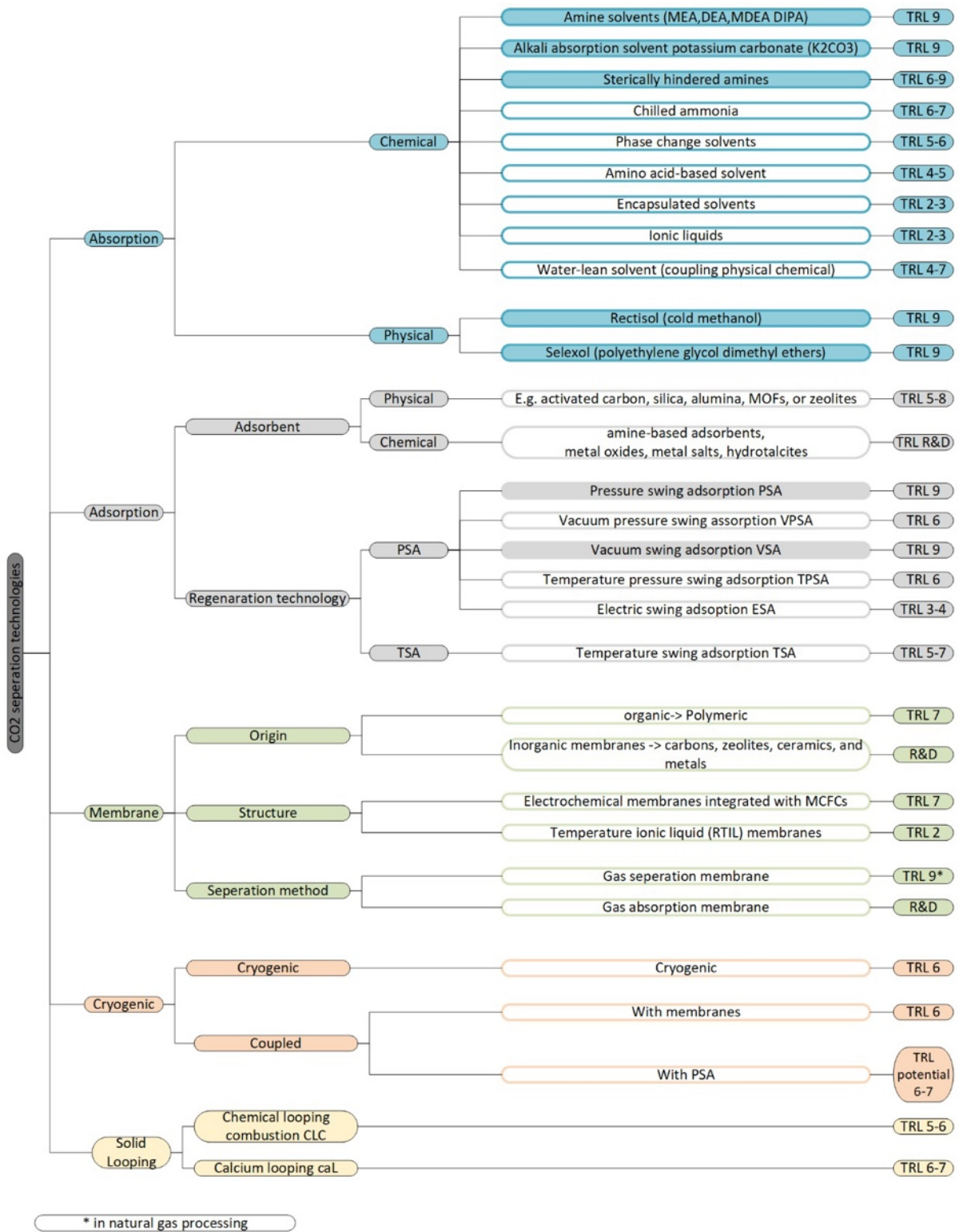


Figure 6: Overview of CO<sub>2</sub> separation technologies and their technological readiness level (TRL) [13]  
 Each CC technology exhibits distinct advantages and limitations. To gain a more comprehensive understanding for this diversity, a selection of these technologies is examined in the following sub-chapters.

### 2.3.1 Chemical absorption

Chemical absorption stands as the most advanced method for CO<sub>2</sub> recovery, especially with monoethanolamine (MEA) as a scrubbing agent [11]. The CO<sub>2</sub> separation is facilitated by its interaction with the solvent, resulting in a new intermediate through either a reversible or irreversible chemical transformation and is carried out in columns, as illustrated in Figure 7 [14].

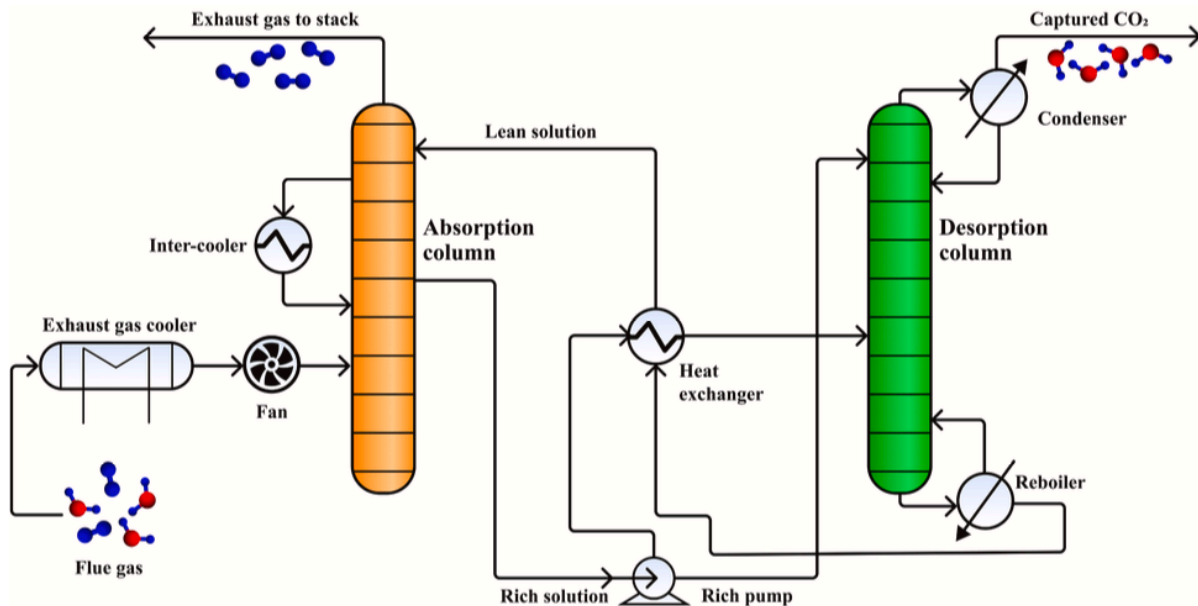


Figure 7: Simplified process flow diagram of CO<sub>2</sub> capture by chemical absorption [14]

Barlow et al. [15] report that this technology is applicable to exhaust gases from industrial sources with CO<sub>2</sub> concentrations below 30%. In the absorption column, the phase transition of CO<sub>2</sub> is achieved through elevated pressure and low temperature, while the regeneration step relies on reduced pressure and higher temperatures. To enhance mass transfer between the gas and CO<sub>2</sub>-selective liquid phases within the columns, build-in packings enlarge the effective surface area for exchange. Owing to the specific process conditions, the MEA scrubber demand a comparatively high energy input of 3.0-4.5 GJ<sub>th</sub> per tonne CO<sub>2</sub> [16], [17]. However, newer amines have been developed for this process, demanding significantly less energy, reported at 2.4 to 2.8 GJ<sub>th</sub> per tonne of CO<sub>2</sub> [15]. Song et al. [18] describe that the required thermal energy of amine-based scrubber accounts for 80% of their total energy demand.

### 2.3.2 Physical adsorption

Physical adsorption relies on Van der Waals forces to attach molecules to the surface of an adsorbent. CO<sub>2</sub>-selective adsorbents, such as activated carbon, silicate, alumina, or zeolites, are commonly employed in porous forms like foams or particle beds [14]. Notably, the binding forces in this process are reversible, allowing a repeating separation of CO<sub>2</sub> from the adsorbent after recovering it from the flue gas. Figure 8 illustrates an adsorption and regeneration system.



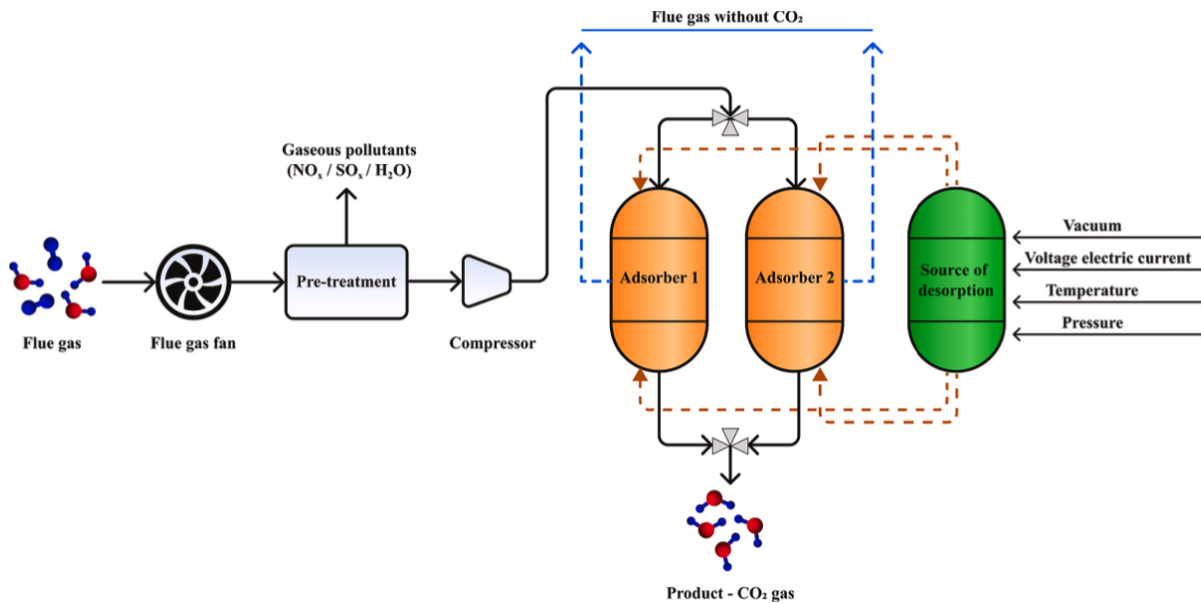


Figure 8: Schematic diagram of a CO<sub>2</sub> adsorption system [14]

The adsorption process takes place within apparatuses filled with CO<sub>2</sub>-selective adsorbents. To enhance cleaning efficiency and safeguard the adsorbents against contamination, the exhaust gas can undergo pre-treatment to eliminate any constituents in advance [19]. Once the adsorbent's surface is saturated, it necessitates regeneration for reusability. An established method for regeneration is pressure swing adsorption (PSA), which involves the following steps: (1) pressurization of the inlet gas, (2) adsorption under high-pressure conditions, (3) depressurization, resulting in the release of CO<sub>2</sub> at the bottom of the desorber, and (4) desorption of CO<sub>2</sub> gas from the adsorbent using purging gas [20]. Adsorption systems can involve several stages, and one of the simplest configurations is the 4-step Skarstrom's [21] cycle, which comprises two parallel connected fixed beds. In this setup, exhaust gas containing 10-15% CO<sub>2</sub> can initially be concentrated to 40-60% in the first stage and then further purified to over 99% in the second stage [22].

Bahamon et al. [23] chose the two step configuration for their energetic evaluation and found that operating at adsorption pressures of 10-20 bar and subsequent regeneration at 1 bar, the electricity requirement ranges between 2.9-4.2 GJ per tonne CO<sub>2</sub> by using zeolite adsorbents. Employing two step vacuum pressure swing adsorption (VPSA), where adsorption occurs under pressure and regeneration by vacuum, can further reduce energy demands to 2.4-3.0 GJ per tonne CO<sub>2</sub>, as reported in literature [24], [25].

### 2.3.3 Membrane separation

Recovering CO<sub>2</sub> from flue gas mixtures using selective membranes represents an innovative approach in separation technology. These membranes function as semipermeable barriers, allowing specific gases to permeate through while other components are retained within the mixture. Due to excellent permeability, selective performance, and ease in pore size regulation, polymers are recognized as highly suitable materials. Concerning the CO<sub>2</sub> transport

mechanism, two main categories of membranes exist: gas separation membranes and gas absorption membranes, as illustrated in Figure 9. [26]

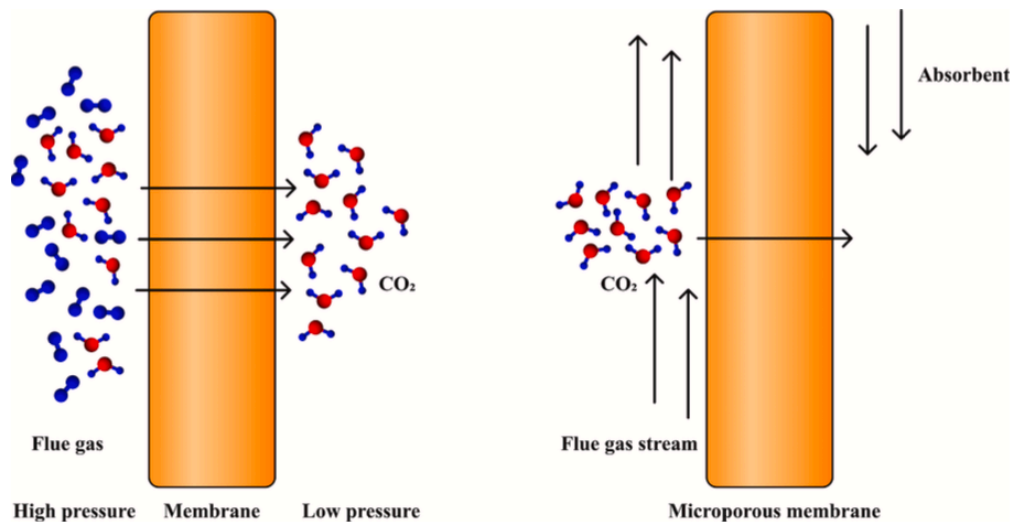


Figure 9: Scheme of membrane separation (on the left) and gas absorption membrane (on the right) [26]

CO<sub>2</sub> separation from the gas mixture occurs when a driving force, such as a pressure difference, temperature gradient, or electric potential, is applied. In gas separation membranes, the transport mechanism relies on dissolution into, and diffusion through the membrane material. The components of a flue gas are separated due to different solubilities and diffusion rates. In the case of gas-absorbing membranes, CO<sub>2</sub> is transferred through the membrane's pores into the liquid absorbent on the other side. The mechanism of this type depends on both the pore size of the membrane and the type of absorbing liquid used. [19] Bounaceur et al. [27] report overall compression energy inputs ranging from 0.5 to 1.0 GJ per tonne CO<sub>2</sub> when employing pressure-driven membrane separation to a gaseous N<sub>2</sub>/CO<sub>2</sub> mixture with CO<sub>2</sub> concentrations starting from 20%.

Membrane separation technology is able to remove CO<sub>2</sub> across a wide concentration range [15]. While it appears to offer energetic advantages, its application is currently limited to natural gas sweetening and biogas upgrading, particularly for CH<sub>4</sub> separation, leading research to actively focus on the separation of additional impurities to enhance its utility in carbon capture systems [28].

### 2.3.4 Cryogenic carbon capture

Cryogenic technologies separate CO<sub>2</sub> from other flue gas components, such as SO<sub>2</sub>, NO<sub>x</sub>, H<sub>2</sub>O, CH<sub>4</sub>, and NH<sub>3</sub>, by harnessing their distinct condensation and desublimation properties [18]. Although this technology is currently under investigation at industrial scales, it is presented in this work due to its potential to achieve remarkable CO<sub>2</sub> recovery rates of up to 99.99% and CO<sub>2</sub> purity levels of up to 99.99% from flue gas point sources [29]. Figure 10 provides a simplified process flow diagram illustrating a cryogenic separation system.

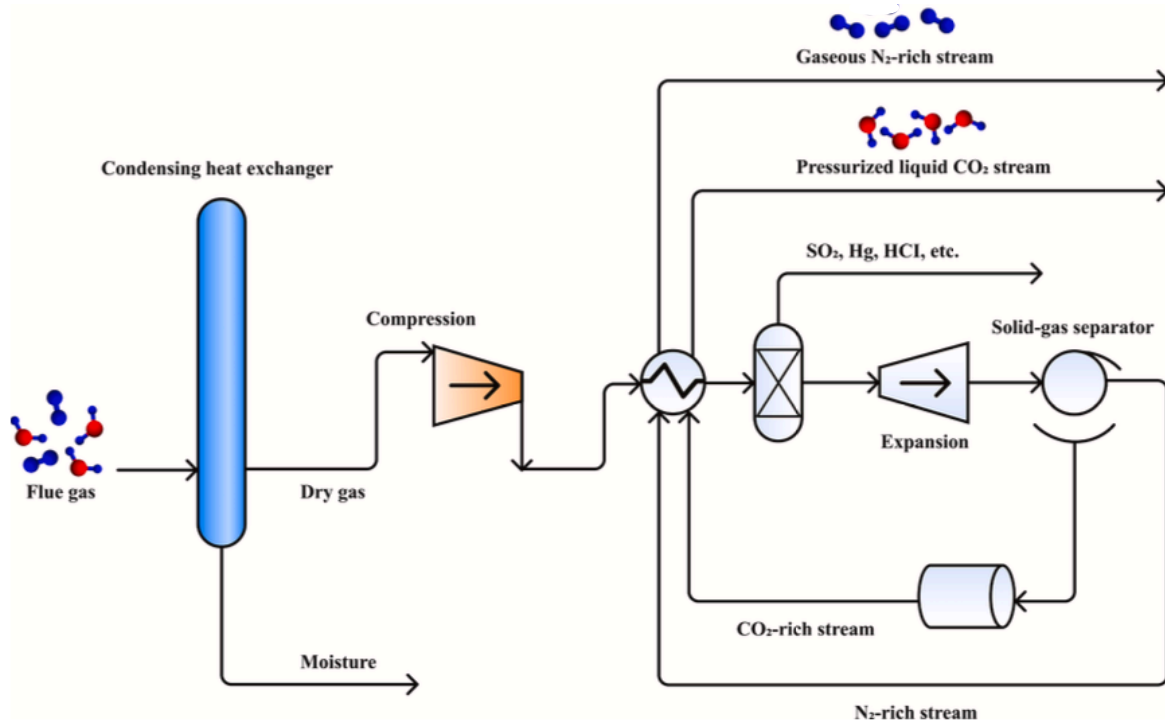


Figure 10: Simplified process flow diagram of cryogenic carbon capture system [30]

Carbon dioxide is forced to phase changes in numerous stages of compressing the flue gas mixture and subsequently cooling it to the required temperature at high pressure. The separated  $\text{CO}_2$  results in a liquid or solid form, often as dry ice, which facilitates its ease of transport to further utilization or storage capabilities. Notably, this separation process requires no additional chemical reagents. [13] The electrical energy consumption typically falls within the range of 1.0 to 3.6 GJ per tonne  $\text{CO}_2$  [31], [32].

Cryogenic carbon capture is indeed capable of extracting  $\text{CO}_2$  in a very pure form, but so far, economical operation is only feasible for gaseous streams with high  $\text{CO}_2$  concentrations above 50% [33], [15]. Therefore, combining cryogenic methods with other CC technologies is recommended [34]. For example, Barlow et al. [15] report on adsorption assisted cryogenic systems. In these systems,  $\text{CO}_2$  concentrations  $\leq 15\%$  are initially concentrated from an exhaust gas stream using physical adsorption with PSA, after which the concentrated  $\text{CO}_2$  is introduced into the cryogenic process.

### 2.3.5 Solid looping

In solid looping technologies, metal oxides circulate between two reactors, both designed as fluidised beds. Chemical looping systems involve the alternate oxidation and reduction of these carrier materials to transport  $\text{O}_2$ , whereas in the calcium looping process the carrier agent  $\text{CaO}$  is carbonated by  $\text{CO}_2$  and subsequently regenerated, as illustrated in Figure 11. [35]

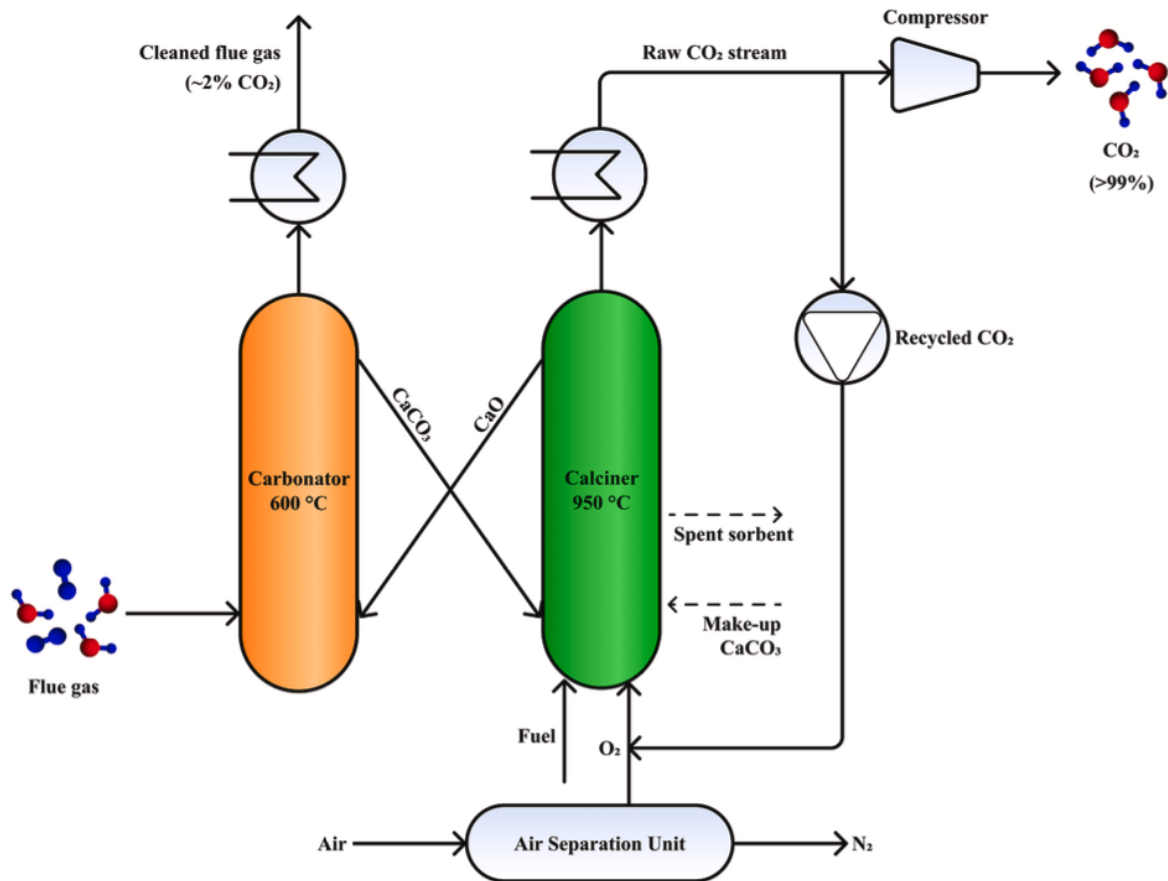


Figure 11: Schematic diagram of CO<sub>2</sub> capture from flue gas by calcium looping [13]

The calcium looping process operates on the reversible reaction between calcium oxide and carbon dioxide. In the first reactor, solid carrier particles capture CO<sub>2</sub> from the flue gas through carbonation. Once calcium carbonate is formed, it is transferred to the second reactor for calcination, where it decomposes back into CaO and CO<sub>2</sub>. To achieve a high purity CO<sub>2</sub> stream, the calciner stage employs oxy-combustion, providing the necessary heat for sorbent regeneration. [35] Hilz et al. [36] explored this technology at pilot scales, noting thermal energy requirements ranging between 6 and 10 MJ per kg of CO<sub>2</sub> captured.

## 2.4 CO<sub>2</sub> utilization pathways

Recovered carbon dioxide from various sources can be processed in numerous ways. These methods broadly fall into two categories: direct applications, such as using it as a working fluid (e.g., in enhanced oil recovery) or in the food and beverage industry, and processes that involve a conversion of CO<sub>2</sub> [36]. CCU technologies offer a wide range of alternative production methods by chemical alternation. The resulting products aid to substitute conventional ones, thereby contributing to the reduction of emissions and the conservation of natural resources. Possible utilization pathways of CCU technologies that employ CO<sub>2</sub> as a key component are summarized in Figure 12.

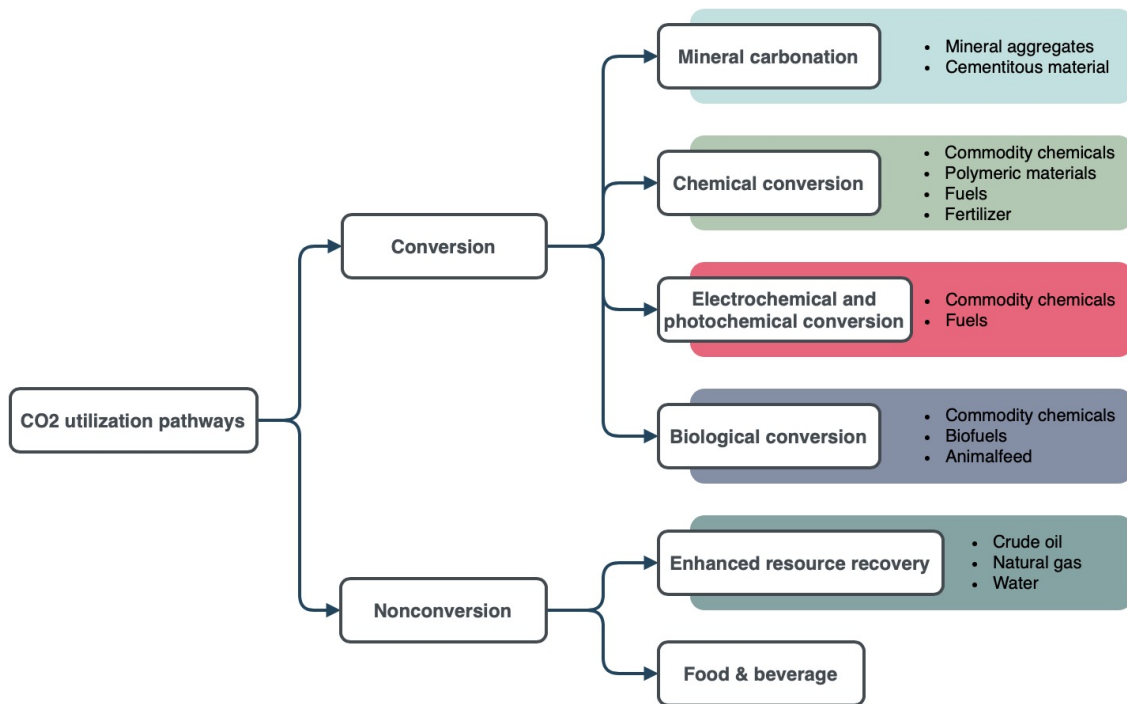
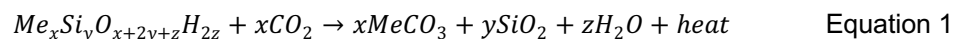


Figure 12: Overview of CO<sub>2</sub> utilization pathways in CCU technologies and product examples based on literature [36], [37]

Tracing CO<sub>2</sub> along its journey through the illustrated pathways reveals a range of products that can serve as potential carbon sinks. The following subchapters will detail the fundamental mechanisms associated with the most maturity conversion techniques. Enhanced oil recovery falls outside the scope of this study.

### 2.4.1 Mineral carbonation

Technologies of the mineral carbonation route exploit the naturally occurring reaction between metal (Me) oxides or silicates and carbon dioxide into thermodynamically stable carbonates, according to the following reaction family [38].



In nature, calcium and magnesium usually exist in silicates such as serpentine, olivine and wollastonite but utilizing these materials is not cost-effective in many cases of ex-situ carbonation because of slow reaction kinetics and the required large-scale mining operation [39], [40]. Consequently, the use of secondary raw materials, such as alkaline solid wastes from industrial processes like steel slag, fly ash or recycled concrete aggregates, is increasing due to their advantages: faster reaction rates, lower energy input, higher carbonate conversion efficiency compared to natural solids and the potential for implementing a circular economy [34].

## 2.4.2 Chemical conversion

The chemical conversion of CO<sub>2</sub> within CCU technologies involves methods like hydrogenation or nitration, usually catalyzed to enhance efficiency. In these conversion routes, CO<sub>2</sub> can be transformed into products such as synthetic natural gas or more reactive carbon monoxide, the latter being a versatile intermediate for further conversion into fuels or commodity chemicals. Figure 13 provides a comprehensive overview of chemical utilization pathways. [37]

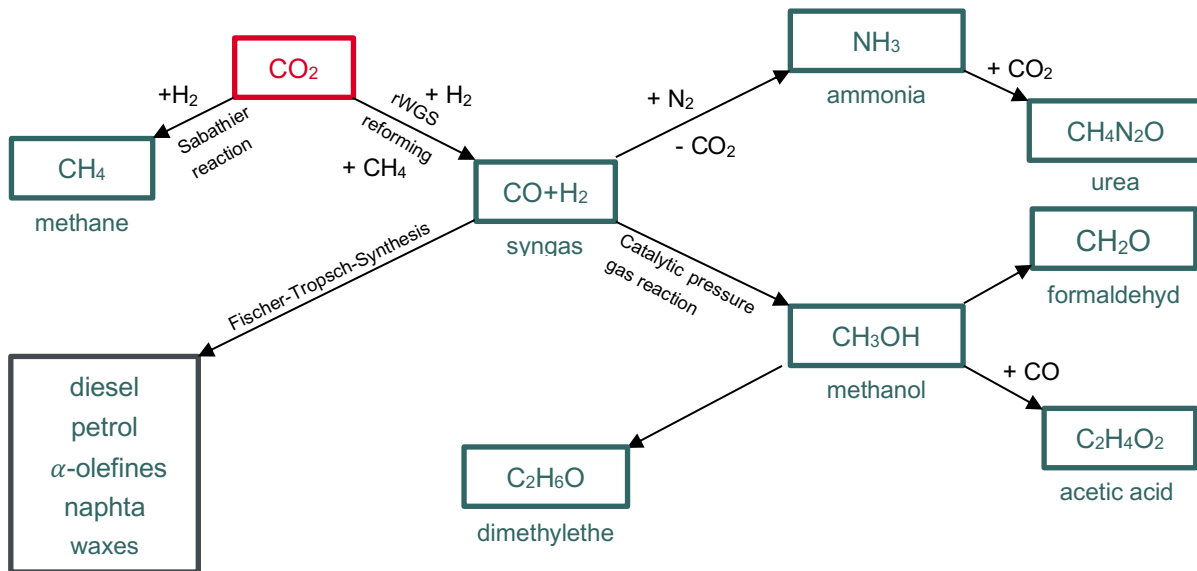


Figure 13: Overview of chemical CO<sub>2</sub> utilization pathways in CCU technologies [37]

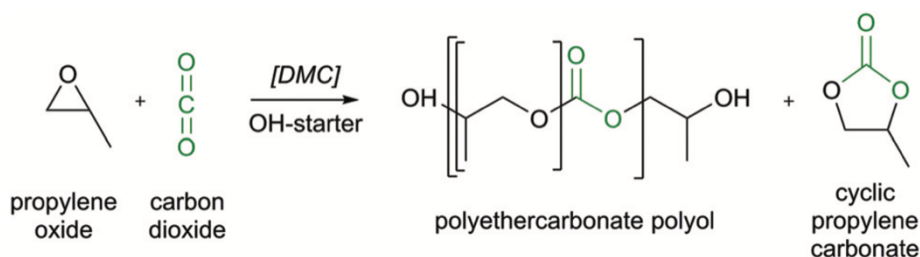
Hydrogen is a crucial reactant in many chemical conversion processes. Achieving a net reduction in CO<sub>2</sub> emissions through CCU requires hydrogen production to be conducted in a low-emissions manner. This objective aligns with the Austrian climate target strategy, as mentioned earlier, and can be accomplished by combining renewable energy sources with electrolysis processes. [42]

Conceivable CCU technologies involving chemical conversions of CO<sub>2</sub> are discussed in Chapter 4. The fundamental reactions associated with these technologies, along with reaction enthalpies under standard conditions (25°C and 1 atm) showing heat demand or release, are listed in Table 1.

Table 1: Fundamental reactions of chemical CO<sub>2</sub> conversion methods (enthalpies calculated based on Lange's Handbook of Chemistry [43])

Conversion method	Chemical reaction		Ref.
Sabatier reaction	$CO_2 + 4H_2 \rightleftharpoons CH_4 + 2H_2O$	$\Delta H_R^0 = -165 \text{ kJ/mol}$	[44]
rWGS reaction	$CO_2 + H_2 \rightleftharpoons CO + H_2O$	$\Delta H_R^0 = 41.2 \text{ kJ/mol}$	[44]
Dry reforming	$CH_4 + CO_2 \rightleftharpoons 2H_2 + 2CO$	$\Delta H_R^0 = 247 \text{ kJ/mol}$	[45]
Fischer-Tropsch-synthesis	$nCO_2 + (3n + 1)H_2 \rightarrow C_nH_{2n+2} + 2nH_2O$ $nCO + (2n + 1)H_2 \rightarrow C_nH_{n+2} + nH_2O$		[45]
Urea synthesis	$2NH_3 + CO_2 \rightleftharpoons H_2N - COONH_4$	$\Delta H_R^0 = -88.4 \text{ kJ/mol}$	[46]
	$H_2N - COONH_4 \rightleftharpoons NH_4CNO + H_2O$	$\Delta H_R^0 = 78.0 \text{ kJ/mol}$	
Hydrogenation (FA)	$CO_2 + H_2 \rightleftharpoons HCOOH$	$\Delta H_R^0 = -31.5 \text{ kJ/mol}$	[45]
Hydrogenation (MeOH)	$CO_2 + 3H_2 \rightleftharpoons CH_3OH + H_2O$	$\Delta H_R^0 = -131 \text{ kJ/mol}$	[45]
DMM reduction	$3CO_2 + 8H_2 \rightarrow CO_2 + 2CH_3OH + 2H_2 \rightarrow DMM$		[45]

Also the copolymerization of CO<sub>2</sub> and epoxides for the synthesis of polyethercarbonate polyols represents a potential conversion method within CCU technologies. Assen and Bardow [47] describe the reaction mechanism according to Figure 14.

Figure 14: Polymerization reaction of propylene oxide and CO<sub>2</sub> to polyethercarbonate polyols [47]

Some of the reaction mechanisms discussed are already in use within industrial applications, while others are currently undergoing trials. The development stage of CCU technologies employing these mechanisms, as well as possible reaction conditions and involved catalysts are reviewed in Chapter 4.

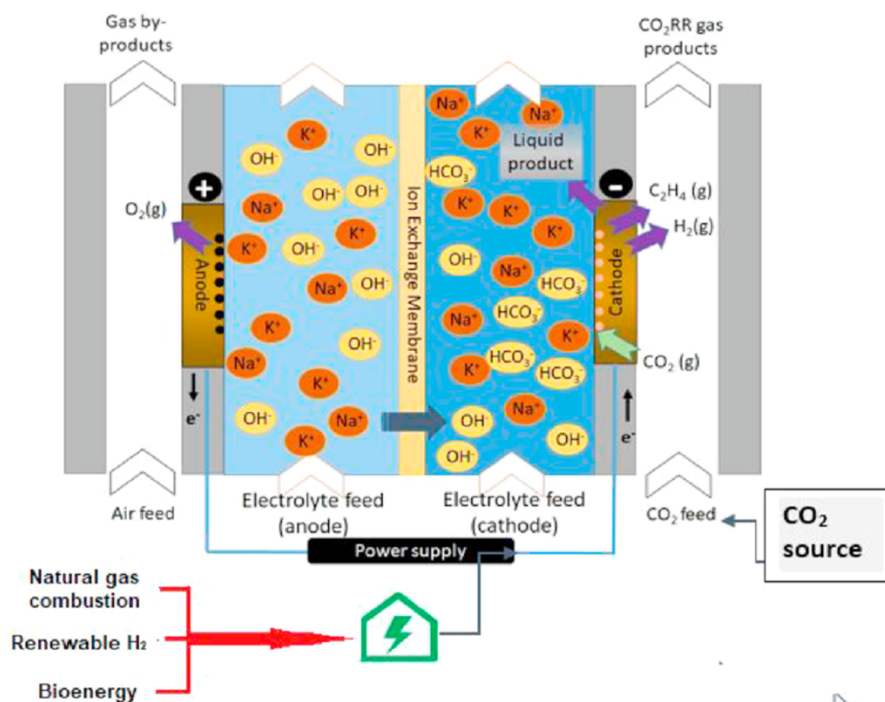
### 2.4.3 Electrochemical conversion

The electrochemical reduction of carbon dioxide, referred to as CO<sub>2</sub>RR, can be effectively carried out in an electrolysis cell. Employing specific equilibrium potentials ( $E^0$ ), enables the reaction to various products, as detailed in Table 2.

Table 2: CO<sub>2</sub> reduction pathways and their equilibrium potentials at ambient conditions [48]

Electrochemical reaction	E <sup>0</sup> [V vs. RHE]
$CO_2 + 2H^+ + 2e^- \rightarrow CO + H_2O$	-0.10
$CO_2 + 2H^+ + 2e^- \rightarrow HCOOH$	-0.12
$CO_2 + 6H^+ + 6e^- \rightarrow CH_3OH + H_2O$	0.03
$2CO_2 + 8H^+ + 8e^- \rightarrow CH_3COOH + 3H_2O$	0.11
$2CO_2 + 10H^+ + 10e^- \rightarrow CH_3CHO + 3H_2O$	0.06
$2CO_2 + 12H^+ + 12e^- \rightarrow C_2H_5OH + 3H_2O$	0.09
$2CO_2 + 12H^+ + 12e^- \rightarrow C_2H_4 + 4H_2O$	0.08
$2CO_2 + 14H^+ + 14e^- \rightarrow C_2H_6 + 4H_2O$	0.14
$2CO_2 + 16H^+ + 16e^- \rightarrow C_2H_5COH + 5H_2O$	0.09
$3CO_2 + 18H^+ + 18e^- \rightarrow C_2H_5COH + 5H_2$	0.10

These electrochemical reactions encompass multiple electron transfer steps. Influential factors, including the electrolyte composition, local conditions at the electrolyte-catalyst interface, and the method of CO<sub>2</sub> transport to the catalyst surface, play significant roles in the formation and utilization of reaction intermediates. As a result, a variety of electrochemical cell designs, engineered for CO<sub>2</sub>RR, have been conceptualized. [49] As an example the flow cell is illustrated in Figure 15, to demonstrate the conversion mechanism for ethylene.

Figure 15: Electrolytic flow cell for the reduction of CO<sub>2</sub> to ethylene [50]

The electrolytic flow cell is equipped with two external gas channels, one of which is flowed through by air and the other by CO<sub>2</sub> gas. By applying electrical voltage, oxygen is removed from the solvent at the anode into the air channel. The remaining cations pass through the ion exchange membrane to the cathode and are available for reaction with CO<sub>2</sub> to form ethylene. [50]



## 2.4.4 Biological conversion

Autotrophic microorganisms can utilize CO<sub>2</sub> as a carbon source to build biomass and produce industrially relevant compounds. The incorporation of CO<sub>2</sub> to form organic compounds is known as carbon fixation, and six major metabolic pathways have been identified for this process. [51] Table 3 presents these pathways along with natural occurrences and key enzymes.

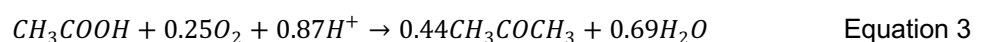
Table 3: Metabolic processes for CO<sub>2</sub>-fixation [51], [52]

Metabolic process	Occurrence	Key enzymes
Calvin-Benson cycle	Plants, algae, cyanobacteria, most aerobic or facultatively anaerobic eubacteria	Ribulose- 1,5-bisphosphate carboxylase/oxygenase (RuBisCO)
Wood-Ljungdahl pathway	Methanogens and sulfate-reducing euryarchaeota, acetogenic firmicutes, etc.	Acetyl-CoA-Synthase/CO-Dehydrogenase
Reductive tricarboxylic acid cycle	Chlorobiales, proteobacteria	2-Oxogluteratesynthase Isocitrate Dehydrogenase Pyruvate synthase
3-hydroxypropionate/ 4-hydroxybutyrate cycle	Aerobic sulfolobales	Acetyl-CoA/Propionyl-CoA carboxylase
Decarboxylate/ 4-hydroxybutyrate cycle	Anaerobic thermoproteales	4-Hydroxybutyryl-CoA-Dehydratase
3-hydroxypropionate bicycle	Chloroflexaceae	Malonyl-CoA-Reduktase, Propionyl-CoA-Synthase, Malyl-CoA-Lyase

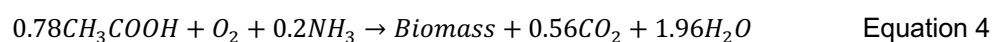
Five of these six pathways involve the mechanism of carboxylation, for instance, through modified photosynthesis. The Wood-Ljungdahl pathway, however, uses the mechanism of reduction. This pathway is recognized as more energy-efficient and can occur in both anaerobic and aerobic gas fermentation [53], [51]. Equation 2 demonstrates anaerobic gas fermentation using H<sub>2</sub> as an energy source to produce acetic acid while simultaneously supporting biomass growth [54]:



This reaction is implemented in the first reactor of the technology described in Chapter 4.9. The intermediate product, acetic acid, is then converted into acetone using aerobic thermophilic bacteria, as depicted in Equation 3 [54]:



In parallel to this conversion, biomass production occurs, represented by Equation 4 [54]:



Other reaction mechanisms related to biological CO<sub>2</sub> conversion are not further explored here, as they fall outside the scope of this thesis.

## 2.5 Lifetime of CCU products

After the successful production and subsequent use of a CCU product, the captured CO<sub>2</sub> is eventually released back into the atmosphere. Accurately assessing the end-of-life emissions of CCU products necessitates consideration of their respective carbon sequestration periods. For instance, CO<sub>2</sub> used in fuel production is typically re-emitted within a few days, whereas carbonates can sequester it for much longer periods, potentially keeping it out of the atmosphere for millennia [37]. Table 4 presents a summary of various product categories along with their estimated average CO<sub>2</sub> storage durations.

Table 4: CCU product categories and their average lifetime

Product category	Product example	Lifetime [years]	Ref. [-]
Direct use	Agricultural greenhouse gas	0-0.5	[55]
Fuels and chemicals	Methanol, methane, DMM	0.5	[55], [56]
Stable chemicals	Polyethylene, polypropylene, polyols	50	[55], [56]
Construction materials	Mineral carbonates, carbonated blocks	>100	[57], [58]

Due to the long-term storage capability of carbonated products, their production can be classified as CDR if the converted carbon dioxide originates from biological or atmospheric sources, and its amount exceeds the GHG emissions associated with the CCU process.

## 2.6 CCU emissions

Quantifying GHG emissions associated to a CCU product enables to determine whether the implementation of a CCU technology results in CDR or serves as an emission reduction measure. Therefore, a CO<sub>2</sub> balance is carried out. According to De Kleijne et al. [59] the GHG emission factor of the CCU product  $E_{CCU}$  (in kg CO<sub>2</sub>e/kg CO<sub>2</sub> utilized) is calculated by Equation 5,

$$E_{CCU} = -E_{utilized} + E_{capture\ process} + E_{conversion} + E_{released} * v_{storage} + E_{other} \quad \text{Equation 5}$$

where  $E_{utilized}$  is CO<sub>2</sub> utilized in production of the CCU product,  $E_{capture\ process}$  are GHG emissions associated with the CO<sub>2</sub> recovery process,  $E_{conversion}$  GHG emissions caused by conversion processes of CO<sub>2</sub> into the end product and  $E_{released}$  GHG emissions of utilized CO<sub>2</sub> into the atmosphere at the end of life of the product.  $E_{other}$  stands for other GHG emissions associated with the CCU product, for example if fossil feedstock is added in conversion processes.

Equation 1 demonstrates that  $E_{CCU}$  can attain a negative value if the amount of CO<sub>2</sub> utilized exceeds the total amount released. However, when interpreting  $E_{CCU}$  values, it is crucial to consider the origin of the carbon dioxide, as mentioned earlier. The following Table 5 presents examples for three emission cases to demonstrate the interpretation of the resulting values in connection with the CO<sub>2</sub> origin.

Table 5: Interpretation of  $E_{CCU}$  values depending on CO<sub>2</sub> origin

Emissions case	Biogenic or atmospheric CO <sub>2</sub>	Fossil or geogenic CO <sub>2</sub>
Case 1: negative CCU emissions $E_{CCU} = -0.8 \frac{kg CO_2e}{kg CO_2utilized}$	80% CO <sub>2</sub> removal 20% CO <sub>2</sub> circulation	80% CO <sub>2</sub> reduction 20% CO <sub>2</sub> postponed
Case 2: zero CCU emissions $E_{CCU} = 0 \frac{kg CO_2e}{kg CO_2utilized}$	100% CO <sub>2</sub> circulation	100% CO <sub>2</sub> postponed
Case 3: positive CCU emissions $E_{CCU} = 0.1 \frac{kg CO_2e}{kg CO_2utilized}$	100% CO <sub>2</sub> circulation 10% CO <sub>2</sub> accumulation	100% CO <sub>2</sub> postponed 10% CO <sub>2</sub> accumulation

For carbon dioxide derived from fossil or geogenic origins, a high utilization rate may lead to negative emission values. Yet, these values do not completely offset the emissions generated by the other stages of the CCU process. Although the release of CO<sub>2</sub> of fossil origin from primary processes into the atmosphere is prevented, the CCU process itself still results in GHG emissions. The use of fossil or geogenic CO<sub>2</sub> is considered as CDR only if the limit value of  $E_{CCU}$  falls below  $-1 \frac{kg CO_2e}{kg CO_2utilized}$ . Negative values exceeding this threshold typically indicate an atmospheric accumulation, as illustrated in Table 5 (emissions case 1), where they are categorized as postponed emissions from the upstream process. In this scenario, a negative emission value represents a relative reduction in GHG emissions compared to conventional pathways, thus qualifying as an emissions reduction measure. In contrast, for CO<sub>2</sub> from biogenic or atmospheric origins, a negative  $E_{CCU}$  value truly signifies CDR, since both the utilized and released CO<sub>2</sub> are part of the existing carbon cycle.

In the second scenario, where total emissions amount to zero, the quantity of carbon dioxide utilized is equivalent to the GHG released by the CCU process. While biogenic or atmospheric CO<sub>2</sub> is circulated and additional atmospheric accumulation is prevented, CO<sub>2</sub> from fossil or geogenic origins increases additionally in the atmosphere. Therefore, emissions from a primary process cannot be regarded as reduced; instead, their eventual release should be viewed as merely postponed.

Positive CCU emissions are interpreted in accordance with case 3, as outlined in Table 5. In dependence to the origin of the utilized CO<sub>2</sub>, it is either partially recycled in the carbon cycle or postponed (as described in case 2). Any portion that exceeds zero is released into the atmosphere, contributing to cumulative emissions.

### 3 Climate target compatibility of CCU technologies

In Austria, CCU technologies are defined as potential if they align with the established climate targets for 2030 or 2040. Therefore, commercial availability in time, as well as a sufficient reduction of CO<sub>2</sub> emissions is required. While the majority status can be obtained from publications on current projects, emissions must be derived from a life cycle assessment (LCA) that details the GWP of the resulting products. To ensure comparability among various CCU technologies, these studies need to be harmonized. This section includes methods for such harmonization and for classifying the availability of the specific technologies. It concludes with the definition of limits to Austrian climate targets compatibility of CCU technologies.

#### 3.1 Harmonization of LCAs

Life cycle assessment is a tool used to evaluate the environmental impacts associated with products and is often employed in the development of new technologies. Typically, these analyses are conducted for existing products based on data from industrial-scale operations. However, applying LCAs to a wide range of CCU technologies, which are currently in development at laboratory or pilot scales, presents challenges due to limited data availability. [60] Nonetheless, if the gathered data is harmonized, LCA results can effectively facilitate the comparison of different technologies. De Kleijne et al. [59] utilized this approach to assess the Paris Agreement compatibility of various CCU technologies. In this work, harmonization is specifically applied to the Austrian context, aiming to evaluate alignment with national climate targets and to explore the potential of CCU within Austria, as detailed later.

The study results from LCAs of CCU technologies are harmonized considering several factors: the functional unit, system boundaries, electricity mix, hydrogen mix, heat supply, CO<sub>2</sub> recovery, multifunctionality, and storage effects, as will be discussed in the following sections.

##### 3.1.1 Functional unit

In most LCA studies, the functional unit relates to the manufactured product, such as kg or MJ product. As all CCU technologies use CO<sub>2</sub> as an input variable, the gathered data is converted to 1 kg CO<sub>2</sub> utilized, thus the functional unit is standardized across various studies.

##### 3.1.2 System boundaries

System boundaries for both CCU products and substituted products are set using a cradle-to-grave approach. This is necessary to determine the accumulation of carbon dioxide in the atmosphere after a products life cycle. Cradle-to-gate data is harmonized by adding end-of-life (EOL) emissions, as proposed by Fernández-Dacosta et al. [61]. Emissions from production infrastructure and transport are taken from the respective LCAs, as they have negligible impact on the overall GHG intensity [62], [63]. Table 6 lists cradle-to-gate emissions of conventional products, which could be substituted by CCU alternatives.

Table 6: Cradle-to-gate emissions of conventional products

Conventional product	Cradle-to-gate emissions		Ref.
Portland cement (PC)	0.76	kg CO <sub>2</sub> e/kg PC	[64]
PC-based concrete blocks	0.12	kg CO <sub>2</sub> e/kg block	[64], [65]
Natural gas (NG)	0.52	kg CO <sub>2</sub> e/kg NG	[66]
Methanol from syngas	0.82	kg CO <sub>2</sub> e/kg MeOH	[42]
Diesel	0.88	kg CO <sub>2</sub> e/MJ diesel	[67]
Urea from natural gas	1.0	kg CO <sub>2</sub> e/kg urea	[68]
Ethylene from steam cracking	1.56	kg CO <sub>2</sub> e/kg ethylene	[69], [70]
DMM based on methanol and formaldehyde	0.41	kg CO <sub>2</sub> e/kg DMM	[66], [71]
Polyether polyols	4.22	kg CO <sub>2</sub> e/kg polyol	[72]
Acetone	2.39	kg CO <sub>2</sub> e/kg acetone	[54]

To compare these emissions with those from CCU products, a 1:1 replacement is assumed, and similar EOL emissions are considered. These EOL emissions can be obtained from the re-emissions of the CO<sub>2</sub> input used in the CCU product, under consideration of storage effects. By referring to the standardized functional unit and conversion to cradle-to-grave system boundaries, comparability between CCU and conventional products is enhanced.

### 3.1.3 Electricity mix

Energy-related emissions, particularly those resulting from the purchase of electricity for capture and conversion processes, as well as hydrogen production via electrolysis, are directly linked to the electricity mix selected in an LCA study. As outlined in Section 2.1, the entirely supply of electricity from renewable sources by 2030 is one of Austria's climate targets. Consequently, this work assumes a renewable electricity mix as detailed in Table 7.

Table 7: Assumed Austrian renewable electricity mix by 2030 and emission factors

Electricity source	Distribution	Emission factors [73]
	[%]	[gCO <sub>2</sub> e/kWh]
Hydropower (run-of-river)	41	5
Hydropower (pumped storage)	21	47
Photovoltaics	16	40
Wind power	22	8

GHG emissions associated with renewable energy facilities originate from indirect emissions due to the supply of necessary infrastructure and raw materials during the construction phase. The electricity mix specified here amounts to 20 gCO<sub>2</sub>e/kWh and is this harmonization step.

### 3.1.4 Hydrogen mix

Many of the CO<sub>2</sub> utilization pathways currently under investigation require hydrogen as an additional feedstock. The defossilization of hydrogen production is another Austrian climate target, as mentioned earlier. While conventional production via steam reforming emits

16.1 kg CO<sub>2</sub>e/kg H<sub>2</sub> [74], the projected GHG intensity is expected to decrease to 4.02 kg CO<sub>2</sub>e/kg H<sub>2</sub> in 2030, and further to 1.00 kg CO<sub>2</sub>e/kg H<sub>2</sub> in 2040, in line with the national energy and climate plans and the assumed electricity mix, detailed in the previous chapter.

### 3.1.5 Heat supply

The heat requirements for endothermic conversion processes in certain CCU technologies vary across LCA studies, resulting in different approaches for supply. For example, Hoppe et al. [75] propose that in some systems, waste heat can fulfill the thermal energy needs, with natural gas serving as a backup for any additional demand. Conversely, Di Maria et al. [65] suggest using diesel to generate the required heat. To maintain consistency in this harmonization step, the assumption is made that efforts will be directed towards de-fossilizing heat production, and synthetic natural gas will be employed to supply heat for CCU technologies as needed. Based on stoichiometric considerations and the combustion enthalpy of methane (-890.6 kJ/mol CH<sub>4</sub> [76]), an emission factor of 0.18 kg CO<sub>2</sub>e/kWh is calculated for thermal energy requirements.

### 3.1.6 CO<sub>2</sub> recovery

Numerous carbon capture technologies exist for recovering CO<sub>2</sub> from specific sources or directly from the atmosphere, resulting in a range of variations in available LCAs. To enable a more comparable assessment of the CO<sub>2</sub> utilization units, two possible capture methods are considered in this section. The first is amine based chemical absorption, a mature technique and thus implementable in CCU technologies by 2030. The second method, combined physical adsorption (VPSA) and cryogenic carbon capture, is assumed for CCU technologies that are expected to become commercially available by 2040. It should be noted that the technologies detailed in Chapter 4 are not exclusively associated with either of these recovery methods. The aim of this harmonization is to standardize the energy requirements and resulting emissions for the capture units. Table 8 lists the selected CO<sub>2</sub> recovery technologies along with their average energy consumption.

Table 8: Selected CO<sub>2</sub> capture technologies and their average energy demands

Capture technology	Thermal energy demand [kWh/t CO <sub>2</sub> captured]	Electricity demand [kWh/t CO <sub>2</sub> captured]
Chemical absorption	722.2	144.4
Physical adsorption & cryogenic	-	1013.9

Given the variability in energy requirements for carbon capture depending on the specific characteristics of the exhaust gas from the primary process, the values here should be viewed as approximate estimates.

### 3.1.7 Multifunctionality

Facilities with CCU are multifunctional when a primary production process (e.g. steel or cement production) is extended by a secondary CCU process. Therefore, all CCU-systems can be considered as multifunctional, with the expectation of CCU in combination with DAC. These systems can be considered as independent CCU plants when coupled with manufacturing processes. However, in a CO<sub>2</sub> balance, GHG emissions must be divided between primary and CCU products. Utilized carbon dioxide is attributed to the CCU product, which can substitute a conventional product. It is important to understand, that the CO<sub>2</sub> balance of the primary product remains unchanged.

According to De Kleijne et al. [66] the GHG emissions of the CCU product are calculated by Equation 5 (see Chapter 2.6). Furthermore, their multifunctionality harmonization approach is based on a transition scenario to a zero-emissions economy, assuming the absence of unabated emissions by 2050. By then, they no longer account  $-E_{utilized}$  from fossil CO<sub>2</sub> sources to CCU technologies. In this work Equation 5 is applied for both the Austrian target years 2030 and 2040, and for CO<sub>2</sub> from all sources because even calculation scenarios including strict measures, such as the transition scenario (see Chapter 2.1) or the progressive pathway (see Chapter 2.2.1), indicate that process-related, hard-to-abate emissions will remain.

### 3.1.8 Storage effects

The diverse lifespans of CCU products and their limited CO<sub>2</sub> sequestration durations are discussed in Chapter 2.5. De Kleijne et al. [66] defined storage factors to include these effects into the GWP of a CCU product. As demonstrated in Equation 5, these factors are applied to the end-of-life emissions  $E_{Released}$ , but they do not account for any emissions from the use of necessary fossil inputs in conversion processes of some technologies. The storage factors, depending on the lifetime of a CCU product, are detailed in Table 9.

Table 9: Storage factors of CCU products depending on their expected lifetime [77]

Lifetime [years]	0-0.5	0.5-1	1	5	10	25	50	≥100
$u_{storage}$	1	0.99	0.98	0.92	0.85	0.67	0.42	0

## 3.2 Technological Readiness Level

The concept of technology readiness levels (TRL) is applied to CCU technologies to categorize their majority status and allows to estimate whether a technology could be available by 2030 or 2040. The technology is placed on a scale comprised of 9 levels, as detailed in the table below.

Table 10: TRL scale for CCU evaluation [78], [79]

TRL	Description by European Commission [78] for different technologies	Description by Chauvy et al. [79] for CCU technologies in particular
1	Basic principles observed	Published research that identifies the principles that underlie the technology
2	Technology concept formulated	Publication or other references that outline the application being considered, and that provide analysis to support the concept. The step up from TRL1 to TRL2 moves the ideas from pure to applied research. A major part of the work is analytical or paper studies. Experimental work is designed to corroborate the basic scientific observations made during TRL1 work.
3	Experimental proof of concept	Active research and development (R&D) has been initiated. At TRL3, the work has moved beyond the publication phase to experimental work
4	Technology validated in lab	TRL4-6 represents the bridge from scientific research to engineering. TRL4 is the first step in determining whether the individual components will work together as a system.
5	Technology validated in relevant environment	The basic technological components are integrated so that the system configuration is similar to the final application in almost all respects.
6	Technology demonstrated in relevant environment	This represents a major step up in a technology's demonstrated readiness. TRL6 begins true engineering development of the technology as an operational system.
7	System prototype demonstration in operational environment	TRL7 is a significant step beyond TRL6, requiring an actual system prototype.
8	System complete and qualified	This TRL represents the end of true system development. The technology has been proven to work in its final form and under expected conditions.
9	Actual system proven in operational environment	The technology is in its final form and operates under the full range of operating mission conditions.

Kramer and Haigh [80] assume that progressing from TRL 1 to TRL 9 might take 20-30 years. Chauvy et al. [79] suggest that a CCU technology should be at least at TRL 6 in 2020 to be considered available for 2030, and further provide an estimated timeframe of 10-15 years for the transition from laboratory to industrial scale.



### 3.3 Compatibility limits for CCU with climate targets

Based on the outlined requirements for technology availability and anticipated levels of defossilisation, limiting criteria for the CCU technologies with Austrian climate targets are presented in Table 11. Additionally, it contains characteristics of technologies that align with the 2030 or 2040 targets, found by De Kleijne et al. [72].

Table 11: Compatibility limits for CCU technologies in 2030 and 2040 and technology characteristics

Target year	CO <sub>2</sub> source	Availability criteria	Decarbonization criteria	Technology characteristics [72]
2030	Fossil, geogenic, biogenic, atmosphere	$TRL \geq 6$	$\frac{E_{CCU}}{E_{substitute}} \leq 54\%$	<ul style="list-style-type: none"> <li>• Preventing (high) capture emissions</li> <li>• Preventing (high) conversion emissions</li> <li>• Preventing re-emission of CO<sub>2</sub></li> <li>• Replacing an emission intensive process</li> </ul>
	Biogenic, atmosphere	$TRL \geq 4$	$E_{CCU} \leq 0 \frac{kg CO_2e}{kg CO_2utilized}$	<ul style="list-style-type: none"> <li>• Preventing re-emission of CO<sub>2</sub></li> <li>• Only using zero-emission energy</li> </ul>
2040	Fossil, geogenic	$TRL \geq 4$	$E_{CCU} \leq -1 \frac{kg CO_2e}{kg CO_2utilized}$	<ul style="list-style-type: none"> <li>• Utilizing CO<sub>2</sub> from atmosphere (biogenic/DAC)</li> </ul>

The established compatibility criteria provide a framework for assessing the feasibility of implementing a specific CCU technology in Austria. Technologies deemed conceivable under this framework either meet these criteria or are within proximity to the defined limits.

## 4 Conceivable CCU technologies

Identifying CCU technologies that could contribute to Austria's defossilisation in alignment with its national climate targets, requires an extensive literature review. Certain LCAs that are clearly unsuitable can be excluded from the outset. These include technologies with TRL less than 4, those with a higher GWP than conventional products, or those linked to enhanced oil recovery processes. The gathered studies are evaluated using the methods outlined in Chapter 3, and the results are presented in Figures 16 and 17.

Figure 16 presents the performance of the analyzed technologies in terms of their compatibility with the 2030 criteria.

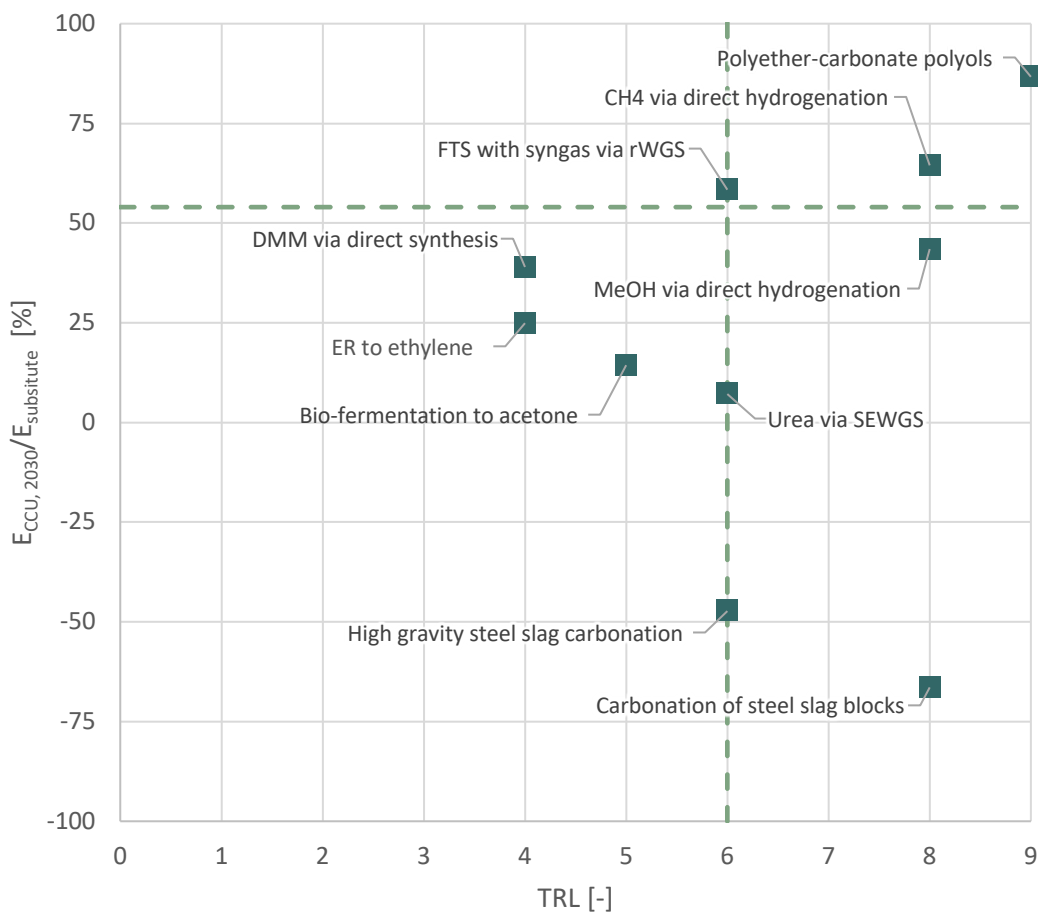


Figure 16: Comparison of CCU technologies related to 2030 climate target compatibility criteria

Four out of ten investigated technologies align with Austria's climate targets set for 2030. However, the implementation of all ten technologies result in less GHG emissions compared to conventional production routes, categorizing them as reduction measures.

The alignment of the analyzed technologies with the 2040 compatibility limits are presented in Figure 17.

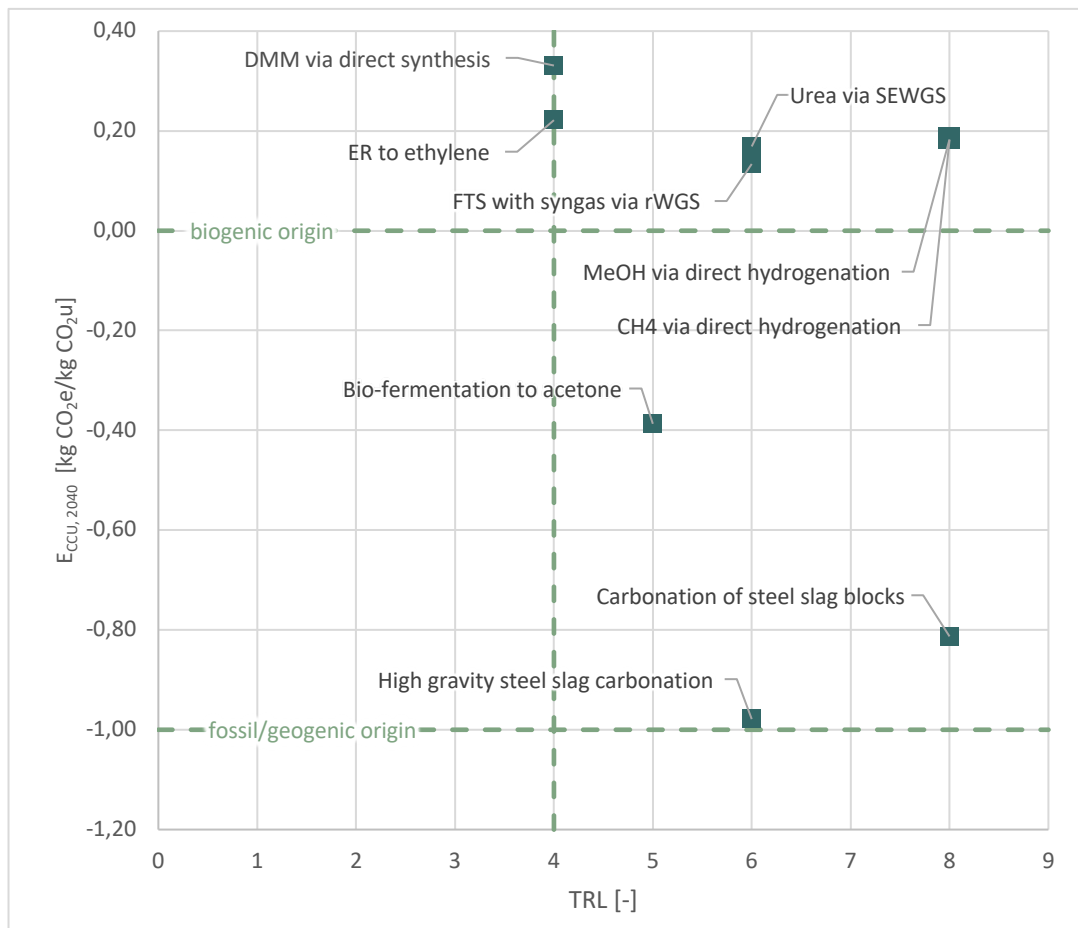


Figure 17: Comparison of CCU technologies related to 2040 climate target compatibility criteria

The analysis of CCU emissions for 2040 reveals that three technologies can align with national climate targets when utilizing biogenic CO<sub>2</sub>. Due to energy-related emissions inherent in conversion processes, none of the technologies strictly meet the 2040 climate targets.

The desired shift towards a fossil-poor energy supply positively impacts the carbon footprint of CCU products. When energy demands of the regarding technologies are met exclusively by electricity from renewable sources, and if no fossil-based reactants are needed, GHG emissions mainly occur from purging activities or at the end of a product's life cycle. Therefore, an accurate assessment of CCU technologies requires a thorough quantification of their energy demands. This step not only aids in evaluating their energy-related GHG emissions but also assigns a price to their emission reduction potential, namely in the form of energy as a valuable commodity. Figure 18 illustrates the energy demands of the investigated CCU technologies. The results demonstrate that production routes without the need of hydrogen as a chemical feedstock are energetically advantageous.

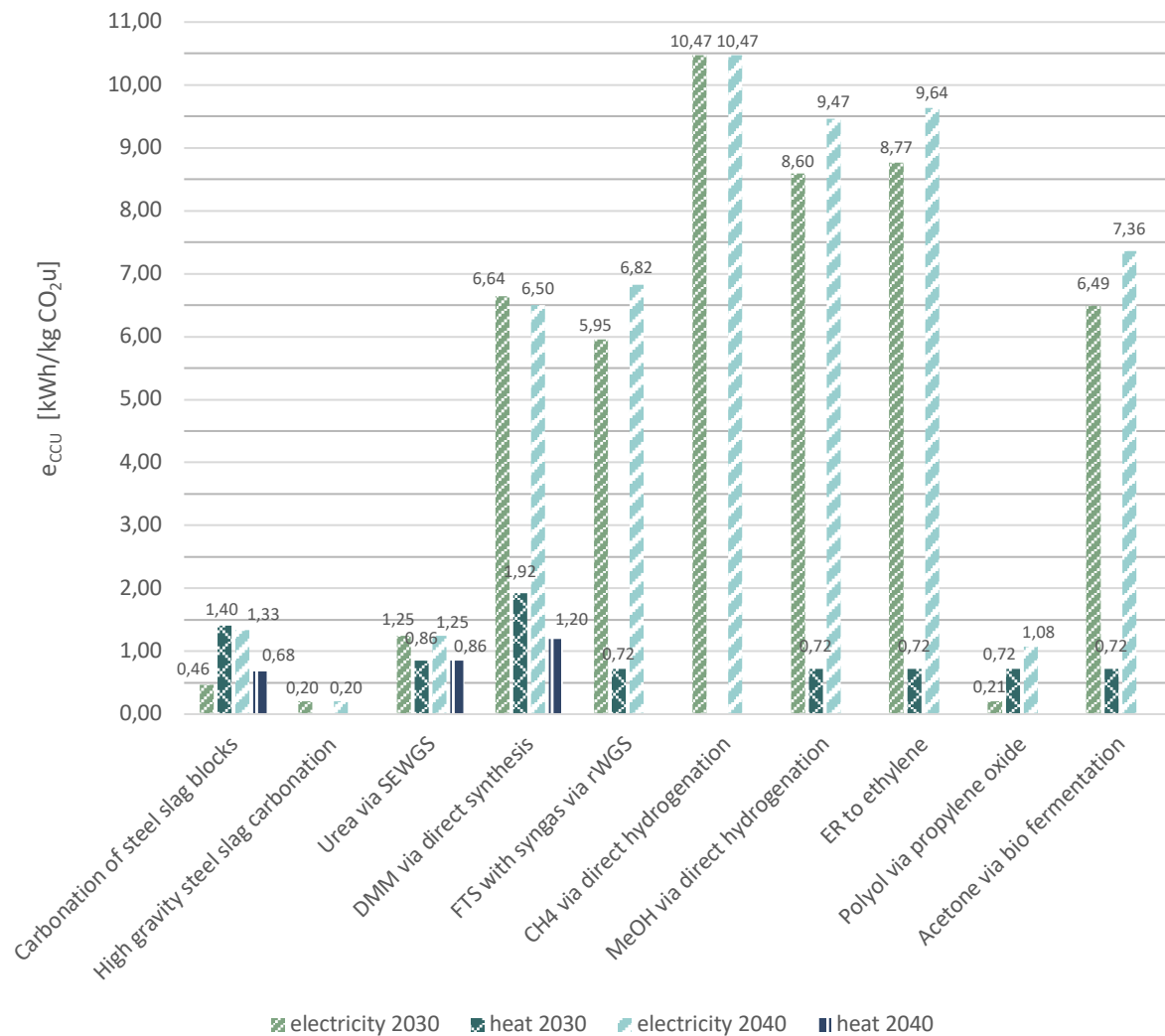


Figure 18: Energy consumption of the investigated CCU technologies

Conceivable CCU technologies include all those that meet the compatibility criteria for at least one target year. Additionally, technologies that are close to the defined limits and exhibit lower emissions compared to hard-to-defossilize systems are considered. The selected technologies are detailed in the following subchapters.

#### 4.1 Carbonation of steel slag construction blocks

Carbonation of steel slag construction blocks refers to a gas-solid carbonation process. This technology modifies the traditional manufacturing approach for producing PC-based concrete blocks by using CO<sub>2</sub> as the curing agent instead of steam. In this method, ordinary cement is replaced with granulated stainless steel slag (SSS). The company Orbix [81] operates a demonstration plant (TRL 8) employing this process to produce a product known as Carbstone. Figure 19 below offers an illustration of the flow scheme at their production site.

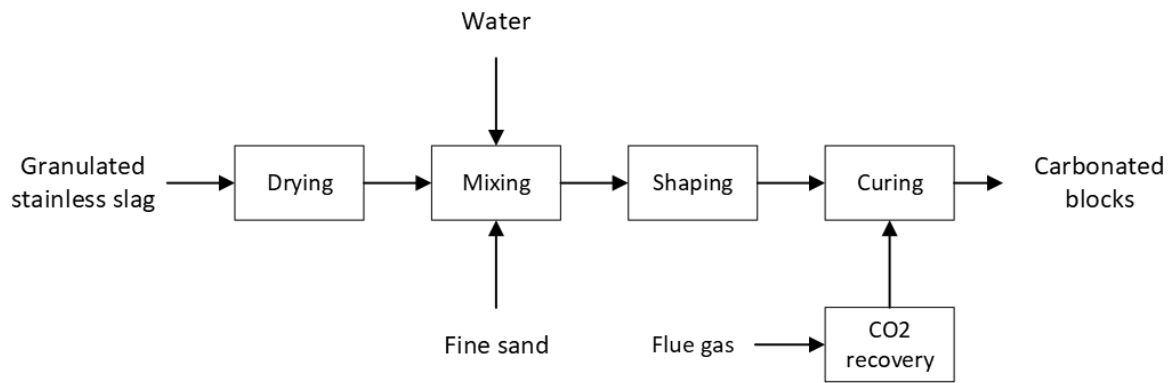


Figure 19: Flow scheme for the production of carbonated blocks, modified from [65], [82]

Wet granulated SSS enters the carbonation plant and is dried in the first step. Afterwards dry SSS, water and fine sand are introduced into a batch-mixer. Once the batch is mixed, it is then poured into molds, where the concrete is compacted using pressure and vibration. The blocks are subsequently removed from the molds and placed within an autoclave using CO<sub>2</sub> as the curing agent. Reactions of CO<sub>2</sub> between Ca and Mg bearing minerals form carbonates that yield the required compressive strength of the final product. The resulting carbonated blocks are immediately ready to be commercialized.

Based on LCA data from Di Maria et al. [65] and stoichiometric analysis, this system carbonates ~20% of the available MgO and CaO. The study proposes the production of carbonated blocks (20 cm x 10 cm x 4 cm) with a compressive strength of 43 MPa. Associated operating conditions and the composition of the input material are listed in Table 12.

Table 12: Operation parameters for the production of carbonated blocks from stainless steel slag [65] and input material composition [82]

Parameter	Unit	Value
Particle size SSS	mm	0-60
Autoclave pressure	bar	5
Autoclave CO <sub>2</sub> -concentration	vol.-%	>90
Wet SSS-sand-ratio	kg:kg	1:1
Wet SSS-water-ratio	kg:kg	1:0.22
Input material	Stainless steel slag	
CaO	wt.-%	45 ± 0.5
MgO	wt.-%	9.3 ± 2.3
Fe <sub>2</sub> O <sub>3</sub>	wt.-%	1.5 ± 0.9
MnO	wt.-%	1.4 ± 0.09
SiO <sub>2</sub>	wt.-%	31 ± 5.3
Al <sub>2</sub> O <sub>3</sub>	wt.-%	3.0 ± 0.1

Quaghebeur et al. [82] studied this technology in lab-scale, achieving CO<sub>2</sub> uptakes ranging from 100 to 150 g CO<sub>2</sub>/kg slag. Their findings recommend autoclave pressures of up to 2 MPa and temperatures between 20 to 140°C, with the specific range dependent on whether the

input material is BOF- or SS-slag. Notably, they demonstrated that purification isn't mandatory, and direct use of flue gases is feasible but provides longer carbonation times. Their research contains further details of the optimization of various process parameters, including temperature, pressure, CO<sub>2</sub> concentration, particle size, and compaction forces.

To assess the compatibility of this technology the LCA results from Di Maria et al. [65] have been harmonized. Carbonated steel slag blocks can substitute ordinary building elements. To check the compatibility of the product with the 2030 targets, PC-based concrete blocks with 0.14 kgCO<sub>2</sub>e/kg product are selected [65]. Cao et al. [83] observe that with PC-based concrete, sponge effects occur, resulting in the reabsorption of 30% of its production emissions over the lifespan. Table 13 shows the results of the availability and CCU emissions assessment, together with their compatibility to Austrian climate targets 2030 and 2040.

Table 13: Compatibility of carbonation of steel slag construction blocks with Austria's climate targets

Compatibility Criteria		2030	2040	
		all sources	biogenic	fos./geo.
Availability	TRL 8	✓	✓	✓
Substitution 2030	$\frac{E_{CCU}}{E_{substitute}} = -66\%$	✓	✓	✗
CCU emissions 2040	$E_{CCU} = -0.81 \frac{kg CO_2e}{kg CO_2 utilized}$	✓	✓	✗

In connection with biogenic CO<sub>2</sub> sources, the technology facilitates CDR, aligning it with the Austrian climate targets set for 2030 and 2040. Regarding the use of fossil or geogenic CO<sub>2</sub>, the substitution approach applied to conventional construction blocks renders it compatible with the 2030 objectives. However, this approach does not fully align with the more stringent 2040 targets. Despite this, implementing the technology with fossil or geogenic CO<sub>2</sub> could still act as an effective measure for reducing GHG emissions.

## 4.2 High gravity steel slag carbonation

High gravity steel slag carbonation integrates the production of cementitious materials with the treatment of wastewater from cold-rolling processes, utilizing carbon dioxide. Pan et al. [58] conducted field tests at a blast furnace plant in Kaohsiung, Taiwan, therefore achieving TRL 6. The direct aqueous carbonation technology can be applied according to the following flow scheme.

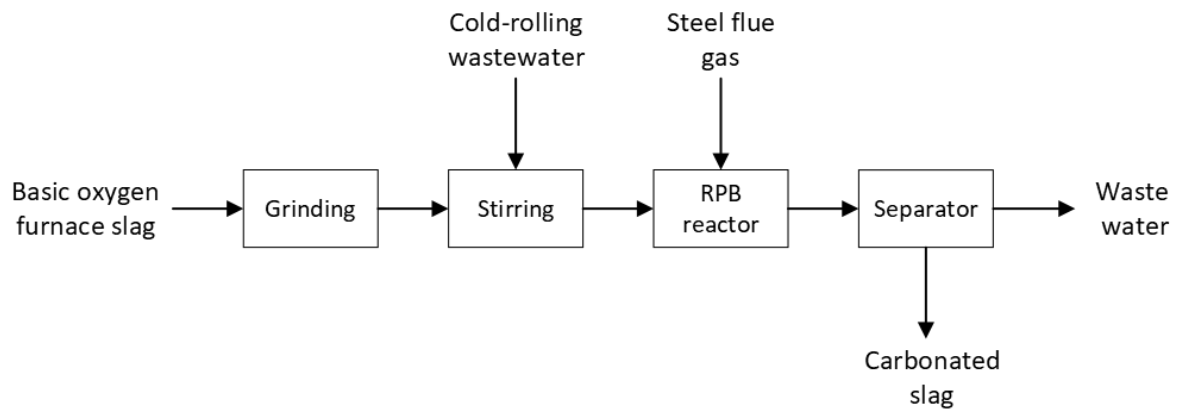


Figure 20: Flow scheme of the HiGCarb process for the production of cementitious material [84]

BOFS from blast furnace plant is ground and added to a stirring reactor along with alkaline Cold-Rolling Wastewater (CRW). The resulting slurry is then fed into a rotating packed bed reactor, where the high centrifugal force accelerates carbonation reactions with CO<sub>2</sub>-containing flue gas. Subsequently, neutralized CRW (pH~6.3) is separated from the cementitious material product. [84]

Pan et al. [58] chose the operating conditions, listed in Table 14, for the production of BOFS-based cement substitute utilizing 316 kg CO<sub>2</sub> per tonne BOFS. The packed bed has an arithmetic diameter of 46.5 cm, and an axial height of 19.9 cm, while the mesh size of the stainless steel wire is 1 cm x 1 cm (thickness 0.3mm). Additionally, the table includes compositions of the input materials, based on earlier research by Chang et al. [85]. The system attains a capture efficiency of 98.3%, eliminating the necessity for a separate CO<sub>2</sub> recovery unit.

Table 14: Operation parameters for the production carbonated cement substitute, based on LCA results by Pan et al. [58] and input material composition from Chang et al. [85]

Parameter	Unit	Value
Particle size $D_{80}$	$\mu\text{m}$	125
RPB rotation speed	rpm	400
Gas flow rate	$\text{m}^3/\text{min}$	0.38
Slurry flow rate	$\text{m}^3/\text{h}$	0.33
Flue gas $\text{CO}_2$ -concentration	vol.-%	28-32
BOFS-CRW-ratio	kg:kg	1:15.0
Input material	BOF slag	
$\text{SiO}_2$	wt.-%	10.59
$\text{Al}_2\text{O}_3$	wt.-%	2.24
$\text{Fe}_2\text{O}_3$	wt.-%	24.41
CaO	wt.-%	41.15
MgO	wt.-%	9.21
$\text{SO}_3$	wt.-%	0.13
$\text{P}_2\text{O}_5$	wt.-%	2.88
$\text{TiO}_2$	wt.-%	0.42
$\text{Cr}_2\text{O}_3$	wt.-%	0.19
$\text{K}_2\text{O}$	wt.-%	0.02
$\text{Na}_2\text{O}$	wt.-%	0.03
MnO	wt.-%	2.75
Input material	CRW	
pH	-	11.26
$\text{Na}^+$	mg/L	791
$\text{K}^+$	mg/L	37.1
$\text{Ca}^{2+}$	mg/L	85.3
$\text{Mg}^{2+}$	mg/L	0.158
$\text{Fe}^{3+}$	mg/L	1.99
$\text{OH}^-$	mg/L	0.0018
$\text{NO}_3^-$	mg/L	0.1
$\text{HCO}_3^-$	mg/L	2.11
$\text{CO}_3^{2-}$	mg/L	17.95
$\text{SO}_4^{2-}$	mg/L	157

High gravity carbonation of BOFS enables the production of cementitious material, which can substitute ordinary PC with an emissions factor of 0.709 kg  $\text{CO}_2\text{e}/\text{kg}$  ordinary PC [86]. Taking EOL impacts into account, it is presumed that PC-based blocks absorb 30% of their production emissions over their lifespan [83]. The assessment of the technologies availability and emissions criteria is illustrated in Table 15.



Table 15: Compatibility of high gravity steel slag carbonation with Austria's climate targets

Compatibility Criteria		2030 all sources	2040 biogenic	2040 fos./geo.
Availability	TRL 6	✓	✓	✓
Substitution 2030	$\frac{E_{CCU}}{E_{substitute}} = -47\%$	✓	✓	✗
CCU emissions 2040	$E_{CCU} = -0.98 \frac{kg CO_2e}{kg CO_2 utilized}$			

High gravity steel slag carbonation aligns with the Austrian climate targets for 2030 and, specifically for CO<sub>2</sub> from biogenic origin, also meets the 2040 targets. Operating with fossil-poor electricity, the conversion process achieves close to zero emissions. However, utilizing fossil-derived carbon dioxide slightly misses the 2040 targets due to assumed losses from the indicated capture efficiency factor of 98.3% and the chosen electricity mix. Despite this, the technology significantly reduces fossil CO<sub>2</sub> emissions, resulting in minimal atmospheric accumulation.

### 4.3 Urea via SEWGS from BOFG

Urea production can utilize BOFG as an alternative source for the required chemical components when it's pre-treated with the sorption enhanced water gas shift (SEWGS) process. De Kleijne et al. [68] describe the procedure in the flow chart shown in Figure 21. Given that SEWGS has attained a TRL 6 [87], [88], while the other process steps are state of the art, this system can be classified at a TRL 6.

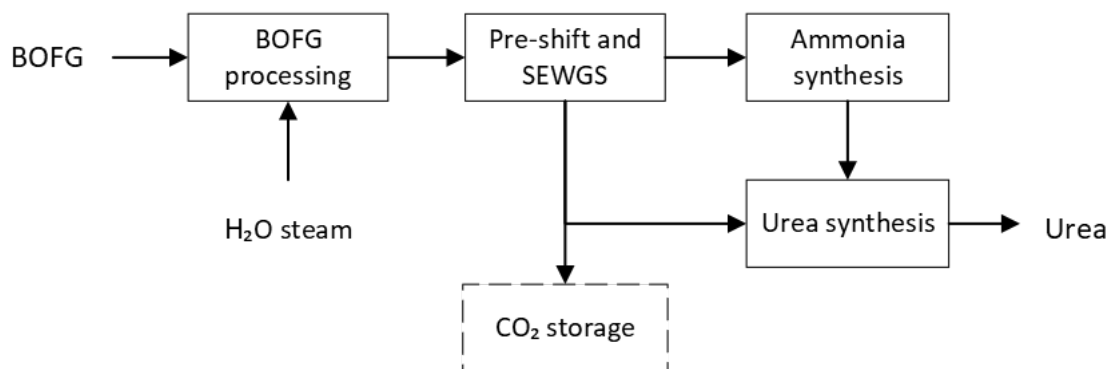


Figure 21: Flow scheme of urea production via SEWGS from BOFG [68]

BOFG from the steel production site enters the system and is compressed, heated, and mixed with steam in the first step. The mixture is lead into a pre-shift reactor where CO is converted to CO<sub>2</sub> and H<sub>2</sub> to the thermodynamic equilibrium, depending on the reactor conditions. In the next step, the product gas is treated by SEWGS. SEWGS combines the WGS reaction and

CO<sub>2</sub> removal, due to a reactive pressure swing adsorption process in a single operation unit [89]. De Kleijne et al. [68] illustrates the process according Figure 22.

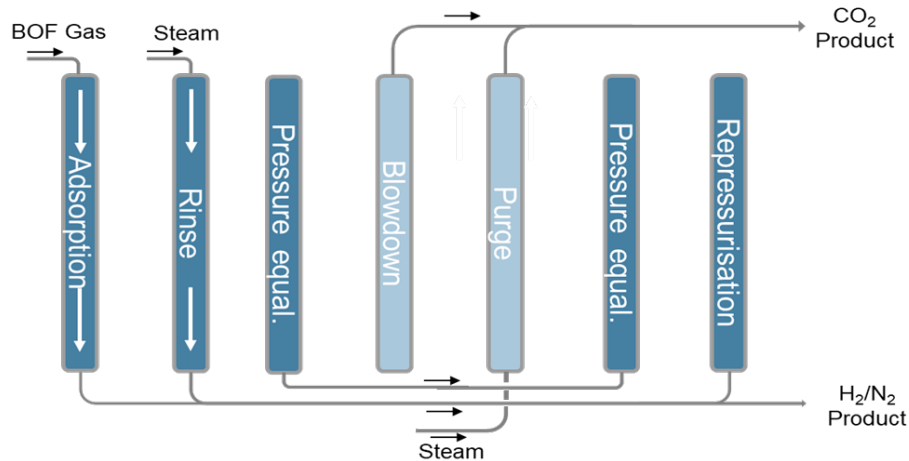


Figure 22: Schematic of the SEWGS reaction [68]

Several columns are filled with potassium-promoted hydrotalcite adsorbent and each of them undergoes a series of phases: adsorption, rinsing, depressurization, blowdown, purge, repressurisation, and finally, repressurisation using feed. The hydrogen/nitrogen-rich stream emerges during the adsorption phase, while the CO<sub>2</sub>-rich product is generated during blowdown and purge phases [90], [91].

Impurities like sulfur or oxygen compounds are removed from the generated H<sub>2</sub>/N<sub>2</sub> mixture, as they can impair the NH<sub>3</sub> catalyst of the following ammonia synthesis process step. A higher H<sub>2</sub>/N<sub>2</sub>-ratio corresponds to an increased yield of ammonia. The produced ammonia is then cooled into a liquid state and stored. From the storage, the ammonia is compressed for urea synthesis, together with 20.6% of the CO<sub>2</sub> obtained from the SEWGS unit. The remaining 79.4% can be transported and stored in the underground [68].

De Kleijne et al. [68] simulated the process described, under operation conditions listed in Table 16.

Table 16: Operation parameters and BOFG composition for the production of urea, from LCA by de Kleijne et al. [68]

Parameter	Unit	Value
<i>BOFG processing</i>		
Temperature	°C	370
Pressure	bar	25
<i>Ammonia synthesis</i>		
H <sub>2</sub> :N <sub>2</sub> ratio	-	2.4
<i>Urea synthesis</i>		
Pressure	bar	300
Input material	BOFG	
CO	mol%	60
N <sub>2</sub>	mol%	24
CO <sub>2</sub>	mol%	16
O <sub>2</sub>	mol%	0.3
H <sub>2</sub>	mol%	0.02
CH <sub>4</sub>	mol%	0.02

Urea from flue gases can replace products based on natural gas. To evaluate the alignment of the presented technology with Austria's 2030 climate targets, urea from conventional steam reforming, which has an emission factor of 1.73 kg CO<sub>2</sub>e/kg urea (including EOL-emissions) [66], is used as the benchmark. The results of the compatibility assessment are presented in Table 17 below.

Table 17: Compatibility of urea production via SEWGS from BOFG with Austria's climate targets

Compatibility Criteria		2030 all sources	2040 biogenic	2040 fos./geo.
Availability	TRL 6	✓	✓	✓
Substitution 2030	$\frac{E_{CCU}}{E_{substitute}} = 7.1\%$	✓	✗	✗
CCU emissions 2040	$E_{CCU} = 0.17 \frac{kg CO_2e}{kg CO_2 utilized}$			

The production of urea from BOFG is not strictly 2040 compatible since carbon dioxide from fossil sources or thermal processes is not stored permanently in urea. Additionally, not all CO<sub>2</sub> obtained can be fully converted into urea due to its excess. Hence, it's crucial to integrate this technology with storage solutions (e.g., in the underground or in carbonates) to prevent the remaining carbon dioxide from being directly released into the atmosphere. As per the LCA conducted by De Kleijne et al. [68], the unconverted carbon dioxide surplus is quantified to be about 0.84 kg CO<sub>2</sub> per kg of urea.

## 4.4 Direct hydrogenation of CO<sub>2</sub>

The direct hydrogenation of CO<sub>2</sub> for the production of basic chemicals such as methane, methanol, and syngas is extensively discussed in literature [42], [92], [93], making it a potentially promising method for CO<sub>2</sub> sequestration. Since industrial-scale production of both methanol and methane has been successfully demonstrated using this pathway [97] - [99], this technology has reached at least TRL 8 in recent years. A schematic diagram describing the process is taken from Bargiacchi et al. [92] and Hoppe et al. [42] and is shown in Figure 23.

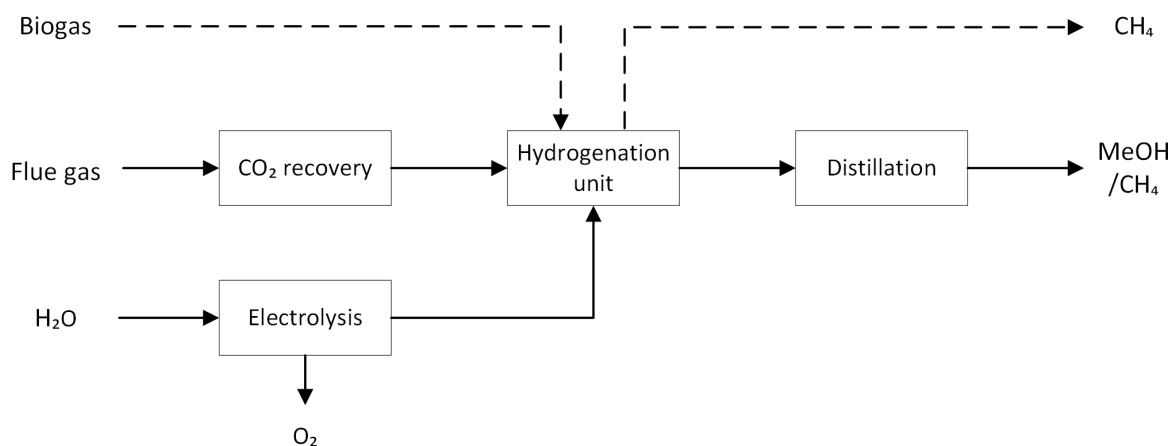


Figure 23: Flow scheme of direct CO<sub>2</sub> hydrogenation for the production of methanol and methane [42], [92], and biogas upgrading (dashed line) [97]

Water is split into hydrogen and oxygen through either alkaline or proton exchange membrane electrolysis [92]. Depending on the desired end product, such as methanol or synthetic natural gas, various pathways are documented within this technology [100] - [102].

The power-to-gas plant in Gabersdorf, Austria, serves as an example of methanation. Biogas is directly supplied to the hydrogenation unit, a plate-type heat exchanger methanation reactor, bypassing progressive CO<sub>2</sub> recovery. The CO<sub>2</sub> undergoes catalytic reaction with H<sub>2</sub> to form CH<sub>4</sub>, producing synthetic natural gas with an output of approximately 240 kW. [97]

Another example is the synthesis of methanol at the Carbon Recycling International plant in Iceland. Described by Bargiacchi et al. [98], CO<sub>2</sub> from carbon capture is combined with an H<sub>2</sub> stream and fed into a fixed-bed reactor for catalytic conversion to methanol. The product, a mixture of methanol and water, is then separated by distillation.

Possible reaction conditions for the synthesis of both methane and methanol are taken from the mentioned studies and presented in Table 18.

Table 18: Operation parameters for the production of methane or methanol via direct hydrogenation [98], [97]

Parameter	Unit	Methane	Methanol
Reactor type	-	Fixed bed	Plate-type heat exchanger
CO <sub>2</sub> :H <sub>2</sub> ratio	-	1:4	1:3
Catalyst	-	Ni	Cu-ZnO-Al <sub>2</sub> O <sub>3</sub>
Reactor temperature	°C	200	200
Reactor pressure	bar	8	50
Distillation temperature	°C	-	25
Distillation pressure	bar	-	20

The assessment of the climate target compatibility is based on LCA-results by Hoppe et al. [42], whereby in the scenario of biogas upgrading via methane synthesis the carbon capture unit is bypassed. Cradle-to-gate data is derived from literature [42], [77], and by adding EOL-emissions, their life spans result in 3.21 kg CO<sub>2</sub>e/kg methane and 2.19 kg CO<sub>2</sub>e/kg methanol.

Table 19: Compatibility of direct hydrogenation of CO<sub>2</sub> to produce methane and methanol

Compatibility Criteria Methane		2030	2040	
		all sources	biogenic	fos./geo.
Availability	TRL 8	✓	✓	✓
Substitution 2030	$\frac{E_{CCU}}{E_{substitute}} = 64\%$	✗	✗	✗
CCU emissions 2040	$E_{CCU} = 0.18 \frac{kg CO_2e}{kg CO_2 utilized}$			
Compatibility Criteria Methanol		2030	2040	
		all sources	biogenic	fos./geo.
Availability	TRL 8	✓	✓	✓
Substitution 2030	$\frac{E_{CCU}}{E_{substitute}} = 43\%$	✓	✗	✗
CCU emissions 2040	$E_{CCU} = 0.18 \frac{kg CO_2e}{kg CO_2 utilized}$			

Considering a 1:1 substitution of conventional products, the production of methanol meets the compatibility criteria for the year 2030. Both hydrogenation technologies exceed the upper limit set for 2040 climate target compatibility, due to only short CO<sub>2</sub> sequestration, but can act as reduction measures if conventional products are substituted.

To confirm these results, LCA data for the production of methane via direct hydrogenation from Bargiacchi et al. [92] were also harmonized. For the year 2040, CCU emissions of 0.19 kgCO<sub>2</sub>e/kgCO<sub>2</sub> utilized were found, and for the 2030 substitution approach, a deviation of 2% was observed. This discrepancy can be attributed to different assumptions regarding the CO<sub>2</sub> utilization quantity.

#### 4.5 FT fuel from syngas via rWGS

Fischer-Tropsch synthesis (FTS) is a well-established technology used to convert solid or gaseous energy sources (i.e., coal, natural gas or biomass) into synthetic crude oil that can be further refined to produce products like fuels, waxes, and lubricants [100]. The feedstock is transformed into synthesis gas (or syngas), a mixture of carbon monoxide and hydrogen and the reaction takes place on the surface of a catalyst, mostly cobalt or iron [101]. CO<sub>2</sub> can serve as an alternative feedstock for FTS if it is reduced in a reversed water gas shift (rWGS) reaction, which is currently TRL 6. Based on literature [101], [102], the production of FT fuel from CO<sub>2</sub> is illustrated in Figure 24.

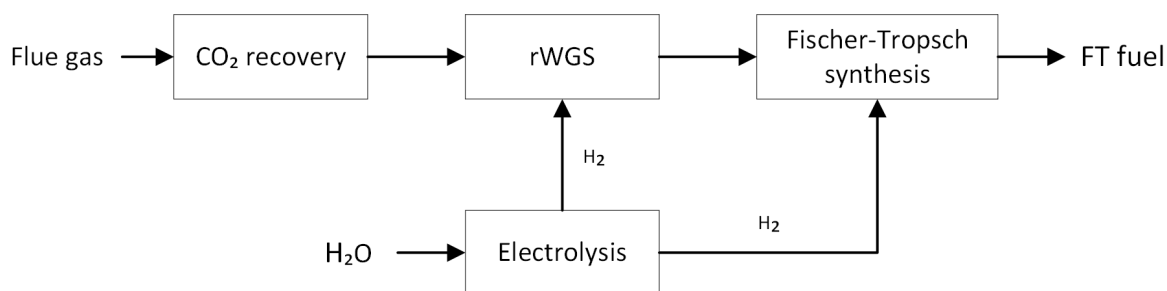


Figure 24: Flow scheme of FT-fuel production from syngas via rWGS [101], [102]

Hydrogen is produced through a water electrolysis process for the conversion of carbon dioxide into fuel, following these distinct steps. The fuel synthesis starts with the conversion of CO<sub>2</sub> to CO and water, facilitated by the rWGS reaction. González-Castaño et al. [103] comprehensively reviewed research findings related to rWGS processes, encompassing efficient catalytic systems, reactor units, and pilot scale processes, while highlighting concurrent research needs to advance systems towards industrial scale applications. However, van der Giesen et al. [102] proposed the use of a fixed-bed reactor for the endothermic equilibrium reaction, employing the operating conditions listed in Table 20. Once syngas is generated, the FTS process is employed to produce CO<sub>2</sub>-based fuels. For example, this step is executed in multi-tubular fixed bed reactors [104].

The table below presents operating conditions employed in the study by van der Giesen et al. [102]. They highlight that 80% of the energy in the syngas is converted into fuel, whereas the remaining 20% is retained in short hydrocarbon chains. These chains cannot be transformed into fuel but provide enough energy to operate the gas-to-liquid plant.

Table 20: Operation parameters for the production of FT-fuels via rWGS reaction [96]

Parameter	Unit	Value
<i>rWGS-process</i>		
Pressure	bar	25
Temperature	°C	230
CO <sub>2</sub> -input	kg CO <sub>2</sub> /kg CO	1,57
H <sub>2</sub> -input	kg H <sub>2</sub> / CO	0,07
<i>Fischer-Tropsch process</i>		
Pressure	bar	25
Temperature	°C	230
Energy efficiency (syngas to fuel)	%	80

FT-fuels, produced from CO<sub>2</sub> via rWGS processes are compared to the emissions factor of 88 g CO<sub>2</sub>e/MJ for the production and combustion of ordinary diesel [67]. The compatibility assessment is based on LCA data by Liu et al. [101]. Results are presented in Table 21 below.

Table 21: Compatibility of FT-fuel from syngas via rWGS

Compatibility Criteria		2030 all sources	2040 biogenic	2040 fos./geo.
Availability	<i>TRL 6</i>	✓	✓	✓
Substitution 2030	$\frac{E_{CCU}}{E_{substitute}} = 58\%$	✗	✗	✗
CCU emissions 2040	$E_{CCU} = 0.13 \frac{kg CO_2e}{kg CO_2 utilized}$			

Liu et al. [101] investigated this technology combined with DAC. For assessing its applicability in the Austrian energy and industrial sectors, the CO<sub>2</sub> recovery unit is harmonized as described in Chapter 3.1.6 and chemical absorption for 2030 and physical adsorption including VPSA followed by cryogenic capture is considered instead. FT-fuels from syngas via rWGS slightly fail the national climate targets established for 2030 and but can serve as a reduction measure when replacing conventional fuel production with the CCU alternative.

Numerous studies in literature suggest achieving a reduction via the rWGS process before the conversion into FT-fuel [101], [105], [106]. However, as demonstrated by the reaction equations in Table 1, direct conversion is also feasible. This direct approach is currently being implemented in a pilot plant in Graz [107].

## 4.6 Direct synthesis of DMM via CO<sub>2</sub> hydrogenation in methanol

Oxymethylene ethers (OMEs) represent a promising category of synthetic fuels, with dimethoxymethane (DMM) or OME<sub>1</sub> being the simplest compound within this group. Traditionally, DMM production involves a two-step process: first, methanol is oxidized into formaldehyde (FA) using either silver or iron-molybdenum catalyst. This is followed by the reaction of FA with methanol in an acid-catalyzed process to generate DMM [108]. Due to huge energy consumption, ongoing research aims to optimize the DMM synthesis route and Thenert et al. [108] validated the ruthenium-catalyzed synthesis utilizing CO<sub>2</sub> at a lab scale, TRL 4. Deutz et al. [71] further explored this approach in their LCA, outlining the process as described in Figure 25.

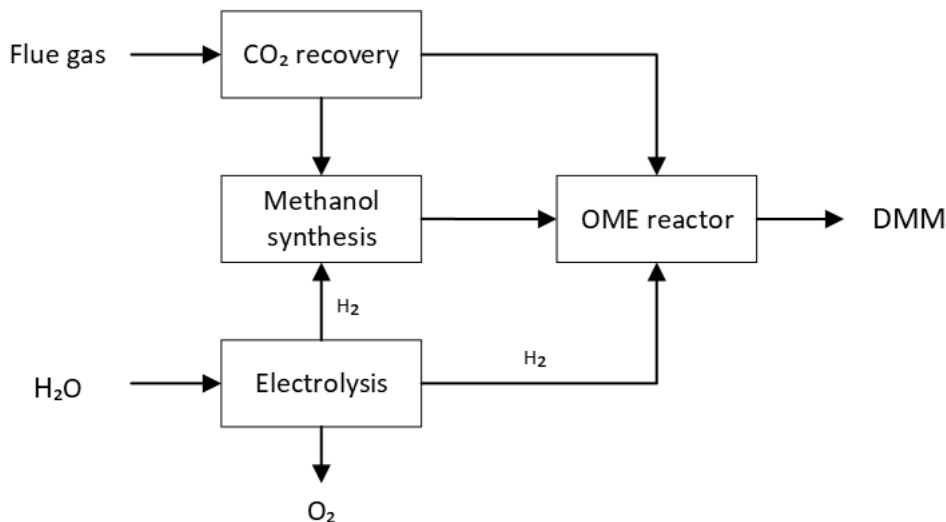


Figure 25: Flow scheme of DMM production via CO<sub>2</sub> hydrogenation in methanol [71]

Hydrogen is supplied by PEM electrolysis and methanol is further obtained from CO<sub>2</sub> via catalytic reduction. DMM is directly produced from methanol, CO<sub>2</sub> and H<sub>2</sub> in one reactor. [71] Applying the molecular catalyst Ru(triphos) in combination with the Lewis acid Al(OTf)<sub>3</sub> enables the reaction pathway, shown in Figure 26 [108].

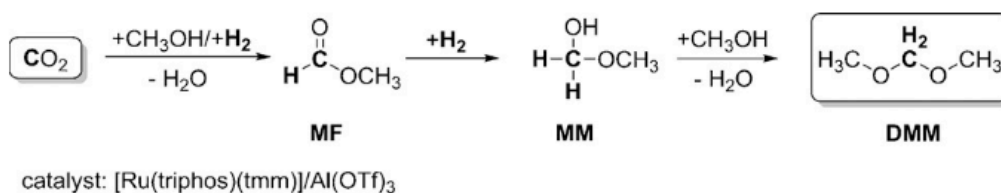


Figure 26: Possible reaction pathway for the Ru(triphos)/Al(OTf)<sub>3</sub>-catalyzed synthesis of DMM using methanol, CO<sub>2</sub> and H<sub>2</sub> [108]

Possible operating conditions are given by Deutz et al. [71] in terms of reactor pressure and temperature, and by Thenert et al. [108] in terms of optimum partial pressures, as shown in



Table 22. For process description concerning the methanol synthesis readers are directed to Chapter 4.4.

Table 22: Operation parameters for the production of DMM via direct synthesis with methanol, CO<sub>2</sub> and H<sub>2</sub> [71], [108]

Parameter	Unit	Value
<i>PEM-electrolysis</i>		
Pressure	bar	75
<i>OME<sub>1</sub> reaction</i>		
Total pressure	bar	80
Temperature	°C	80
CO <sub>2</sub> partial pressure	bar	20
H <sub>2</sub> partial pressure	bar	60
Ru(triphos)-concentration	mmol/l	3,00
Al(OTf) <sub>3</sub> -concentration	mmol/l	12,5

OMEs can be combusted in conventional diesel engines, therefore selecting 88 gCO<sub>2</sub>e/MJ for diesel in the substitution approach [67]. Table 23 summarizes the compatibility of the presented technology with the Austrian climate targets.

Table 23: Compatibility of DMM production via direct CO<sub>2</sub> hydrogenation in methanol

Compatibility Criteria		2030 all sources	2040 biogenic	2040 fos./geo.
Availability	<i>TRL 4</i>	✗	✓	✓
Substitution 2030	$\frac{E_{CCU}}{E_{substitute}} = 39\%$	✓	✗	✗
CCU emissions 2040	$E_{CCU} = 0.33 \frac{kg CO_2e}{kg CO_2 utilized}$			

It should be noted, that OME<sub>1</sub> must be blended with fossil diesel, due to its low boiling point and vapor pressure, leading Deutz et al. [71] to estimate a substitution ratio of 24%. Owing to its restricted applicability and early stage of development, this technology is not expected to reach commercial viability before 2040.

## 4.7 Electrochemical CO<sub>2</sub> reduction to ethylene

The electrochemical CO<sub>2</sub> reduction reaction can convert carbon dioxide into valuable chemical compounds. Figure 27 illustrates potential conversion products and highlights the endothermic nature of the overall reactions.

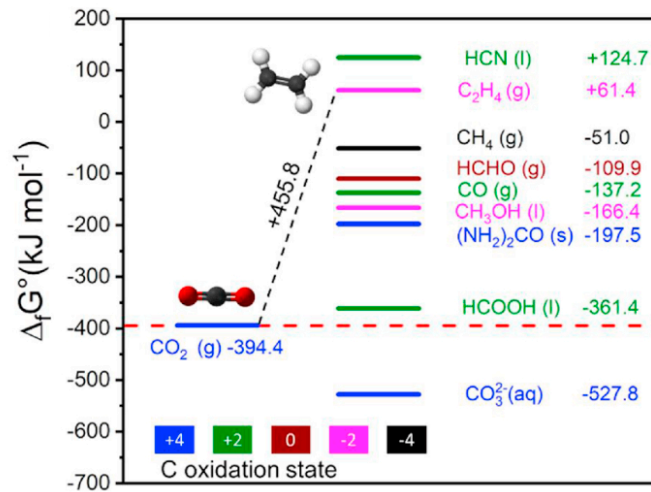


Figure 27: Standard Gibbs free energy of formation for CO<sub>2</sub> and various possible chemical products [50], [109]

Given the substantial market value of ethylene, Khoo et al. [50] focused on its production through this method in their LCA study. Since laboratory bench success is reported [50], the technology is categorized at TRL 4. A possible flow scheme for large-scale CO<sub>2</sub> reduction is depicted in Figure 28.

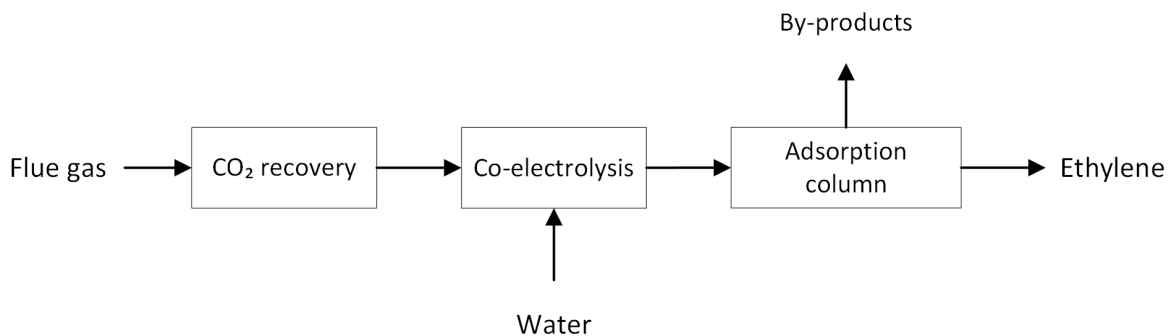


Figure 28: Flow scheme of ethylene production by electrochemical CO<sub>2</sub> reduction [50]

Carbon dioxide, captured through MEA-absorption, is introduced into the electrochemical cell along with water. This cell comprises an anion exchange membrane with a high surface area, CuO-derived Cu as the working electrode, and CO<sub>2</sub>-saturated 1M aqueous KHCO<sub>3</sub> as the supporting electrolyte [50]. In this process, known as co-electrolysis, O<sub>2</sub> is generated at the anode, H<sub>2</sub> and C<sub>2</sub>H<sub>4</sub> at the cathode. Khoo et al. [50] assume a 100% CO<sub>2</sub> conversion through recycling. Further, they add a distillation column to separate the main product from the additional gases. These by-products could either be recovered or released into the air. As this technology has only been validated in lab-scale, the operating conditions listed in Table 24 are based on experimental data.

Table 24: Operating parameters of electrochemical CO<sub>2</sub> reduction to ethylene [50]

Parameter	Unit	Value
Temperature	°C	25
Pressure	atm	1
Optimum operation point		
Voltage efficiency	%	45
Faradaic efficiency	%	75

Conventional ethylene production involves steam cracking of hydrocarbons, with a reported GWP of 1.56 kg CO<sub>2</sub> per kg of ethylene [70]. By adding the CO<sub>2</sub> release at the end of the CCU products life cycle, the cradle-to-grave emissions are estimated to account 6.12 kgCO<sub>2</sub>/kg C<sub>2</sub>H<sub>4</sub>. The assessment of CO<sub>2</sub>RR technology's alignment with Austrian climate targets is based on LCA from Khoo et al. [50] and results are shown in Table 25.

Table 25: Compatibility of electrochemical CO<sub>2</sub> reduction to ethylene

Compatibility Criteria		2030 all sources	2040 biogenic	2040 fos./geo.
Availability	TRL 4	✗	✓	✓
Substitution 2030	$\frac{E_{CCU}}{E_{substitute}} = 25\%$	✓	✗	✗
CCU emissions 2040	$E_{CCU} = 0.22 \frac{kg CO_2e}{kg CO_2 utilized}$			

Ethylene via electrochemical CO<sub>2</sub> reduction aligns with the substitution criteria when powered by renewable energy sources but is not expected to be commercially available in 2030. Khoo et al. [50] have made assumptions regarding air emissions from the adsorption column, leading to a marginally positive  $E_{CCU}$  value. This implies that the technology fails the climate targets set for 2040 but could act as a reduction measure.

## 4.8 CO<sub>2</sub>-based polyol production

Polyols can be further processed into polyurethane (PU) foams and are therefore categorized as stable chemicals. The synthesis of conventional polyether polyols typically involves feedstocks like ethylene oxide, propylene oxide, and multifunctional alcohols. In the production of polyether-carbonate polyols, CO<sub>2</sub> is used to substitute the ethylene oxide stream, offering a pathway for GHG reduction. [47]

With the commercial availability of CO<sub>2</sub>-based polyols already reported [110], this technology has reached TRL 9. The production process is illustrated in Figure 29 below.

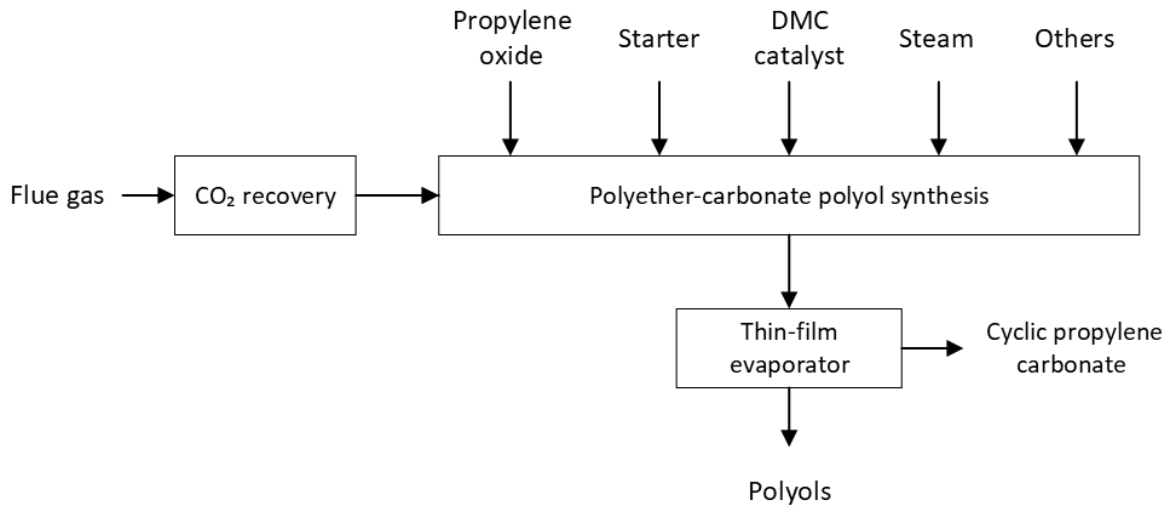


Figure 29: Flow scheme of CO<sub>2</sub>-based polyol production [47]

Carbon dioxide from flue gas is recovered by carbon capture technology and redirected to the main process of the utilization stage. In the production of polyether-carbonate polyols a feedstock comprising of propylene oxide, CO<sub>2</sub>, and a multifunctional alcohol starter, like glycerol is added to a vigorous stirring reactor. The use of a double metal cyanide (DMC) catalyst minimizes the formation of the cyclic propylene carbonate by-product. Remaining by-product is separated from the polyols by processing the reactor output through a thin-film evaporator. [47]

Buchner et al. [111] conducted a techno-economic assessment on CO<sub>2</sub> based polyol production and created a block flow diagram including characteristic process conditions, which is illustrated in Figure 30.

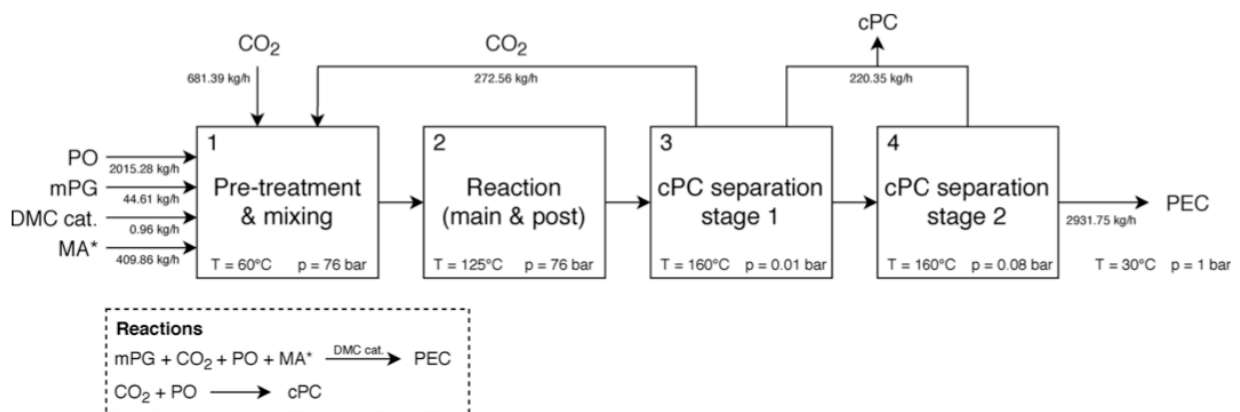


Figure 30: Block flow diagram for production of polyols containing CO<sub>2</sub> (PEC) under characteristic process conditions (PO – propylene oxide, mPG – monomeric propylene glycol, DMC cat. – double metal cyanide catalyst, MA – maleic anhydride, cPc – cyclic propylene carbonate) [111]

During literature review, several LCA studies [45], [47], [60] related to the production of CO<sub>2</sub>-based polyols were discovered. For the examination of the technology and to assess its

alignment with Austrian climate targets, the study by Thoneman and Pizzol [45] has been selected. Substitute emissions for production of conventional polyether polyols, inclusive EOL impacts, are referenced from De Kleijne et al. [72], indicating 6.47 kg CO<sub>2</sub>e/kg polyol. The results are presented in Table 26.

Table 26: Compatibility of CO<sub>2</sub>-based polyol production

Compatibility Criteria		2030 all sources	2040 biogenic	2040 fos./geo.
Availability	TRL 9	✓	✓	✓
Substitution 2030	$\frac{E_{CCU}}{E_{substitute}} = 87\%$	✗	✗	✗
CCU emissions 2040	$E_{CCU} = 35 \frac{kg CO_2e}{kg CO_2 utilized}$			

The result of 35 kg CO<sub>2</sub>e per kg CO<sub>2</sub> utilized in the CCU emissions primarily stems from the input of GHG intensive raw materials, including propylene oxide. Although the synthesis of polyether-carbonate polyols may not meet climate targets, it can still be regarded as a method for reducing emissions compared to the conventional hard-to-defossilize product. An earlier LCA study by Von der Assen and Bardow [47] reports emission reductions of 11-19% compared to conventional products, aligning with the findings presented in this work.

## 4.9 CO<sub>2</sub> bio-fermentation to acetone

Acetone serves not only as a solvent but also as a chemical intermediate in the synthesis of various products, including methyl methacrylate, bisphenol A, and diacetone alcohol. Its significant consumption in the production of acrylic glass (polymethyl methacrylate) categorizes it as a stable chemical, owing to the products lifespan. [112] Given the substantial market demand and the fact that acetone production is presently predominantly reliant on fossil feedstock, the Norwegian PyroCO<sub>2</sub> project is developing an alternative thermophilic microbial bioprocess [54]. This technology is intended for demonstration in a pilot plant by 2026 [113]. In the absence reports on its current development stage, a TRL of 5 is chosen.

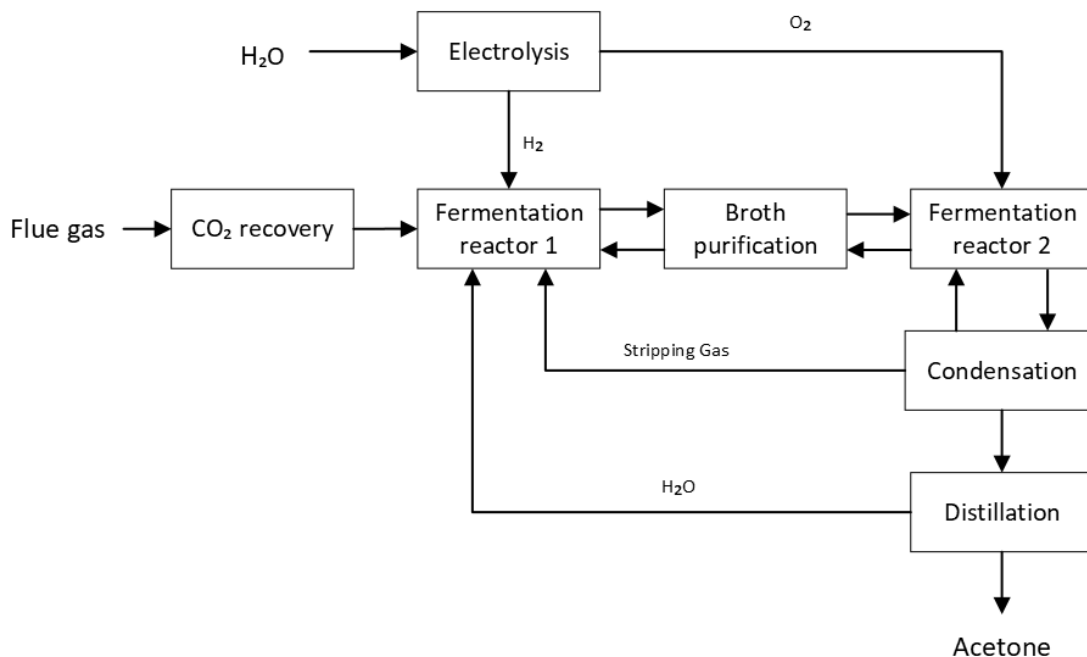


Figure 31: Flow scheme of acetone production from CO<sub>2</sub> via bio-fermentation [54]

In this process, CO<sub>2</sub> is recovered and purified from industrial off-gases using a carbon capture unit, before being introduced into the first fermentation reactor of the CCU system. Water is split via electrolysis to meet the hydrogen requirements for the initial fermentation step and oxygen needs for the subsequent fermentation step. The first reactor houses thermophilic bacteria that convert H<sub>2</sub> and CO<sub>2</sub> into acetic acid. This reaction broth then progresses to the second fermentation reactor, where aerobic thermophilic bacteria further convert it into acetone. To prevent contamination of the reactors, membrane filtration is employed to purify both the output from the first reactor and the recirculated stream from the second. The output from the second reactor, comprising acetone, water, and stripping gas, is then separated by condensation and subsequent distillation. The acetone is isolated as the final product, while the stripping gas and water are recirculated back into the first reactor. [54]

Jiresten and Larsson [54] highlight that this technology is currently in the development phase. They assume operating conditions for their study, which are detailed in Table 27. The bacteria feed recipe remains undisclosed due to confidentiality concerns [54].

Table 27: Operation parameters for the production of acetone from CO<sub>2</sub> via bio-fermentation [54]

Parameter	Unit	Value
<i>Fermentation 1</i>		
Reactor volume	m <sup>3</sup>	943
Temperature	°C	60
Pressure	bar	10
pH	-	6.0-6.7
Cell density	g cDW/l	20
Space-Time-Yield	g/l h	2
Acetic acid concentration	g/l	40
<i>Fermentation 2</i>		
Reactor volume	m <sup>3</sup>	250
Temperature	°C	60
Pressure	bar	10
pH	-	6-7
Cell density	g cDW/l	20
Space-Time-Yield	g/l h	2.5
Acetone concentration	g/l	25
<i>Membrane filter</i>		
Maximum pressure	kPa	20
Flux	l/m <sup>2</sup> h	10
<i>Condensation</i>		
Temperature	°C	12
<i>Distillation</i>		
Temperature	°C	56

Conventional methods for producing acetone involve the 2-propanol dehydrogenation process, cumene oxidation, and propene oxidation [112]. These fossil-based approaches constitute over 95% of global acetone production. In Europe, the average production of acetone generates 4.26 kgCO<sub>2</sub>e per kg of acetone, including EOL emissions. The results of the assessment for Austrian climate target compatibility, based on LCA data from Jiresten and Larsson [54], are outlined in the table below. Their input-output analysis indicates that the system effectively utilizes the heat generated during specific process steps, which suffices to maintain the low operational temperatures.

Table 28: Compatibility of CO<sub>2</sub> bio-fermentation to acetone

Compatibility Criteria		2030	2040	
		all sources	biogenic	fos./geo.
Availability	<i>TRL 5</i>	✗	✓	✓
Substitution 2030	$\frac{E_{CCU}}{E_{substitute}} = 14\%$	✓	✓	✗
CCU emissions 2040	$E_{CCU} = -0.39 \frac{kg CO_2e}{kg CO_2 utilized}$			

Given its current stage of development, it is anticipated that this technology will not be commercially available by 2030, but rather in 2040. In terms of substitution criteria, it meets the Austrian climate target compatibility, and the utilization of biogenic CO<sub>2</sub> even contributes to CDR, based on the possibility of mid-term sequestration.



## 5 Potential of CCU in Austria

Quantifying the potential of CCU in Austria requires allocating the available CO<sub>2</sub> emissions from domestic point sources to suitable CC technologies, and subsequently adapting these technologies to conceivable utilization options. The data compiled by Hochmeister et al. [8] serve as a basis for this analysis, offering insights into the volume of emissions from point sources and identifying industry-specific CO<sub>2</sub> concentrations in their exhaust gases. Furthermore, a progressive calculation scenario helps to trace the origin of carbon dioxide from industrial processes in the years 2030 and 2040. The following table shows the expected industrial CO<sub>2</sub> emissions in 2030 and their origins, categorized into 28 sub-sectors of the sectors industry and energy.

Table 29: Sectoral distribution of CO<sub>2</sub> emissions in 2030, CO<sub>2</sub> exhaust concentrations and origins [8]

Sector (branch)	Total emissions [ktCO <sub>2</sub> e]	CO <sub>2</sub> concentration [%]	Geogenic CO <sub>2</sub> [ktCO <sub>2</sub> e]	Fossil CO <sub>2</sub> [ktCO <sub>2</sub> e]	Biogenic CO <sub>2</sub> [ktCO <sub>2</sub> e]
Primary steel production	7759	13-40	0	6640	1119
Pulp and paper	5292	7-20	0	469	4823
Natural gas CHP	3382	3-5	0	3139	242
Cement	2828	14-33	1770	1034	25
MSWI	2662	9.1-10.2	0	1384	1278
Reffinery	2272	10-15	0	2272	0
Biomasse CHP	1780	3-14	0	0	1780
Wood and wood products	828	14	0	43	785
Lime production	722	21	314	378	29
Bricks	495	18	216	259	20
Compressor stations	398	3-5	0	370	29
Chemical industry	394	7-10	0	366	28
Methanol	329	18-20	0	114	215
Ammonia	258	98-100	0	90	169
Magnesia	255	14-33	167	82	6
Food and beverage	227	7-10	0	170	58
Glass production	218	13	39	167	13
Biomass heating	202	3-14	0	0	202
Secondary steel making	193	40	0	106	87
Bioethanol	120	98-99	0	0	120
Iron and steel processing	89	7-10	0	82	7
Alumina	86	3-10	0	57	29
Machinery	49	7-10	0	31	18
Natural gas storage	39	3-5	0	36	3
Gas processing plants	36	96-99	0	36	0
Copper	33	7-10	0	22	11
Nitric acid, urea, fertilizer	0.38	98-100	0.0	0.13	0.25
Natural gas heating	0.029	7-10	0.00	0.029	0.00

The domestic industrial emissions projected for 2040, based on the progressive calculation scenario applied by Hochmeister et al. [8], are listed in Table 30.

Table 30: Sectoral distribution of CO<sub>2</sub> emissions in 2040, CO<sub>2</sub> exhaust concentrations and origins [8]

Sector (branch)	Total emissions [ktCO <sub>2</sub> e]	CO <sub>2</sub> concentration [%]	Geogenic CO <sub>2</sub> [ktCO <sub>2</sub> e]	Fossil CO <sub>2</sub> [ktCO <sub>2</sub> e]	Biogenic CO <sub>2</sub> [ktCO <sub>2</sub> e]
Pulp and paper	4920	7-20	0	0	4920
Cement	2676	14-33	1770	883	24
MSWI	1952	9.1-10.2	0	1015	937
Biomass CHP	1722	3-14	0	0	1722
Wood and wood products	826	14	0	0	826
Primary steel production	550	13-40	0	0	550
Chemical industry	386	7-10	0	0	386
Lime production	341	21	314	0	27
Biomass heating	236	3-14	0	0	236
Bricks	234	18	216	0	18
Secondary steel making	193	40	0	0	193
Magnesia	183	14-33	167	0	16
Food and beverage	171	7-10	0	0	171
Natural gas CHP	133	3-5	0	0	133
Bio-ethanol	120	98-99	0	0	120
Glass production	50	13	48	0	3
Alumina	46	3-10	0	0	46
Machinery	28	7-10	0	0	28
Iron and steel processing	24	7-10	0	0	24
Gas processing plants	18	96-99	0	18	0
Copper	18	7-10	0	0	18
Compressor	13	3-5	0	0	13
Ammonia	2.4	98-100	0	0	2.4
Natural gas storage	1.3	3-5	0	0	1.3
Nitric acid, urea, fertilizer	0.14	98-100	0	0	0.14
Natural gas heating	0.0019	7-10	0	0	0.0019

Carbon dioxide from these industrial sectors can serve as a raw material in CCU processes. Technology-specific emission factors and a comparison with emissions associated with manufacturing equivalent conventional products, enable the estimation of reduction potentials. The approach for quantifying the potential of CO<sub>2</sub> from point sources as an alternative raw material through CCU implementation in Austria is elaborated in the following subchapter.

## 5.1 Estimating CCU potentials

The resulting GHG emissions corresponding to a CCU technology  $Q_{CCU}$  (in ktCO<sub>2</sub>e) are determined using Equation 6,

$$Q_{CCU} = Q_{source} * E_{CCU} \quad \text{Equation 6}$$

where  $Q_{Source}$  is the amount of utilized CO<sub>2</sub> (in ktCO<sub>2</sub>) from a point source,  $E_{CCU}$  is the emissions factor of the CCU technology (kgCO<sub>2</sub>e/kg CO<sub>2</sub> utilized).

Depending on the CO<sub>2</sub> concentration in the exhaust gas of a primary process, as given in Tables 29 and 30, an appropriate recovery method must be selected. Literature provides an array of CC technologies, typical application examples and ranges of input concentrations, as shown in Table 31. Furthermore, to quantify the resulting GHG emissions of a selected recovery method, emission factors are assumed, based on energy consumptions as detailed earlier in Chapter 2.3. Given that the information on CO<sub>2</sub> concentrations for both, the exhaust gases and input streams into recovery systems, refers to ranges, the derived CC emission factors are to be regarded as average values.

Table 31: Carbon capture technologies and their typical CO<sub>2</sub> input concentrations and applications

Carbon capture technology	CO <sub>2</sub> conc. [%]	Application examples	Ref.	$E_{\text{capture process}}$ [kgCO <sub>2</sub> e/kgCO <sub>2</sub> utilized]
Chemical absorption	<30	SMR, cement, lime, steel blast furnace, refineries, biomass power plant, pulp & paper	[15]	0.133
Physical adsorption	>40	Syngas, iron and steel industry, SMR, landfill gas,	[15],	0.0075
4-step cycle	>10	NG sweetening	[22]	0.0150
Membrane separation	>20	NG sweetening, biogas upgrading	[28], [114]	0.00417
Cryogenic capture	>50	SMR, cement, lime, steel blast furnace, refineries, waste	[15],	0.0128
Physical adsorption and cryogenic purification	>15	incineration, biomass power plant, pulp & paper	[33]	0.0203

Emission factors regarding to the utilization part of the investigated technologies from Chapter 4 are presented in the following table. In addition, emission factors for conventional products, including EOL-emissions, are provided for comparison.

Table 32: Emission factors for investigated technologies and conventional products to substitute

Technology	$E_{2030}$ [kgCO <sub>2</sub> e/ kgCO <sub>2</sub> utilized]	$E_{2040}$ [kgCO <sub>2</sub> e/ kgCO <sub>2</sub> utilized]	$E_{Substitute}$ [kgCO <sub>2</sub> e/ kgCO <sub>2</sub> utilized]
Carbonation of steel slag blocks	-0.833	-0.833	1.054
High gravity steel slag carbonation	-0.979	-0.979	2.07
Urea via SEWGS	0.169	0.169	2.37
DMM via direct synthesis	0.706	0.331	1.21
FTS with syngas via rWGS	0.421	0.113	0.949
CH <sub>4</sub> via direct hydrogenation	0.753	0.182	1.17
MeOH via direct hydrogenation	0.561	0.146	1.60
Electrochemical reduction ethylene	0.201	0.201	1.34
Polyol via propylene oxide	34.7	34.7	40.2
Acetone via bio-fermentation	-0.00237	-0.387	0.909

Preference is accorded to utilization pathways that, wherever feasible, exhibit one or more of the following characteristics: (1) CCU products sharing the same market as those derived from the primary process; (2) CCU products that can be reintegrated into the primary process itself; (3) the utilization of by-products or waste materials from the primary process, such as CRW or slags; (4) the long-term sequestration of fossil/geogenic CO<sub>2</sub>, particularly in sectors where such CO<sub>2</sub> is expected to persist in 2040.

After selecting suitable technologies for adapting the primary process, the potential GHG savings  $Q_{Savings}$  (in in ktCO<sub>2</sub>e) achievable through substituting conventional products with CCU-manufactured alternatives can be quantified by a straightforward subtraction, as demonstrated in Equation 7.

$$Q_{Savings} = Q_{Substitute} - Q_{CCU} \quad \text{Equation 7}$$

In this context, emissions associated with the production of the equivalent amount of conventional product ( $Q_{Substitute}$  in ktCO<sub>2</sub>e) are calculated similar to Equation 6, using the relevant emission factors  $E_{Substitute}$  in kgCO<sub>2</sub>e/kg CO<sub>2</sub> utilized.

To provide a comprehensive overview of the calculations and the interpretation of ensuing results, two different cases of involving CCU technologies within domestic industry sectors are examined in the following subchapters.

### 5.1.1 MSWI sector

First, the case of involving CCU technologies within the municipal solid waste incineration sector (MSWI) for the target year 2040 is presented. As indicated in Table 30, the corresponding exhaust gas contains 9.1-10.2 % of carbon dioxide, therefore choosing chemical absorption as the CO<sub>2</sub> capture technology. This step is followed by carbonation of steel slag blocks as the utilization method. The GHG emissions resulting from the deployment of this CCU technology are calculated based on Equation 6, detailed as follows:

$$Q_{CCU} = Q_{Source} * E_{CCU} = 1952 \text{ ktCO}_2\text{e} * \left( 0.133 \frac{\text{ktCO}_2\text{e}}{\text{ktCO}_2\text{utilized}} - 0.833 \frac{\text{ktCO}_2\text{e}}{\text{ktCO}_2\text{utilized}} \right)$$

$$= -1367 \text{ ktCO}_2\text{e}$$

Negative  $Q_{CCU}$  emissions may be viewed as a mitigation for the primary process, as illustrated in Figure 32.

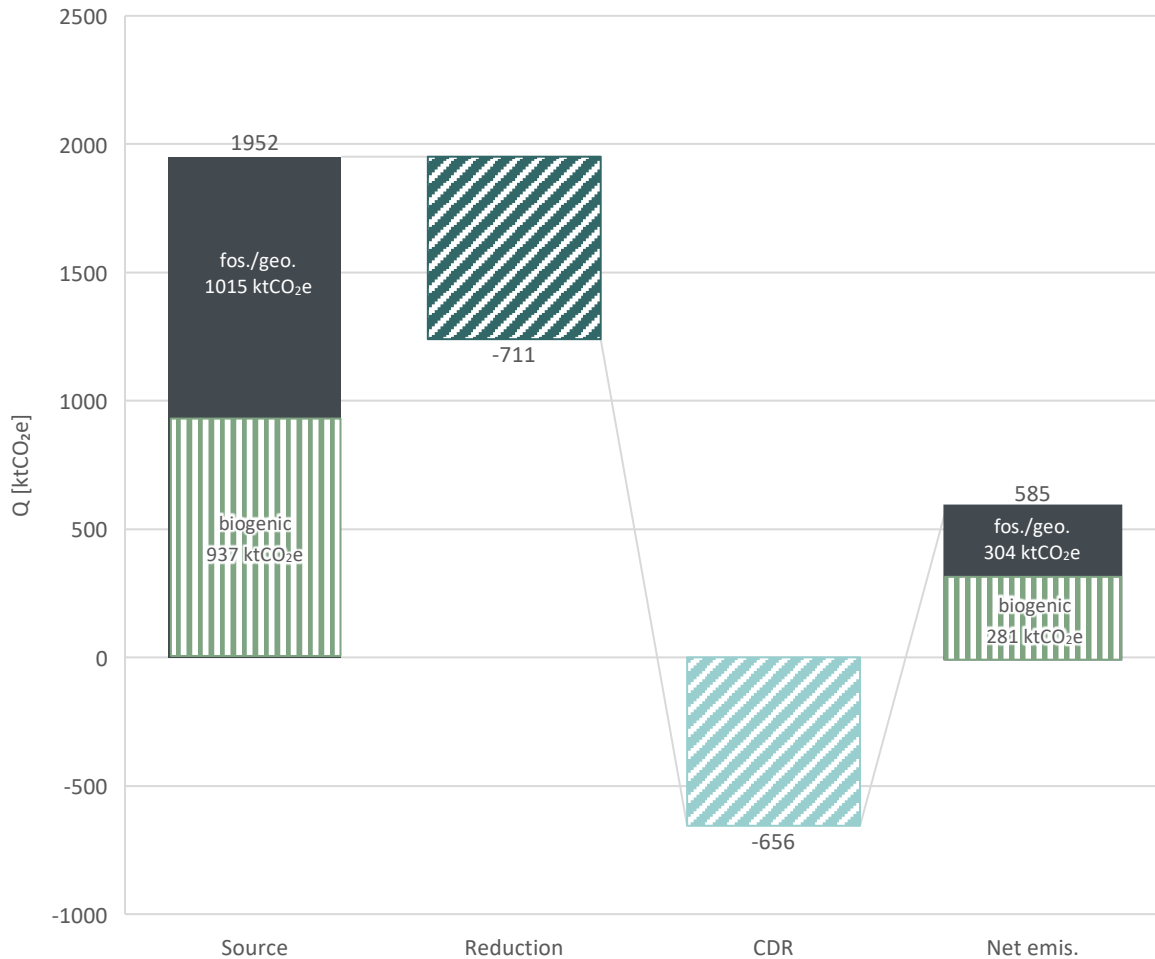


Figure 32: Emissions of MSWI sector combined with CCU technologies (chemical absorption via MEA and carbonation of steel slag blocks) in 2040

Analysis of the CO<sub>2</sub> origin in conjunction with the interpretation of  $E_{CCU}$  values outlined in Chapter 2.6, indicates that -656 ktCO<sub>2</sub>e from biogenic sources can be classified as CDR, while -711 ktCO<sub>2</sub>e from fossil and geogenic sources are considered as reduced. After adopting the CCU technology to the primary MSWI sector, total emissions amount to 585 ktCO<sub>2</sub>e, with 48% from biogenic origins and thus re-entering the carbon cycle, whereas the remaining 52% contribute to atmospheric accumulation.

Compared to conventionally produced Portland cement-based construction blocks, the selected CCU route offers potential emission savings, calculated according to Equation 7.

$$\begin{aligned}
 Q_{Savings} &= Q_{Substitute} - Q_{CCU} = 1952 \text{ ktCO}_2e * 1.054 \frac{\text{ktCO}_2e}{\text{ktCO}_2\text{utilized}} + 1367 \text{ ktCO}_2e \\
 &= 3425 \text{ ktCO}_2e
 \end{aligned}$$

This demonstrates that through the implementation of the selected carbonation route, carbon dioxide from the MSWI sector can be repurposed to produce alternative construction building blocks, leading to net savings of 3425 ktCO<sub>2</sub>e when substituting conventional products.

### 5.1.2 Methanol sector

The CO<sub>2</sub> concentration in exhaust gases emitted in the methanol sector ranges between 18 and 20%, leading to the selection of combined physical adsorption with cryogenic carbon capture. Given the significant proportion of biogenic carbon dioxide this sector presents an appealing opportunity for utilization methods that result in products with short-term CO<sub>2</sub> sequestration properties, such as fuels or chemicals. The direct hydrogenation of carbon dioxide enables to produce an equivalent product and the amount of GHG emitted by implementing this technology in 2030 are calculated by Equation 6:

$$\begin{aligned}
 Q_{CCU} &= Q_{Source} * E_{CCU} = 329 \text{ ktCO}_2e * \left( 0.0203 \frac{\text{ktCO}_2e}{\text{ktCO}_2\text{utilized}} + 0.561 \frac{\text{ktCO}_2e}{\text{ktCO}_2\text{utilized}} \right) \\
 &= 191 \text{ ktCO}_2e
 \end{aligned}$$

Positive  $Q_{CCU}$  emissions fail to mitigate the impact of the primary process, as shown in Figure 33.

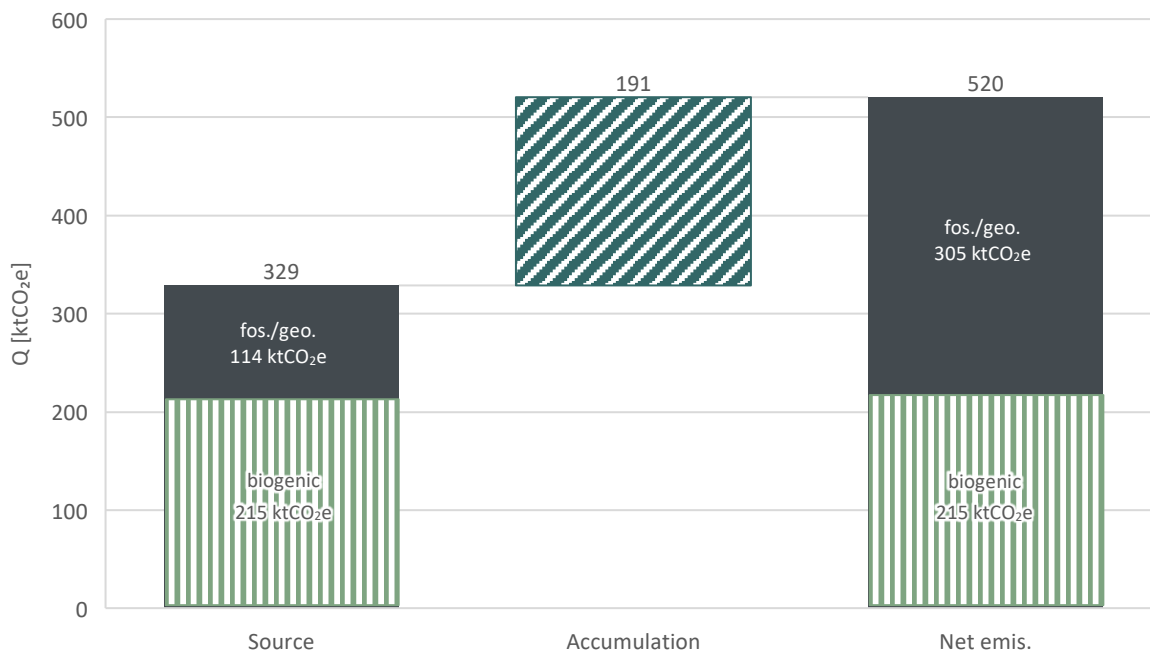


Figure 33: Emissions of methanol sector combined with CCU technologies (physical adsorption and cryogenic carbon capture and direct hydrogenation to methanol) in 2030

The net emissions of 520 ktCO<sub>2</sub>e are derived from both, the primary and the CCU process. This example highlights the necessity of evaluating CCU products in comparison to their

conventionally manufactured counterparts. The substitution of conventional methanol by this alternative, offers the reduction potential, calculated by Equation 6:

$$Q_{Savings} = Q_{Substitute} - Q_{CCU} = 329 \text{ ktCO}_2\text{e} * 1.60 \frac{\text{ktCO}_2\text{e}}{\text{ktCO}_2\text{utilized}} - 191 \text{ ktCO}_2\text{e} = 335 \text{ ktCO}_2\text{e}$$

## 5.2 Resulting reduction potentials for Austria's industrial sectors

The sectors listed in Tables 29 and 30 summarize domestic CO<sub>2</sub> point sources, which are matched with conceivable CCU pathways following the outlined approach. Resulting GHG emissions related to the alternative production methods, as well as their reduction potentials in contrast to their conventional counterparts are presented in the following tables.

Table 33: Conceivable CCU paths for Austrian emitters in 2030, CCU emissions and reduction potentials

Sector (branch)	Capture technology	Utilization technology	Q <sub>CCU</sub> [ktCO <sub>2</sub> e]	Q <sub>Savings</sub> [ktCO <sub>2</sub> e]
Pulp and paper	Chemical abs.	FTS & rWGS	2933	2089
Cement	No capture	High gravity carb.	-2768	8622
MSWI	Chemical abs.	Block carbonation	-1864	4670
Biomass CHP	Chemical abs.	Hydrogenation CH <sub>4</sub>	1576	501
Wood and wood products	PSA & cryogenic	Hydrogenation MeOH	575	747
Primary steel production	PSA & cryogenic	Block carbonation	-6307	14484
Chemical industry	Chemical abs.	Hydrogenation MeOH	274	356
Lime production	No capture	High gravity carb.	-706	2201
Biomass heating	Chemical abs.	Hydrogenation CH <sub>4</sub>	179	56,8
Bricks	PSA & cryogenic	Block carbonation	-402	924
Secondary steel making	Cryogenic	Block carbonation	-159	362
Magnesia	No capture	High gravity carb.	-250	778
Food and beverage	Poly. membrane	Hydrogenation CH <sub>4</sub>	201	64.0
Natural gas CHP	Chemical abs.	Hydrogenation CH <sub>4</sub>	2995	953
Bio-ethanol	No capture	Hydrogenation MeOH	68,9	123
Glass production	Chemical abs.	Block carbonation	-153	383
Alumina	Chemical abs.	Block carbonation	-60.0	150
Machinery	Chemical abs.	FTS & rWGS	27.3	19.5
Iron and steel processing	No capture	High gravity carb.	-87.1	271
Gas processing plants	No capture	Hydrogenation CH <sub>4</sub>	27.1	14.9
Copper	Chemical abs.	Block carbonation	-23.2	58.2
Compressor	Poly. membrane	Hydrogenation CH <sub>4</sub>	353	112
Ammonia	No capture	CO <sub>2</sub> -based polyols	8958	1413
Natural gas storage	Poly. membrane	Hydrogenation CH <sub>4</sub>	34.2	10.9
Nitric acid, urea, fertilizer	No capture	Hydrogenation MeOH	0.222	0.395
Natural gas heating	Chemical abs.	Hydrogenation CH <sub>4</sub>	0.0254	0.0081
Refinery	Chemical abs.	Block carbonation	-1591	3986
Methanol	PSA & cryogenic	Hydrogenation MeOH	191	335

Table 34 lists possible CCU pathways for Austrian emission sectors for the target year 2040.

Table 34: Conceivable CCU paths for Austrian emitters in 2040, CCU emissions and reduction potentials

Sector (branch)	Capture technology	Utilization technology	Q <sub>CCU</sub> [ktCO <sub>2</sub> e]	Q <sub>Savings</sub> [ktCO <sub>2</sub> e]
Pulp and paper	Chemical abs.	FTS & rWGS	1213	3457
Cement	No capture	High gravity carb.	-2619	8158
MSWI	Chemical abs.	Block carbonation	-1367	3425
Biomass CHP	Chemical abs.	Hydrogenation CH <sub>4</sub>	542	1468
Wood and wood products	PSA & cryogenic	Hydrogenation MeOH	230	1088
Primary steel production	PSA & cryogenic	Block carbonation	-447	1026
Chemical industry	Chemical abs.	Bio-fermentation	-98.1	449
Lime production	No capture	High gravity carb.	-334	1039
Biomass heating	Chemical abs.	Hydrogenation CH <sub>4</sub>	74.1	201
Bricks	PSA & cryogenic	Block carbonation	-190	436
Secondary steel making	Cryogenic	FTS & rWGS	23.3	159
Magnesia	No capture	High gravity carb.	-180	559
Food and beverage	Poly. membrane	Hydrogenation CH <sub>4</sub>	53.8	146
Natural gas CHP	Chemical abs.	Hydrogenation CH <sub>4</sub>	42.0	114
Bio-ethanol	No capture	DMM synthesis	41.3	104
Glass production	Chemical abs.	Block carbonation	-35.4	88.6
Alumina	Chemical abs.	Block carbonation	-32.5	81.5
Machinery	Chemical abs.	FTS & rWGS	6.99	19.9
Iron and steel processing	No capture	High gravity carb.	-23.7	73.8
Gas processing plants	No capture	Hydrogenation CH <sub>4</sub>	3.27	17.8
Copper	Chemical abs.	ER to ethylene	6.01	18.1
Compressor	Poly. membrane	Hydrogenation CH <sub>4</sub>	4.08	11.1
Ammonia	No capture	CO <sub>2</sub> -based polyols	82.5	13.0
Natural gas storage	Poly. membrane	Hydrogenation CH <sub>4</sub>	0.396	1.07
Nitric acid, urea, fertilizer	No capture	Bio-fermentation	-0.0515	0.176
Natural gas heating	Chemical abs.	Hydrogenation CH <sub>4</sub>	0.00059	0.0016

This selection exemplifies the impact of CCU implementations across different industrial emitters. For certain sectors, such as the bricks sector or the biomass heating sector, identifying an appropriate CO<sub>2</sub> utilization pathway to produce a suitable product appears straightforward. Conversely, in other sectors that offer a wider product spectrum, multiple CCU technologies might be applicable. For example, in the chemical industry possibilities extend beyond the direct hydrogenation to methanol and involves CO<sub>2</sub>-based production routes for viable chemicals like ethylene, acetone, polyols, etc. The technology specific emission factors calculated in this thesis, detailed in Table 32, facilitate an estimation of the emissions impact and reduction potential by adopting the investigated technologies to an industrial point source.

The potential for GHG savings by substituting conventional products with CCU-derived alternatives initially seems capable of addressing sectors with hard-to-abate emissions. The proposed source to CCU product routes result in total savings potentials of ~44 million tonnes CO<sub>2</sub>e in 2030 and ~22 million tonnes CO<sub>2</sub>e in 2040, theoretically. However, these optimistic



findings do not take into account several limiting factors that could significantly alter their impact. Examples for limiting factors are discussed in the following.

Table 35: Examples and description of limiting aspects on theoretical CO<sub>2</sub> saving potentials

Limiting factor	Description
Raw materials	Adopting a circular economy approach, the utilization of waste as secondary raw materials for carbonation processes is indeed advantageous. However, the actual availability of these materials must be accurately quantified. The variability in the supply of metal oxides, influenced by the primary processes, has led to a substantial body of research aimed at analyzing the composition of industrial waste and its theoretical CO <sub>2</sub> fixation capacities [108]-[119].
Energy	Another challenge is the significant energy consumption of CCU technologies, as illustrated in Figure 18. For example, adapting the wood & wood products sector to the recommended CCU pathway in 2040 requires about 8.2 TWh additional energy from renewable sources.
Hydrogen	The production of green hydrogen as a crucial reaction partner in many chemical CCU routes is energy intensive and the projected electrolysis capacity in 2030 is limited to 1 GW [5]. Based on LCA data [42] and electricity demands of 50 kWh per kg H <sub>2</sub> [129], the conversion of CO <sub>2</sub> available from the biomass CHP sector into synthetic natural gas would result in 1.9 GW.
Capacity	Due to the development stage of the investigated technologies, capacity limits are widely unknown, and assumptions of the primal LCA-studies retain in this work, also after execution of the harmonization. Calculations based on LCA data showed that the high gravity carbonation is an energy efficient option, compared to other CCU technologies. However in this case, the regarding conversion technology deals with capacity limitations of 75 to 150 kgCO <sub>2</sub> /day [58].
Product demand	Prior to CCU implementation, it is crucial to assess the market landscape and demand for the resultant products to ensure their commercial viability and an emissions reduction success by substituting conventional products.
CO <sub>2</sub> dispersion	For short-lived CCU products, although subsequent recovery could reveal new artificial carbon circulations, decentralized CO <sub>2</sub> releases, such as through the combustion of alternative fuels, would necessitate the use of direct air capture technologies.

These limitations are inherently specific to processes of both, the primary and CCU systems. Consequently, to estimate the real impact of adopting existing facilities of the energy and industrial sectors by CCU technologies, individual case studies are indispensable.

## 6 Conclusions

This thesis investigates conceivable CCU pathways for commercial deployment in Austria by either 2030 or 2040, with focus on technologies that transform carbon dioxide captured from point sources within the domestic industrial and energy sectors into viable alternatives to conventional products. A comprehensive literature review reveals appropriate CO<sub>2</sub> utilization methods, their process flows, and possible operation conditions. Overall, ten distinct technologies are identified, categorized as follows: six technologies within chemical conversion methods, two pertaining to mineral carbonation routes, and one each within bio-chemical and electrochemical pathways. The found technologies are evaluated for compatibility with Austrian climate targets and subsequently assessed for their potential in reducing GHG emissions.

The analysis is grounded in LCA studies that address the environmental aspects of CCU technologies and quantify the associated GHG emissions. Given the diversity of processes and solutions, along with the varied assumptions and conditions across these studies, a harmonization approach is applied. This ensures alignment with Austrian standards and enhances the comparability between innovative technologies and traditional production methods. The findings are presented as emission factors, detailing the amount of GHG emitted or sequestered per unit of CO<sub>2</sub> input for each technology.

National climate target compatibility is evaluated in accordance with NECPs [5]. Within this framework, a substitution criterion is established for the target year 2030, setting an upper boundary for CCU emissions at 54% relative to conventional counterparts. For the target year 2040, the emissions criterion mandates net-zero emissions. Additionally, TRLs are specified as majority criteria for both target years, requiring at least TRL 6 for availability by 2030 and at least TRL 4 by 2040. Four out of ten technologies meet Austria's 2030 climate targets: (1) carbonation of steel slag blocks, (2) high gravity steel slag carbonation, (3) direct hydrogenation to methanol, and (4) urea synthesis via SEWGS. Both carbonation technologies also meet the climate target compatibility for 2040 when utilizing biogenic CO<sub>2</sub>, as it is part of the natural carbon cycle. CO<sub>2</sub>-based bio-fermentation to acetone also satisfies these criteria. The corresponding emission factors indicate CDR, categorizing the resulting products as carbon sinks and allocating the greatest potential towards the carbonation routes, due to long-term sequestration characteristics. Since the 2040 target seeks to prevent further accumulation of fossil or geogenic carbon dioxide in the atmosphere, these sources are not considered as suitable feedstocks for CCU applications, due to potential re-emissions after the product's life cycle or the conversion process itself, effectively shifting emissions from primary to CCU processes. However, the substitution approach indicates that all investigated CCU technologies may act as GHG reduction measures, even if the utilized CO<sub>2</sub> stems from fossil or geogenic origins.

The projected availability of carbon dioxide for CCU technologies from Austrian industrial and energy sector emitters is estimated at 31 million tonnes in 2030 and 15 million tonnes in 2040, derived from comprehensive data collections and progressive calculation scenarios [8].

Aspects such as the origin of CO<sub>2</sub>, typical concentrations in exhaust gases, and sector-specific conditions inform the recommendation of suitable CCU pathways for each sector. This procedure culminates in the quantification of related GHG emissions and reduction potentials, leveraging the technology-specific emission factors. The proposed adaptations reveal a total CO<sub>2</sub> savings potential of approximately 44 million tonnes by 2030 and around 22 million tonnes by 2040, offering a strategy to mitigate emissions from sectors where abatement is particularly challenging. However, these results are preliminary and serve as an initial step in assessing the real reduction potential, as they do not account for a number of limiting factors.

The assessment of real reduction potentials through the implementation of CCU technologies is challenged by the diversity of both, the primary production sites and the CCU routes. CCU encompasses a wide range of capture and conversion processes as well as product-specific properties and utilizing CO<sub>2</sub> as a climate mitigation option is no homogenous technology. The requirements for energy, hydrogen, and other raw materials vary significantly and pose critical constraints. Additional aspects that determine the effectiveness of the technologies include consideration about CO<sub>2</sub> conversion capacities, possible plant locations and supply infrastructure. Although the theoretical GHG reduction potentials discussed in this thesis seem promising, these limiting factors could not be taken into account as individual and more detailed analysis of specific combinations are required.

The presented technologies enable operators of the Austrian industry and energy sectors to devise tailored solutions within their framework, taking a step towards minimizing GHG emissions that are difficult to abate. Associated CCU emissions and the reduction potentials from substituting conventional products underscore the value of CO<sub>2</sub> from point sources as an alternative raw material. The selection of suitable CCU technologies should emphasize the prevention of atmospheric accumulation of carbon dioxide from geogenic and fossil origins. In these cases technologies capable to ensure long-term sequestration are recommended to align with national climate target strategies.

## 7 Appendices

### 7.1 References

- [1] "Project CaCTUS." Accessed: Jul. 17, 2023. [Online]. Available: <https://project-cactus.at>
- [2] "European Climate Law," *Official Journal of the European Union*, vol. 2021, 2021.
- [3] Österreichische Bundesregierung, "Aus Verantwortung für Österreich: Zusammenfassung des Regierungsprogrammes 2020-2024," 2020.
- [4] Bundesministerium für Nachhaltigkeit und Tourismus, "Langfriststrategie 2050 - Österreich," 2019.
- [5] Bundesministerium für Nachhaltigkeit und Tourismus, "Integrierter nationaler Energie- und Klimaplan für Österreich," *Report*, no. 663, p. 272, 2019.
- [6] C. Diendorfer *et al.*, "Klimaneutralität Österreichs bis 2040," 2021.
- [7] Umweltbundesamt, "Austria's National Inventory Report 2023," 2023.
- [8] S. Hochmeister *et al.*, "Carbon Management für ein klimaneutrales Österreich," EnInnov, 2024.
- [9] Voestalpine, "Corporate Responsibility Report 2021," 2021.
- [10] United States Accountability Office, "United States Government Accountability Office Decarbonization Status, Challenges, and Policy Options for Carbon Capture, Utilization, and Storage," 2022.
- [11] P. Wolf-Zöllner, H. Langitz, and M. Lehner, "CCCA Fact Sheet Carbon Capture," 2024.
- [12] R. M. Cuéllar-Franca and A. Azapagic, "Carbon capture, storage and utilisation technologies: A critical analysis and comparison of their life cycle environmental impacts," *Journal of CO2 Utilization*, vol. 9, pp. 82–102, 2015, doi: 10.1016/j.jcou.2014.12.001.
- [13] B. Dziejarski, R. Krzyżyńska, and K. Andersson, "Current status of carbon capture, utilization, and storage technologies in the global economy: A survey of technical assessment," *Fuel*, vol. 342, no. December 2022, 2023, doi: 10.1016/j.fuel.2023.127776.
- [14] B. Dziejarski, R. Krzyżyńska, and K. Andersson, "Current status of carbon capture, utilization, and storage technologies in the global economy: A survey of technical assessment," *Fuel*, vol. 342, no. February, 2023, doi: 10.1016/j.fuel.2023.127776.

- [15] H. Barlow, S. Shahi, and M. Loughrey, "State of the art: Carbon Capture Storage Technologies 2023," 2023.
- [16] W. Elliott, A. Benz, J. Gibbins, and S. Michailos, "An open-access FEED study for a post-combustion CO<sub>2</sub> capture plant retrofit to a CCGT," *SSRN Electronic Journal*, no. October, 2022, doi: 10.2139/ssrn.4286280.
- [17] J. A. Garcia, M. Villen-Guzman, J. M. Rodriguez-Maroto, and J. M. Paz-Garcia, "Technical analysis of CO<sub>2</sub> capture pathways and technologies," *J Environ Chem Eng*, vol. 10, no. 5, p. 108470, 2022, doi: 10.1016/j.jece.2022.108470.
- [18] C. Song, Q. Liu, S. Deng, H. Li, and Y. Kitamura, "Cryogenic-based CO<sub>2</sub> capture technologies: State-of-the-art developments and current challenges," *Renewable and Sustainable Energy Reviews*, vol. 101, no. November 2018, pp. 265–278, 2019, doi: 10.1016/j.rser.2018.11.018.
- [19] B. Dziejarski, R. Krzyżyńska, and K. Andersson, "Current status of carbon capture, utilization, and storage technologies in the global economy: A survey of technical assessment," *Fuel*, vol. 342, no. February, 2023, doi: 10.1016/j.fuel.2023.127776.
- [20] D. A. Bell, B. F. Towler, and M. Fan, *Coal Gasification and Its Applications*. 2011. doi: 10.1016/b978-0-8155-2049-8.10015-4.
- [21] C. W. Skarstrom, "Method and apparatus for fractionating gaseous mixtures by adsorption," 1960
- [22] J. H. Park, H. T. Beum, J. N. Kim, and S. H. Cho, "Numerical analysis on the power consumption of the PSA process for recovering CO<sub>2</sub> from flue gas," *Ind Eng Chem Res*, vol. 41, no. 16, pp. 4122–4131, 2002, doi: 10.1021/ie010716i.
- [23] D. Bahamon, A. Díaz-Márquez, P. Gamallo, and L. F. Vega, "Energetic evaluation of swing adsorption processes for CO<sub>2</sub> capture in selected MOFs and zeolites: Effect of impurities," *Chemical Engineering Journal*, vol. 342, no. December 2017, pp. 458–473, 2018, doi: 10.1016/j.cej.2018.02.094.
- [24] S. Cho, J.-H. Park, H.-T. Beum, S.-S. Han, and J.-N. Kim, "A 2-stage PSA process for the recovery of CO<sub>2</sub> from flue gas and its power consumption," *Studies in Surface Science and Catalysis - STUD SURF SCI CATAL*, vol. 153, pp. 405–410, Dec. 2004, doi: 10.1016/S0167-2991(04)80287-8.
- [25] L. Wang *et al.*, "CO<sub>2</sub> Capture from Flue Gas in an Existing Coal-Fired Power Plant by Two Successive Pilot-Scale VPSA Units," *Ind Eng Chem Res*, vol. 52, pp. 7947–7955, Jun. 2013, doi: 10.1021/ie4009716.

- [26] M. K. Mondal, H. K. Balsora, and P. Varshney, "Progress and trends in CO<sub>2</sub> capture/separation technologies: A review," *Energy*, vol. 46, no. 1, pp. 431–441, 2012, doi: 10.1016/j.energy.2012.08.006.
- [27] R. Bounaceur, N. Lape, D. Roizard, C. Vallieres, and E. Favre, "Membrane processes for post-combustion carbon dioxide capture: A parametric study," *Energy*, vol. 31, no. 14, pp. 2556–2570, 2006, doi: 10.1016/j.energy.2005.10.038.
- [28] Z. Dai and L. Deng, "Membranes for CO<sub>2</sub> capture and separation: Progress in research and development for industrial applications," *Sep Purif Technol*, vol. 335, no. November 2023, p. 126022, 2023, doi: 10.1016/j.seppur.2023.126022.
- [29] A. Brunetti, F. Scura, G. Barbieri, and E. Drioli, "Membrane technologies for CO<sub>2</sub> separation," *J Memb Sci*, vol. 359, no. 1–2, pp. 115–125, 2010, doi: 10.1016/j.memsci.2009.11.040.
- [30] L. Baxter, A. Baxter, and S. Burt, "Cryogenic CO<sub>2</sub> capture as a cost-effective CO<sub>2</sub> capture process," *26th Annual International Pittsburgh Coal Conference 2009, PCC 2009*, vol. 1, no. January 2009, pp. 762–775, 2009.
- [31] M. J. Tuinier, M. Van Sint Annaland, and J. A. M. Kuipers, "A novel process for cryogenic CO<sub>2</sub> capture using dynamically operated packed beds-An experimental and numerical study," *International Journal of Greenhouse Gas Control*, vol. 5, no. 4, pp. 694–701, 2011, doi: 10.1016/j.ijggc.2010.11.011.
- [32] S. M. Safdarnejad, J. D. Hedengren, and L. L. Baxter, "Plant-level dynamic optimization of Cryogenic Carbon Capture with conventional and renewable power sources," *Appl Energy*, vol. 149, pp. 354–366, Jul. 2015, doi: 10.1016/j.apenergy.2015.03.100.
- [33] P. Feron, "Absorption-Based Post-Combustion Capture of Carbon Dioxide," Woodhead publishing series in energy, no. 101, 2016, ISBN: 9783131450715
- [34] A. Meisen and X. Shuai, "Research and development issues in CO<sub>2</sub> capture," *Energy Convers Manag*, vol. 38, no. SUPPL. 1, pp. 37–42, 1997, doi: 10.1016/s0196-8904(96)00242-7.
- [35] M. P. S. Santos and D. P. Hanak, "Carbon capture for decarbonisation of energy-intensive industries: a comparative review of techno-economic feasibility of solid looping cycles," *Front Chem Sci Eng*, vol. 16, no. 9, pp. 1291–1317, 2022, doi: 10.1007/s11705-022-2151-5.
- [36] United States Government Accountability Office, "Decarbonization," 2022.
- [37] M. Lehner, "Abscheidung, Nutzung und Speicherung von CO<sub>2</sub> als Maßnahme des Klimaschutzes, Vorlesungsteil: Carbon Capture and Utilization (CCU)," Montanuniversität Leoben, 2022.

- [38] A. A. Olajire, "A review of mineral carbonation technology in sequestration of CO<sub>2</sub>," *J Pet Sci Eng*, vol. 109, pp. 364–392, 2013, doi: 10.1016/j.petrol.2013.03.013.
- [39] C. A. Myers, T. Nakagaki, and K. Akutsu, "Quantification of the CO<sub>2</sub> mineralization potential of ironmaking and steelmaking slags under direct gas-solid reactions in flue gas," *International Journal of Greenhouse Gas Control*, vol. 87, 2018, pp. 100–111, 2019, doi: 10.1016/j.ijggc.2019.05.021.
- [40] F. Wang, D. Dreisinger, M. Jarvis, T. Hitchins, and D. Dyson, "Quantifying kinetics of mineralization of carbon dioxide by olivine under moderate conditions," *Chemical Engineering Journal*, vol. 360, pp. 452–463, 2019, doi: 10.1016/j.cej.2018.11.200.
- [41] H. Ostovari, L. Kuhrmann, F. Mayer, H. Minten, and A. Bardow, "Towards a European supply chain for CO<sub>2</sub> capture, utilization, and storage by mineralization: Insights from cost-optimal design," *Journal of CO<sub>2</sub> Utilization*, vol. 72, 2023, doi: 10.1016/j.jcou.2023.102496.
- [42] W. Hoppe, N. Thonemann, and S. Bringezu, "Life Cycle Assessment of Carbon Dioxide–Based Production of Methane and Methanol and Derived Polymers," *J Ind Ecol*, vol. 22, no. 2, pp. 327–340, 2018, doi: 10.1111/jiec.12583.
- [43] J. G. Speight, *Lange's Handbook of Chemistry*, 17th ed. Mc Graw Hill Education, 2017.
- [44] S. Rönsch *et al.*, "Review on methanation - From fundamentals to current projects," *Fuel*, vol. 166, pp. 276–296, 2016, doi: 10.1016/j.fuel.2015.10.111.
- [45] N. Thonemann and M. Pizzol, "Consequential life cycle assessment of carbon capture and utilization technologies within the chemical industry," *Energy Environ Sci*, vol. 12, no. 7, pp. 2253–2263, 2019, doi: 10.1039/c9ee00914k.
- [46] M. Hamidipour, N. Mostoufi, and R. Sotudeh-Gharebagh, "Modeling the synthesis section of an industrial urea plant," *Chemical Engineering Journal*, vol. 106, no. 3, pp. 249–260, 2005, doi: 10.1016/j.cej.2004.12.020.
- [47] N. Von Der Assen and A. Bardow, "Life cycle assessment of polyols for polyurethane production using CO<sub>2</sub> as feedstock: Insights from an industrial case study," *Green Chemistry*, vol. 16, no. 6, pp. 3272–3280, 2014, doi: 10.1039/c4gc00513a.
- [48] S. Nitopi *et al.*, "Progress and Perspectives of Electrochemical CO<sub>2</sub> Reduction on Copper in Aqueous Electrolyte," *Chem Rev*, vol. 119, no. 12, pp. 7610–7672, 2019, doi: 10.1021/acs.chemrev.8b00705.
- [49] J. Lin, Y. Zhang, P. Xu, and L. Chen, "CO<sub>2</sub> electrolysis: Advances and challenges in electrocatalyst engineering and reactor design," *Materials Reports: Energy*, vol. 3, no. 2, p. 100194, 2023, doi: 10.1016/j.matre.2023.100194.

- [50] H. H. Khoo, I. Halim, and A. D. Handoko, "LCA of electrochemical reduction of CO<sub>2</sub> to ethylene," *Journal of CO<sub>2</sub> Utilization*, vol. 41, no. May, p. 101229, 2020, doi: 10.1016/j.jcou.2020.101229.
- [51] B. Hüsing, H. Aichinger, C. Moll, F. Marscheider-Weidemann, and Wietschel, "Technologie- und Marktstudie: Übersicht über Technologien zur bioinspirierten CO<sub>2</sub>-Fixierung und -Nutzung sowie der Akteure in Baden-Württemberg," p. 143, 2020.
- [52] M. Kumar, S. Sundaram, E. Gnansounou, C. Larroche, and I. S. Thakur, "Carbon dioxide capture, storage and production of biofuel and biomaterials by bacteria: A review," *Bioresour Technol*, vol. 247, no. September 2017, pp. 1059–1068, 2018, doi: 10.1016/j.biortech.2017.09.050.
- [53] C. A. Cotton, C. Edlich-Muth, and A. Bar-Even, "Reinforcing carbon fixation: CO<sub>2</sub> reduction replacing and supporting carboxylation," *Curr Opin Biotechnol*, vol. 49, pp. 49–56, 2018, doi: 10.1016/j.copbio.2017.07.014.
- [54] E. Jiresten and O. Larsson, "Life Cycle Assessment of acetone production from captured carbon dioxide Using bio-fermentation at the PYROCO<sub>2</sub>-pilot plant," 2022.
- [55] M. Mazzotti *et al.*, "Mineral carbonation and industrial uses of carbon dioxide," in *IPCC special report on carbon dioxide capture and storage*, Cambridge University Press, 2005.
- [56] C. Hepburn *et al.*, "The technological and economic prospects for CO<sub>2</sub> utilization and removal," *Nature*, vol. 575, no. 7781, pp. 87–97, 2019, doi: 10.1038/s41586-019-1681-6.
- [57] A. Sanna, M. Uibu, G. Caramanna, R. Kuusik, and M. M. Maroto-Valer, "A review of mineral carbonation technologies to sequester CO<sub>2</sub>," *Chem Soc Rev*, vol. 43, no. 23, pp. 8049–8080, 2014, doi: 10.1039/c4cs00035h.
- [58] S. Y. Pan, A. M. Lorente Lafuente, and P. C. Chiang, "Engineering, environmental and economic performance evaluation of high-gravity carbonation process for carbon capture and utilization," *Appl Energy*, vol. 170, pp. 269–277, 2016, doi: 10.1016/j.apenergy.2016.02.103.
- [59] K. de Kleijne, S. V. Hanssen, L. van Dinteren, M. A. J. Huijbregts, R. van Zelm, and H. de Coninck, "Limits to Paris compatibility of CO<sub>2</sub> capture and utilization," *One Earth*, vol. 5, no. 2, pp. 168–185, 2022, doi: 10.1016/j.oneear.2022.01.006.
- [60] N. Tsoy, B. Steubing, and J. B. Guinée, "Ex-ante life cycle assessment of polyols using carbon captured from industrial process gas," *Green Chemistry*, vol. 25, no. 14, pp. 5526–5538, 2023, doi: 10.1039/d3gc00799e.



- [61] C. Fernández-Dacosta, L. Shen, W. Schakel, A. Ramirez, and G. J. Kramer, "Potential and challenges of low-carbon energy options: Comparative assessment of alternative fuels for the transport sector," *Appl Energy*, vol. 236, no. November 2018, pp. 590–606, 2019, doi: 10.1016/j.apenergy.2018.11.055.
- [62] W. Hoppe, S. Bringezu, and N. Thonemann, "Comparison of global warming potential between conventionally produced and CO<sub>2</sub>-based natural gas used in transport versus chemical production," *J Clean Prod*, vol. 121, pp. 231–237, 2016, doi: <https://doi.org/10.1016/j.jclepro.2016.02.042>.
- [63] R. Hischer, S. Hellweg, C. Capello, and A. Primas, "Establishing Life Cycle Inventories of Chemicals Based on Differing Data Availability (9 pp)," *Int J Life Cycle Assess*, vol. 10, no. 1, pp. 59–67, 2005, doi: 10.1065/lca2004.10.181.7.
- [64] International Civil Aviation Or, "ICAO Environmental Report 2016," *Environmental report 2016*, p. 250, 2016.
- [65] A. Di Maria, R. Snellings, L. Alaert, M. Quaghebeur, and K. Van Acker, "Environmental assessment of CO<sub>2</sub> mineralisation for sustainable construction materials," *International Journal of Greenhouse Gas Control*, vol. 93, no. May 2019, p. 102882, 2020, doi: 10.1016/j.ijggc.2019.102882.
- [66] K. de Kleijne, S. V. Hanssen, L. van Dinteren, M. A. J. Huijbregts, R. van Zelm, and H. de Coninck, "Limits to Paris compatibility of CO<sub>2</sub> capture and utilization," *One Earth*, vol. 5, no. 2, pp. 168–185, 2022, doi: 10.1016/j.oneear.2022.01.006.
- [67] R. Cuéllar-Franca, P. García-Gutiérrez, I. Dimitriou, R. H. Elder, R. W. K. Allen, and A. Azapagic, "Utilising carbon dioxide for transport fuels: The economic and environmental sustainability of different Fischer-Tropsch process designs," *Appl Energy*, vol. 253, no. April, p. 113560, 2019, doi: 10.1016/j.apenergy.2019.113560.
- [68] K. de Kleijne, J. James, S. V. Hanssen, and R. van Zelm, "Environmental benefits of urea production from basic oxygen furnace gas," *Appl Energy*, vol. 270, no. April, p. 115119, 2020, doi: 10.1016/j.apenergy.2020.115119.
- [69] O. Mynko *et al.*, "Reducing CO<sub>2</sub> emissions of existing ethylene plants: Evaluation of different revamp strategies to reduce global CO<sub>2</sub> emission by 100 million tonnes," *J Clean Prod*, vol. 362, no. May, 2022, doi: 10.1016/j.jclepro.2022.132127.
- [70] F. Keller, R. P. Lee, and B. Meyer, "Life cycle assessment of global warming potential, resource depletion and acidification potential of fossil, renewable and secondary feedstock for olefin production in Germany," *J Clean Prod*, vol. 250, p. 119484, 2020, doi: 10.1016/j.jclepro.2019.119484.

- [71] S. Deutz *et al.*, “Cleaner production of cleaner fuels: Wind-to-wheel-environmental assessment of CO<sub>2</sub>-based oxymethylene ether as a drop-in fuel,” *Energy Environ Sci*, vol. 11, no. 2, pp. 331–343, 2018, doi: 10.1039/c7ee01657c.
- [72] K. de Kleijne, S. V. Hanssen, L. van Dinteren, M. A. J. Huijbregts, R. van Zelm, and H. de Coninck, “Limits to Paris compatibility of CO<sub>2</sub> capture and utilization,” *One Earth*, vol. 5, no. 2, pp. 168–185, 2022, doi: 10.1016/j.oneear.2022.01.006.
- [73] D. Fritz, M. Gössl, E. Hatzl, S. Poupá, W. Pölz, and H. Schreiber, “Österreichische Treibhausgas-Emissionsfaktoren,” 2023.
- [74] Umweltbundesamt, “Welche Treibhausgasemissionen verursacht die Wasserstoffproduktion?,” no. November, pp. 1–16, 2022.
- [75] W. Hoppe, S. Bringezu, and N. Wachter, “Economic assessment of CO<sub>2</sub>-based methane, methanol and polyoxymethylene production,” *Journal of CO<sub>2</sub> Utilization*, vol. 27, no. July, pp. 170–178, 2018, doi: 10.1016/j.jcou.2018.06.019.
- [76] D. Lide, *CRC Handbook of Chemistry and Physics*, vol. Internet V. 2005.
- [77] K. de Kleijne, S. V. Hanssen, L. van Dinteren, M. A. J. Huijbregts, R. van Zelm, and H. de Coninck, “Limits to Paris compatibility of CO<sub>2</sub> capture and utilization,” *One Earth*, vol. 5, no. 2, pp. 168–185, 2022, doi: 10.1016/j.oneear.2022.01.006.
- [78] European Commission, “Technology Readiness Levels (TRL),” *HORIZON 2020 – WORK PROGRAMME 2014-2015 General Annexes, Extract from Part 19 - Commission Decision C*, no. 2014, p. 1, 2014.
- [79] R. Chauvy, N. Meunier, D. Thomas, and G. De Weireld, “Selecting emerging CO<sub>2</sub> utilization products for short- to mid-term deployment,” *Appl Energy*, vol. 236, no. November 2018, pp. 662–680, 2019, doi: 10.1016/j.apenergy.2018.11.096.
- [80] G. J. Kramer and M. Haigh, “No quick switch to low-carbon energy,” *Nature*, vol. 462, no. 7273, pp. 568–569, 2009, doi: 10.1038/462568a.
- [81] “Orbix NV.” [Online]. Available: <https://www.orbix.be/en/technologies/carbonation>
- [82] M. Quaghebeur, P. Nielsen, L. Horckmans, and D. Van Mechelen, “Accelerated carbonation of steel slag compacts: Development of high-strength construction materials,” *Front Energy Res*, vol. 3, no. DEC, 2015, doi: 10.3389/fenrg.2015.00052.
- [83] Z. Cao *et al.*, “The sponge effect and carbon emission mitigation potentials of the global cement cycle,” *Nat Commun*, vol. 11, no. 1, pp. 1–9, 2020, doi: 10.1038/s41467-020-17583-w.

- [84] S. Y. Pan, P. C. Chiang, Y. H. Chen, C. Da Chen, H. Y. Lin, and E. E. Chang, "Systematic approach to determination of maximum achievable capture capacity via leaching and carbonation processes for alkaline steelmaking wastes in a rotating packed bed," *Environ Sci Technol*, vol. 47, no. 23, pp. 13677–13685, 2013, doi: 10.1021/es403323x.
- [85] E. E. Chang, A. C. Chiu, S. Y. Pan, Y. H. Chen, C. S. Tan, and P. C. Chiang, "Carbonation of basic oxygen furnace slag with metalworking wastewater in a slurry reactor," *International Journal of Greenhouse Gas Control*, vol. 12, pp. 382–389, 2013, doi: 10.1016/j.ijggc.2012.11.026.
- [86] M. B. Ali, R. Saidur, and M. S. Hossain, "A review on emission analysis in cement industries," *Renewable and Sustainable Energy Reviews*, vol. 15, no. 5, pp. 2252–2261, 2011, doi: 10.1016/j.rser.2011.02.014.
- [87] H. A. J. Van Dijk *et al.*, "Cost Effective CO<sub>2</sub> Reduction in the Iron & Steel Industry by Means of the SEWGS Technology: STEPWISE Project," *Energy Procedia*, vol. 114, no. November 2016, pp. 6256–6265, 2017, doi: 10.1016/j.egypro.2017.03.1764.
- [88] TNO, "SEWGS: revolutionary technology for CO<sub>2</sub> reduction." [Online]. Available: <https://www.tno.nl/en/technology-science/technologies/sewgs/#>
- [89] E. R. Van Selow, P. D. Cobden, P. A. Verbraeken, J. R. Hufton, and R. W. Van Den Brink, "Carbon capture by sorption-enhanced water-gas shift reaction process using hydrotalcite-based material," *Ind Eng Chem Res*, vol. 48, no. 9, pp. 4184–4193, 2009, doi: 10.1021/ie801713a.
- [90] J. Boon, P. D. Cobden, H. A. J. van Dijk, C. Hoogland, E. R. van Selow, and M. van Sint Annaland, "Isotherm model for high-temperature, high-pressure adsorption of CO<sub>2</sub> and H<sub>2</sub>O on K-promoted hydrotalcite," *Chemical Engineering Journal*, vol. 248, pp. 406–414, 2014, doi: 10.1016/j.cej.2014.03.056.
- [91] D. P. Harrison, "Sorption-enhanced hydrogen production: A review," *Ind Eng Chem Res*, vol. 47, no. 17, pp. 6486–6501, 2008, doi: 10.1021/ie800298z.
- [92] E. Bargiacchi, N. Thonemann, J. Geldermann, M. Antonelli, and U. Desideri, "Life cycle assessment of synthetic natural gas production from different CO<sub>2</sub> sources: A cradle-to-gate study," *Energies (Basel)*, vol. 13, no. 17, 2020, doi: 10.3390/4579.
- [93] T. B. H. Nguyen and E. Zondervan, "Methanol production from captured CO<sub>2</sub> using hydrogenation and reforming technologies- environmental and economic evaluation," *Journal of CO<sub>2</sub> Utilization*, vol. 34, no. January, pp. 1–11, 2019, doi: 10.1016/j.jcou.2019.05.033.

- [94] Carbon Recycling International, “worlds largest co2 to methanol plant starts production.” [Online]. Available: <https://www.carbonrecycling.is/news-media/worlds-largest-co2-to-methanol-plant-starts-production>
- [95] “Hitachi Zosen Inova EtoGas Power-to-Gas.” [Online]. Available: <https://www.hz-inova.com/de/renewable-gas/etogas/>
- [96] K. Salbrechter, M. Lehner, and K. Neumann, “Renewable Gasfield – eine P2G - Demoanlage,” pp. 1–11, 2020.
- [97] E. Moioli, P. Senn, S. Østrup, and C. Hütter, “Results from the operation of an efficient and flexible large-scale biogas methanation system,” pp. 1–29, 2023.
- [98] E. Bargiacchi, M. Antonelli, and U. Desideri, “A comparative assessment of Power-to-Fuel production pathways,” *Energy*, vol. 183, pp. 1253–1265, 2019, doi: 10.1016/j.energy.2019.06.149.
- [99] A. R. Medved, “The Influence of Nitrogen on Catalytic Methanation,” Montanuniversität Leoben, Doctoral thesis, 2020.
- [100] H. Mahmoudi *et al.*, “A review of Fischer Tropsch synthesis process, mechanism, surface chemistry and catalyst formulation,” *Biofuels Engineering*, vol. 2, no. 1, pp. 11–31, 2017, doi: 10.1515/bfuel-2017-0002.
- [101] C. M. Liu, N. K. Sandhu, S. T. McCoy, and J. A. Bergerson, “A life cycle assessment of greenhouse gas emissions from direct air capture and Fischer-Tropsch fuel production,” *Sustain Energy Fuels*, vol. 4, no. 6, pp. 3129–3142, 2020, doi: 10.1039/c9se00479c.
- [102] C. Van Der Giesen, R. Kleijn, and G. J. Kramer, “Energy and climate impacts of producing synthetic hydrocarbon fuels from CO<sub>2</sub>,” *Environ Sci Technol*, vol. 48, no. 12, pp. 7111–7121, 2014, doi: 10.1021/es500191g.
- [103] M. González-Castaño, B. Dorneanu, and H. Arellano-García, “The reverse water gas shift reaction: A process systems engineering perspective,” *React Chem Eng*, vol. 6, no. 6, pp. 954–976, 2021, doi: 10.1039/d0re00478b.
- [104] A. Hoek and L. B. J. M. Kersten, “The Shell Middle Distillate Synthesis Process: Technology, products and perspective,” *Stud Surf Sci Catal*, vol. 147, pp. 25–30, 2004, doi: 10.1016/s0167-2991(04)80022-3.
- [105] V. Papantoni *et al.*, “Life Cycle Assessment of Power-to-Liquid for Aviation: A Case Study of a Passenger Aircraft,” *E3S Web of Conferences*, vol. 349, pp. 0–5, 2022, doi: 10.1051/e3sconf/202234902003.
- [106] M. Micheli, D. Moore, V. Bach, and M. Finkbeiner, “Life-Cycle Assessment of Power-to-Liquid Kerosene Produced from Renewable Electricity and CO<sub>2</sub> from Direct Air Capture

- in Germany,” *Sustainability (Switzerland)*, vol. 14, no. 17, 2022, doi: 10.3390/su141710658.
- [107] EWO-Austria, “Innovation Flüssige Energie.” [Online]. Available: <https://www.ewo-austria.at/innovation-fluessige-energie/>
- [108] K. Thenert, K. Beydoun, J. Wiesenthal, W. Leitner, and J. Klankermayer, “Ruthenium-Catalyzed Synthesis of Dialkoxymethane Ethers Utilizing Carbon Dioxide and Molecular Hydrogen,” *Angewandte Chemie - International Edition*, vol. 55, no. 40, pp. 12266–12269, 2016, doi: 10.1002/anie.201606427.
- [109] M. Aresta, A. Dibenedetto, and A. Angelini, “Catalysis for the Valorization of Exhaust Carbon: from CO<sub>2</sub> to Chemicals, Materials, and Fuels. Technological Use of CO<sub>2</sub>,” *Chem Rev*, vol. 114, no. 3, pp. 1709–1742, Feb. 2014, doi: 10.1021/cr4002758.
- [110] R. Chauvy and G. De Weireld, “CO<sub>2</sub> Utilization Technologies in Europe: A Short Review,” *Energy Technology*, vol. 8, no. 12, pp. 1–17, 2020, doi: 10.1002/ente.202000627.
- [111] G. A. Buchner, N. Wulfes, and R. Schomäcker, “Techno-economic assessment of CO<sub>2</sub>-containing polyurethane rubbers,” *Journal of CO<sub>2</sub> Utilization*, vol. 36, no. October 2019, pp. 153–168, 2020, doi: 10.1016/j.jcou.2019.11.010.
- [112] A. B. Levy, “Acetone: Ullman’s Encyclopedia of Industrial Chemistry,” 1991, doi: 10.1002/14356007.
- [113] (European Commission), “Scaling up innovative technologies for climate neutrality,” 2023. doi: 10.2777/926968.
- [114] S. Rostami, P. Keshavarz, and S. Raeissi, “Experimental study on the effects of an ionic liquid for CO<sub>2</sub> capture using hollow fiber membrane contactors,” *International Journal of Greenhouse Gas Control*, vol. 69, pp. 1–7, Feb. 2018, doi: 10.1016/j.ijggc.2017.12.002.
- [115] J. Meng, W. Liao, and G. Zhang, “Emerging CO<sub>2</sub>-mineralization technologies for co-utilization of industrial solid waste and carbon resources in p,” *Minerals*, vol. 11, no. 3, pp. 1–16, 2021, doi: 10.3390/min11030274.
- [116] S. K. Kaliyavaradhan, T. C. Ling, and K. H. Mo, “Valorization of waste powders from cement-concrete life cycle: A pathway to circular future,” *J Clean Prod*, vol. 268, p. 122358, 2020, doi: 10.1016/j.jclepro.2020.122358.
- [117] X. WANG, X. YAN, and X. LI, “Environmental risks for application of magnesium slag to soils in China,” *J Integr Agric*, vol. 19, no. 7, pp. 1671–1679, 2020, doi: [https://doi.org/10.1016/S2095-3119\(19\)62835-2](https://doi.org/10.1016/S2095-3119(19)62835-2).

- [118] F. J. Doucet, "Effective CO<sub>2</sub>-specific sequestration capacity of steel slags and variability in their leaching behaviour in view of industrial mineral carbonation," *Miner Eng*, vol. 23, no. 3, pp. 262–269, 2010, doi: 10.1016/j.mineng.2009.09.006.
- [119] S. Teir, S. Eloneva, C.-J. Fogelholm, and R. Zevenhoven, "Dissolution of steelmaking slags in acetic acid for precipitated calcium carbonate production," *Energy*, vol. 32, no. 4, pp. 528–539, 2007, doi: <https://doi.org/10.1016/j.energy.2006.06.023>.
- [120] R. Baciocchi, G. Costa, E. Di Bartolomeo, A. Poletini, and R. Pomi, "Wet versus slurry carbonation of EAF steel slag," *Greenhouse Gases: Science and Technology*, vol. 1, no. 4, pp. 312–319, Dec. 2011, doi: <https://doi.org/10.1002/ghg.38>.
- [121] S. Monkman and Y. Shao, "Assessing the Carbonation Behavior of Cementitious Materials," *Journal of Materials in Civil Engineering - J MATER CIVIL ENG*, vol. 18, Dec. 2006, doi: 10.1061/(ASCE)0899-1561(2006)18:6(768).
- [122] W. J. J. Huijgen and R. N. J. Comans, "Mineral CO<sub>2</sub> sequestration by carbonation of industrial residues," *ECN Clean Fossil Fuels - Environmental Risk Assessment*, no. December, pp. 1–22, 2005.
- [123] P. J. Gunning, C. D. Hills, and P. J. Carey, "Accelerated carbonation treatment of industrial wastes," *Waste Management*, vol. 30, no. 6, pp. 1081–1090, 2010, doi: 10.1016/j.wasman.2010.01.005.
- [124] S. Teramura, N. Isu, and K. Inagaki, "New Building Material from Waste Concrete by Carbonation," *Journal of Materials in Civil Engineering - J MATER CIVIL ENG*, vol. 12, Nov. 2000, doi: 10.1061/(ASCE)0899-1561(2000)12:4(288).
- [125] J. K. Stolaroff, G. V. Lowry, and D. W. Keith, "Using CaO- and MgO-rich industrial waste streams for carbon sequestration," *Energy Convers Manag*, vol. 46, no. 5, pp. 687–699, 2005, doi: 10.1016/j.enconman.2004.05.009.
- [126] Y. Katsuyama, A. Yamasaki, A. Iizuka, M. Fujii, K. Kumagai, and Y. Yanagisawa, "Development of a process for producing high-purity calcium carbonate (CaCO<sub>3</sub>) from waste cement using pressurized CO<sub>2</sub>," *Environmental Progress*, vol. 24, no. 2, pp. 162–170, Jul. 2005, doi: <https://doi.org/10.1002/ep.10080>.
- [127] L. Wang, Y. Jin, and Y. Nie, "Investigation of accelerated and natural carbonation of MSWI fly ash with a high content of Ca," *J Hazard Mater*, vol. 174, no. 1–3, pp. 334–343, 2010, doi: 10.1016/j.jhazmat.2009.09.055.
- [128] M. J. Quina, J. C. Bordado, and R. M. Quinta-Ferreira, "Treatment and use of air pollution control residues from MSW incineration: An overview," *Waste Management*, vol. 28, no. 11, pp. 2097–2121, 2008, doi: 10.1016/j.wasman.2007.08.030.

- [129] H. Groenemans, G. Saur, C. Mittelsteadt, J. Lattimer, and H. Xu, "Techno-economic analysis of offshore wind PEM water electrolysis for H<sub>2</sub> production," *Curr Opin Chem Eng*, vol. 37, p. 100828, 2022, doi: 10.1016/j.coche.2022.100828.

## 7.2 Nomenclature

%	Percentage
°C	Celsius degree
atm	atmosphere
BOFG	Basic oxygen furnace gas
CC	Carbon capture
CCU	Carbon capture and utilization
CDR	Carbon dioxide removal
CHP	Combined heat and power
CH <sub>4</sub>	Methane
C <sub>2</sub> H <sub>4</sub>	Ethylene
CH <sub>2</sub> O	Formaldehyde
CH <sub>3</sub> OH	Methanol
C <sub>2</sub> H <sub>6</sub> O	Dimethylether
C <sub>2</sub> H <sub>4</sub> O <sub>2</sub>	Acetic acid
CH <sub>4</sub> N <sub>2</sub> O	Urea
CO	Carbon monoxide
CO <sub>2</sub>	Carbon dioxide
CO <sub>2</sub> e	Carbon dioxide equivalent
CO <sub>2</sub> RR	Electrochemical reduction of carbon dioxide
CRW	Cold-rolling wastewater
DAC	Direct air capture
DMC	Double metal cyanide
DMM	Dimethoxymethane
EOL	End of life
EU	European Union
FA	Formaldehyde
FTS	Fischer-Tropsch synthesis
GHG	Greenhouse gas
GJ <sub>th</sub>	Gigajoule thermal
GJ <sub>el</sub>	Gigajoule electric
GWP	Global warming potential
H <sub>2</sub>	Hydrogen
HCl	Hydrochloric acid
Hg	Mercury
H <sub>2</sub> O	Water
J	Joule
kg	Kilogramm
kWh	Kilowatt-hour
LCA	Life cycle assessment
m	Meter

Me	Metal
MEA	Monoethanolamine
MSWI	Municipal solid waste incineration
N <sub>2</sub>	Nitrogen
NECP	National energy and climate plans
NG	Natural gas
NO <sub>x</sub>	Nitrogen oxides
NH <sub>3</sub>	Ammonia
O <sub>2</sub>	Oxygen
OME	Oxymethylene ether
PC	Portland cement
PSA	Pressure swing adsorption
PU	Polyurethane
RHE	Reversible hydrogen electrode
rWGS	Reversed water gas shift
R&D	Research and development
SEWGS	Sorption enhanced water gas shift
SSS	Stainless steel slag
SO <sub>2</sub>	Sulphur dioxide
TRL	Technological readiness level
t	Tonnes
UNFCCC	United Nations Framework Convention on Climate Change
V	Voltage
VPSA	Vacuum pressure swing adsorption
W	Watt
WAM	With additional measures
WEM	With existing measures

### 7.3 Formulars

$E^0$	Equilibrium potential [V vs. RHE]
$E_{2030}$	Emission factor in 2030 [kg CO <sub>2</sub> e/kg CO <sub>2</sub> utilized]
$E_{2040}$	Emission factor in 2040 [kg CO <sub>2</sub> e/kg CO <sub>2</sub> utilized]
$E_{CCU}$	CCU emission factor [kg CO <sub>2</sub> e/kg CO <sub>2</sub> utilized]
$E_{utilized}$	Emission factor for utilized CO <sub>2</sub> [kg CO <sub>2</sub> e/kg CO <sub>2</sub> utilized]
$E_{capture\ process}$	Emission factor for CC [kg CO <sub>2</sub> e/kg CO <sub>2</sub> utilized]
$E_{conversion}$	Emission factor for CO <sub>2</sub> conversion [kg CO <sub>2</sub> e/kg CO <sub>2</sub> utilized]
$E_{released}$	Emission factor for EOL-emissions [kg CO <sub>2</sub> e/kg CO <sub>2</sub> utilized]
$E_{other}$	Emission factor for other emissions [kg CO <sub>2</sub> e/kg CO <sub>2</sub> utilized]
$e_{CCU}$	CCU energy factor [kWh/kg CO <sub>2</sub> utilized]
$Q_{Savings}$	Theoretical GHG savings [ktCO <sub>2</sub> e]
$Q_{CCU}$	CCU product emissions [ktCO <sub>2</sub> e]
$Q_{Source}$	Utilized CO <sub>2</sub> from point source [ktCO <sub>2</sub> e]
$Q_{Substitute}$	Conventional product emissions [ktCO <sub>2</sub> e]
$\Delta H_R^0$	Standard reaction enthalpies [kJ/mol]
$u_{storage}$	Storage factor [-]



## 7.4 Tables

Table 1: Fundamental reactions of chemical CO <sub>2</sub> conversion methods (enthalpies calculated based on Lange's Handbook of Chemistry [43]) .....	18
Table 2: CO <sub>2</sub> reduction pathways and their equilibrium potentials at ambient conditions [48] .....	19
Table 3: Metabolic processes for CO <sub>2</sub> -fixation [51], [52].....	20
Table 4: CCU product categories and their average lifetime .....	21
Table 5: Interpretation of <i>ECCU</i> values depending on CO <sub>2</sub> origin.....	22
Table 6: Cradle-to-gate emissions of conventional products.....	24
Table 7: Assumed Austrian renewable electricity mix by 2030 and emission factors.....	24
Table 8: Selected CO <sub>2</sub> capture technologies and their average energy demands .....	25
Table 9: Storage factors of CCU products depending on their expected lifetime [77] .....	26
Table 10: TRL scale for CCU evaluation [78], [79] .....	27
Table 11: Compatibility limits for CCU technologies in 2030 and 2040 and technology characteristics.....	28
Table 12: Operation parameters for the production of carbonated blocks from stainless steel slag [65] and input material composition [82] .....	32
Table 13: Compatibility of carbonation of steel slag construction blocks with Austria's climate targets.....	33
Table 14: Operation parameters for the production carbonated cement substitute, based on LCA results by Pan et al. [58] and input material composition from Chang et al. [85]....	35
Table 15: Compatibility of high gravity steel slag carbonation with Austria's climate targets	36
Table 16: Operation parameters and BOFG composition for the production of urea, from LCA by de Kleijne et al. [68] .....	38
Table 17: Compatibility of urea production via SEWGS from BOFG with Austria's climate targets.....	38
Table 18: Operation parameters for the production of methane or methanol via direct hydrogenation [98], [97].....	40
Table 19: Compatibility of direct hydrogenation of CO <sub>2</sub> to produce methane and methanol .	40
Table 20: Operation parameters for the production of FT-fuels via rWGS reaction [96] .....	42
Table 21: Compatibility of FT-fuel from syngas via rWGS .....	42
Table 22: Operation parameters for the production of DMM via direct synthesis with methanol, CO <sub>2</sub> and H <sub>2</sub> [71], [108] .....	44
Table 23: Compatibility of DMM production via direct CO <sub>2</sub> hydrogenation in methanol .....	44

Table 24: Operating parameters of electrochemical CO <sub>2</sub> reduction to ethylene [50].....	46
Table 25: Compatibility of electrochemical CO <sub>2</sub> reduction to ethylene .....	46
Table 26: Compatibility of CO <sub>2</sub> -based polyol production .....	48
Table 27: Operation parameters for the production of acetone from CO <sub>2</sub> via bio-fermentation [54].....	50
Table 28: Compatibility of CO <sub>2</sub> bio-fermentation to acetone.....	51
Table 29: Sectoral distribution of CO <sub>2</sub> emissions in 2030, CO <sub>2</sub> exhaust concentrations and origins [8] .....	52
Table 30: Sectoral distribution of CO <sub>2</sub> emissions in 2040, CO <sub>2</sub> exhaust concentrations and origins [8].....	53
Table 31: Carbon capture technologies and their typical CO <sub>2</sub> input concentrations and applications.....	54
Table 32: Emission factors for investigated technologies and conventional products to substitute .....	55
Table 33: Conceivable CCU paths for Austrian emitters in 2030, CCU emissions and reduction potentials .....	58
Table 34: Conceivable CCU paths for Austrian emitters in 2040, CCU emissions and reduction potentials .....	59
Table 35: Examples and description of limiting aspects on theoretical CO <sub>2</sub> saving potentials	60

## 7.5 Figures

Figure 1: Development of total GHG-emissions (ETS and non-ETS) 1990-2021 and calculated GHG-scenarios [5].....	4
Figure 2: Overview of CO <sub>2</sub> origins and its journey on CCU pathways .....	6
Figure 3: Share of sectors in Austria's total GHG emissions in 2020 [7] .....	7
Figure 4: Branch specific allocation of GHG emissions from the energy and industry sectors for the target years 2030 and 2040 (data from Hochmeister et al. [8]) .....	8
Figure 5: CO <sub>2</sub> origin distribution in 2019 and their progressive development until target years 2030 and 2040 (data from Hochmeister et al. [8]) .....	9
Figure 6: Overview of CO <sub>2</sub> separation technologies and their technological readiness level (TRL) [13] .....	10
Figure 7: Simplified process flow diagram of CO <sub>2</sub> capture by chemical absorption [14].....	11
Figure 8: Schematic diagram of a CO <sub>2</sub> adsorption system [14] .....	12
Figure 9: Scheme of membrane separation (on the left) and gas absorption membrane (on the right) [26] .....	13
Figure 10: Simplified process flow diagram of cryogenic carbon capture system [30] .....	14
Figure 11: Schematic diagram of CO <sub>2</sub> capture from flue gas by calcium looping [13].....	15
Figure 12: Overview of CO <sub>2</sub> utilization pathways in CCU technologies and product examples based on literature [36], [37] .....	16
Figure 13: Overview of chemical CO <sub>2</sub> utilization pathways in CCU technologies [37].....	17
Figure 14: Polymerization reaction of propylene oxide and CO <sub>2</sub> to polyethercarbonate polyols [47].....	18
Figure 15: Electrolytic flow cell for the reduction of CO <sub>2</sub> to ethylene [50] .....	19
Figure 16: Comparison of CCU technologies related to 2030 climate target compatibility criteria .....	29
Figure 17: Comparison of CCU technologies related to 2040 climate target compatibility criteria .....	30
Figure 18: Energy consumption of the investigated CCU technologies.....	31
Figure 19: Flow scheme for the production of carbonated blocks, modified from [65], [82] ..	32
Figure 20: Flow scheme of the HiGCarb process for the production of cementitious material [84].....	34
Figure 21: Flow scheme of urea production via SEWGS from BOFG [68] .....	36
Figure 22: Schematic of the SEWGS reaction [68].....	37

Figure 23: Flow scheme of direct CO <sub>2</sub> hydrogenation for the production of methanol and methane [42], [92], and biogas upgrading (dashed line) [97] .....	39
Figure 24: Flow scheme of FT-fuel production from syngas via rWGS [101], [102] .....	41
Figure 25: Flow scheme of DMM production via CO <sub>2</sub> hydrogenation in methanol [71] .....	43
Figure 26: Possible reaction pathway for the Ru(triphos)/Al(OTf) <sub>3</sub> -catalyzed synthesis of DMM using methanol, CO <sub>2</sub> and H <sub>2</sub> [108] .....	43
Figure 27: Standard Gibbs free energy of formation for CO <sub>2</sub> and various possible chemical products [50], [109] .....	45
Figure 28: Flow scheme of ethylene production by electrochemical CO <sub>2</sub> reduction [50] .....	45
Figure 29: Flow scheme of CO <sub>2</sub> -based polyol production [47] .....	47
Figure 30: Block flow diagram for production of polyols containing CO <sub>2</sub> (PEC) under characteristic process conditions (PO – propylene oxide, mPG – monomeric propylene glycol, DMC cat. – double metal cyanide catalyst, MA – maleic anhydride, cPc – cyclic propylene carbonate) [111] .....	47
Figure 31: Flow scheme of acetone production from CO <sub>2</sub> via bio-fermentation [54] .....	49
Figure 32: Emissions of MSWI sector combined with CCU technologies (chemical absorption via MEA and carbonation of steel slag blocks) in 2040 .....	56
Figure 33: Emissions of methanol sector combined with CCU technologies (physical adsorption and cryogenic carbon capture and direct hydrogenation to methanol) in 2030 .....	57